

SANDIA REPORT

SAND2003-1755
Unlimited Release
Printed June, 2003

Very High Efficiency Reactor (VHER) Concepts for Electrical Power Generation and Hydrogen Production

Edward J. Parma
Paul S. Pickard
Ahti J. Suo-Anttila

Prepared by
Sandia National Laboratories
Albuquerque, New Mexico 87185 and Livermore, California 94550

Sandia is a multiprogram laboratory operated by Sandia Corporation,
a Lockheed Martin Company, for the United States Department of Energy's
National Nuclear Security Administration under Contract DE-AC04-94AL85000.

Approved for public release; further dissemination unlimited.



Issued by Sandia National Laboratories, operated for the United States Department of Energy by Sandia Corporation.

NOTICE: This report was prepared as an account of work sponsored by an agency of the United States Government. Neither the United States Government, nor any agency thereof, nor any of their employees, nor any of their contractors, subcontractors, or their employees, make any warranty, express or implied, or assume any legal liability or responsibility for the accuracy, completeness, or usefulness of any information, apparatus, product, or process disclosed, or represent that its use would not infringe privately owned rights. Reference herein to any specific commercial product, process, or service by trade name, trademark, manufacturer, or otherwise, does not necessarily constitute or imply its endorsement, recommendation, or favoring by the United States Government, any agency thereof, or any of their contractors or subcontractors. The views and opinions expressed herein do not necessarily state or reflect those of the United States Government, any agency thereof, or any of their contractors.

Printed in the United States of America. This report has been reproduced directly from the best available copy.

Available to DOE and DOE contractors from

U.S. Department of Energy
Office of Scientific and Technical Information
P.O. Box 62
Oak Ridge, TN 37831

Telephone: (865)576-8401
Facsimile: (865)576-5728
E-Mail: reports@adonis.osti.gov
Online ordering: <http://www.doe.gov/bridge>

Available to the public from

U.S. Department of Commerce
National Technical Information Service
5285 Port Royal Rd
Springfield, VA 22161

Telephone: (800)553-6847
Facsimile: (703)605-6900
E-Mail: orders@ntis.fedworld.gov
Online order: <http://www.ntis.gov/help/ordermethods.asp?loc=7-4-0#online>



SAND2003-1755
Unlimited Release
Printed June 2003

Very High Efficiency Reactor (VHER) Concepts for Electrical Power Generation and Hydrogen Production

Edward J. Parma and Paul S. Pickard
Advanced Nuclear Concepts
Sandia National Laboratories
P.O. Box 5800
Albuquerque, NM 87185 - 1141

Ahti J. Suo-Anttila
ITS Corporation
6000 Uptown NE, Suite 300
Albuquerque, NM 87110

Abstract

The goal of the Very High Efficiency Reactor study was to develop and analyze concepts for the next generation of nuclear power reactors. The next generation power reactor should be cost effective compared to current power generation plant, passively safe, and proliferation-resistant. High-temperature reactor systems allow higher electrical generating efficiencies and high-temperature process heat applications, such as thermo-chemical hydrogen production. The study focused on three concepts; one using molten salt coolant with a prismatic fuel-element geometry, the other two using high-pressure helium coolant with a prismatic fuel-element geometry and a fuel-pebble element design. Peak operating temperatures, passive-safety, decay heat removal, criticality, burnup, reactivity coefficients, and material issues were analyzed to determine the technical feasibility of each concept.

LEFT BLANK INTENTIONALLY

CONTENTS

EXECUTIVE SUMMARY	8
1. INTRODUCTION	10
2. DESCRIPITON OF SELECTED REACTOR SYSTEMS	14
2.1 Advanced High Temperature Reactor – Molten Salt - 1000°C.....	15
2.2 Very High Temperature Gas Cooled Reactor - He - 1100°C.....	20
2.3 Ultra High Temperature Gas Cooled Reactor - He - 1200°C.....	24
3. FUEL PARTICLE	29
4. FUEL ELEMENT	32
4.1 Fuel Loading.....	32
4.2 Configuration.....	35
4.3 Thermal Analysis Modeling.....	41
4.4 Thermal Hydraulic Analysis Modeling.....	44
4.5 Thermal and Thermal Hydraulic Analysis for the VHER Concepts.....	46
5. PASSIVE DECAY HEAT REMOVAL	58
5.1 AHTR – Passive Heat Removal Analysis.....	59
5.2 VHTGR – Passive Heat Removal Analysis.....	65
5.3 UHTGR – Passive Heat Removal Analysis.....	67
6. MATERIAL ISSUES	70
6.1 Coolant.....	70
6.2 Core Materials.....	71
6.3 Pressure Vessel, Piping, Heat Exchangers, Pumps.....	72
7. CRITICALITY AND BURNUP	76
7.1 Infinite Reactor Calculations.....	77
7.2 AHTR Neutronics Analysis.....	79
7.3 VHTGR Neutronics Analysis.....	84
7.4 UHTGR Neutronics Analysis.....	84
8. CONCLUSIONS	87
9. REFERENCES	89

TABLES

Table 1. Typical Particle Fuel and Pebble Fuel Elemental Composition.	33
Table 2. Fuel Loading Density for the UHTGR.	34
Table 3. Maximum Fuel Loading Density for the AHTR and VHTGR.	35
Table 4. Flibe Molten Salt Thermo-Physical Properties.	49
Table 5. AHTR Maximum Coolant Channel and Fuel Radius ($T_{max} = 1250^{\circ}C$).	51
Table 6. He Thermo-Physical Properties at 1000 psi and $900^{\circ}C$.	52
Table 7. VHTGR Maximum Coolant Channel and Fuel Radius ($T_{max} = 1400^{\circ}C$).	55
Table 8. UHTGR Thermal Hydraulic Results.	57
Table 9. Dimensions and Properties for the AHTR Passive Heat Removal Analysis.	61
Table 10. Dimensions and Properties for the VHTGR Passive Heat Removal Analysis.	66
Table 11. Dimensions and Properties for the UHTGR Passive Heat Removal Analysis.	68
Table 12. Operating Temperatures for Refractory Metal Alloys in Flibe.	73
Table 13. Operating Temperatures for Refractory Metal Alloys in He With 100 appm O.	74
Table 14. Burnup Results for the UHTGR Using Graphite Moderator.	85
Table 15. Burnup Results for the UHTGR Using Heavy Water Moderator.	85
Table 16. Figure of Merit for the VHER Concepts.	87

FIGURES

Figure 1. The AHTR – Molten Salt Reactor Concept.	17
Figure 2. The VHTGR – Helium Gas Cooled Reactor Concept.....	21
Figure 3. The UHTGR Module Concept – Helium Gas Cooled.	26
Figure 4. The UHTGR concept – 18 Module Configuration.	26
Figure 5. Typical Triso-coated Particle Fuel Composition, Dimensions, and Density.....	30
Figure 6. Illustration of a PBMR Fuel Pebble.....	33
Figure 7. Fuel Element Configuration for the AHTR and VHTGR concepts.	36
Figure 8. Prismatic Fuel Form With Annular and Inner Cooling Channel.....	38
Figure 9. Cooling Channel Options for the Prismatic Fuel Form.....	39
Figure 10. Prismatic Fuel Form Without Additional Moderator.	40
Figure 11. Prismatic Fuel Element Used for Thermal Hydraulic Analysis.....	46
Figure 12. Fuel Compact Peak to Wall Temperature Difference – 5 W/cc, 0.3 W/cm-°C...48	
Figure 13. Fuel Compact Peak to Wall Temperature Difference – 10 W/cc, 0.3 W/cm-°C.48	
Figure 14. AHTR Wall to Bulk Coolant Temperature Difference – 5 W/cc.	50
Figure 15. AHTR Wall to Bulk Coolant Temperature Difference – 10 W/cc.	50
Figure 16. Pumping Power Required for the AHTR.....	52
Figure 17. VHTGR Wall to Bulk Coolant Temperature Difference – 5 W/cc.....	54
Figure 18. VHTGR Wall to Bulk Coolant Temperature Difference – 10 W/cc.....	54
Figure 19. Pumping Power Required for the VHTGR.....	55
Figure 20. Decay Power and Energy Fraction Following a 10-Year Operating History.	59
Figure 21. Plan View of the AHTR Concept.	60
Figure 22. Schematic Diagram of the AHTR Cooling System.....	61
Figure 23. Passive Cooling Results for the AHTR With Conduction Through the Core. ...	63
Figure 24. Passive Cooling Results for the AHTR With Flow Through the Core.....	63
Figure 25. Natural Circulation Passive Cooling Results for the AHTR.....	65
Figure 26. Passive Cooling Results for the VHTGR.....	67
Figure 27. Passive Cooling Results for the UHTGR Module.....	69
Figure 28. Burnup Results for 20% Enriched U-235 Infinite Reactor.	78
Figure 29. Burnup Results for 10% Enriched U-235 Infinite Reactor.	78
Figure 30. Void Reactivity for the 10% Coolant Fraction AHTR.	80
Figure 31. Fission Lifetime for the 10% Coolant Fraction AHTR.	80
Figure 32. Burnup Results for the AHTR With 0.05 U/C Homogeneous Fuel Element.	81
Figure 33. Burnup Results for the AHTR With 0.05 U/C Heterogeneous Fuel Element.....	83
Figure 34. Burnup Results for 0.05 U/C Heterogeneous Fuel Element (Continued).....	83
Figure 35. Dimensions for the UHTGR Module.	85

EXECUTIVE SUMMARY

The Very High Efficiency Reactor (VHER) project examined potential reactor concepts for next generation nuclear power reactor systems. The project focus was on improved performance characteristics for the electrical and hydrogen production applications. High-temperature reactor systems can attain high thermal efficiencies and allow for high-temperature heat applications, such as thermo-chemical hydrogen production. High-temperature gas-cooled systems are considered to provide the most promising approach due to past experience with helium gas coolant, current fuel technology, and current inherently safe designs. This formed the basis for further study.

The goal of the project was to study reactor concepts that could generate exit coolant temperatures from 1000°C to 1200°C, maintained passive safety features, were proliferation resistant, were inherently simple in design, and maintained an attractive fuel cycle. Several approaches were initially considered. From these initial assessments, three reactor concepts were analyzed further:

- 1) Advanced High Temperature Reactor (AHTR) – A low-pressure molten salt-cooled reactor using prismatic graphite fuel elements with current technology coated particle fuel – process heat applications, exit coolant temperature of 1000°C;
- 2) Very High Temperature Gas Cooled Reactor (VHTGR) – A high-pressure helium-cooled reactor using prismatic graphite fuel elements with advanced coated particle fuel – electrical power generation with ~57% thermal efficiency at 1100°C;
- 3) Ultra High Temperature Gas Cooled Reactor (UHTGR) – A high-pressure helium-cooled reactor using fuel pebbles with highly advanced coated particle fuel – electrical power generation with greater than 60% thermal efficiency at 1200°C or higher.

Peak operating temperatures, passive-safety, decay heat removal, criticality, burnup, reactivity coefficients, and material issues were analyzed to determine the technical feasibility of each concept. The results of these analyses are presented in this report.

The AHTR concept maintains the most robust passive safety features, operates at a low pressure, and has the highest efficiency for a given temperature. However the molten salt coolant introduces material compatibility issues that must be more thoroughly addressed. The VHTGR concept is the focus of one of the Generation IV designs. In order to achieve 1100°C exit core temperature, evolutionary materials and fuel designs will be required. The UHTGR concept is a unique design that uses a modular array of fuelled units to form the reactor. In order to achieve 1200°C exit core temperature, additional material and fuel issues must be addressed. There is currently no application identified that benefits from this high temperature. However, some of the unique characteristics of this concept may be used for lower temperature applications. The fuel burnup for all of the concepts can be made comparable to current LWR systems if the uranium loading density in the fuel element is increased a factor of four greater than currently proposed for PBR fuel.

The role of high-temperature reactor systems is essential if the role of nuclear energy is to expand. The near term approach of the U.S. should be to take advantage of existing technology, material performance, and fuel designs using high heat capacity and low pressure. Designs that mitigate high-temperature material performance may be more important than improved material properties. The benefits of extremely high exit temperatures must be weighed against the cost and technological risk associated with the design. The designs presented in this report must be further studied and pursued with regard to cost and feasibility estimates in order to better understand their potential impact on the next generation power reactor.

1. INTRODUCTION

The Very High Efficiency Reactor (VHER) Project focused on developing concepts for the next-generation power reactors that would enable more efficient electricity generation and the production of emissions free hydrogen for future transportation fuels. These next generation reactors would be characterized by lower cost, a more benign waste stream, inherent safety, proliferation resistance, and have performance characteristics that would enable nuclear power to make a larger contribution to the future U.S. energy supply.

Plant costs and construction times are significant barriers to expanding nuclear power in the U.S. These costs include costs for construction, operating and maintenance, and fuel costs including fresh fuel fabrication, storage, and disposal of spent fuel. The large capital cost for a light water reactor (LWR) (including containment, steam supply, pressure vessel, nuclear instrumentation and control, emergency core cooling system, and auxiliary systems) is the primary factor in projecting higher costs for new nuclear plants. Fuel cost for current nuclear power plants is a small fraction of the overall cost. Although the plant cost for a new power reactor concept is difficult to quantify, one obvious approach to lowering the overall cost is to increase electrical generation efficiency for the same thermal power. Also, reducing system component complexity from those required in a water/steam-based coolant/power generating system could significantly reduce the capital cost and overall plant construction time.

Next generation systems also must address the issues of minimizing the nuclear waste stream. These systems should take advantage of more efficient fuel utilization and closed fuel cycles to minimize concerns regarding the back end of the fuel cycle. The nuclear fuel cycle is currently a significant issue facing the nuclear power industry that must be resolved with both technical and political solutions. With the current state of uncertainty, it is difficult to propose advanced nuclear concepts involving optimized fuel cycles. The approach taken in this study was to identify core designs that maximize burnup efficiency for an initial and final fuel loading. These results could then be compared with the current LWR once-through cycle.

The concept of inherent safety or passively-safe nuclear systems has received much more attention since the Three Mile Island event. Although only small quantities of radiation were released to the environment and no fatalities or injuries resulted, the effect on the public perception of nuclear power was dramatic. The political risk of a nuclear accident can exceed the actual impact on the public and the environment. This risk must be included as a factor in estimating plant cost since it directly affects capital cost due to over-design and regulatory burden. The next generation nuclear power plant must have a very robust safety case – that is, it must be inherently safe. In the strictest sense, “inherently safe” means that if all safety systems were to fail, no adverse consequence would result. However, this may be an impossible goal to achieve. A more workable definition is that no active systems are required to be operational after the reactor is shut down to maintain the essential fission product barriers. Therefore, no active system is required to remove decay heat from the system after shutdown. The reactor could potentially be restarted after the problem was resolved. Inherent safety characteristics clearly can impact economics. The pebble bed reactor concept is proposed as being inherently safe, but only operates with a power density of 5 W/cc and generates ~120 MW electric power. However, more than eight of these plants would be required to equal the electricity produced by

one typical LWR. If the plant costs were on the order of 1/8th or less as compared to a typical LWR, then this concept would be viable. However, if the plant costs exceed this value, the benefits of inherent safety would have to be weighed against the cost and risk associated alternative concepts.

“Proliferation-resistant” fuel forms and cycles are generally achieved by using low-enriched U-235 or U-233 fuels (less than 20% enriched). For plutonium, proliferation resistance can be achieved by poisoning the Pu-239 with a plutonium isotope like Pu-238, which has a large spontaneous fission probability. For low enriched fuel, Pu-238 is produced along with Pu-239, making the Pu into a less desirable form.

The Very High Efficiency Reactor study examined several designs that incorporated design features that could address these performance objectives. Reactor systems were analyzed that included the use of high-temperature fuels, high-temperature coolants, highly neutron-efficient systems, and high-burnup core designs. Of these designs, three were chosen as baseline designs for further study. These baseline designs are:

- ***Advanced High Temperature Reactor (AHTR)*** – Molten-salt cooled, pool type, prismatic graphite moderator, coated particle fuel, passive decay-heat removal, H₂ production through heat exchanger and/or indirect cycle electric. This design was originally proposed by ORNL as an alternative to high-temperature, high-pressure gas-cooled systems for hydrogen production.
- ***Very High Temperature Gas Cooled Reactor (VHTGR)*** – Helium cooled, loop type, graphite moderated/reflected, axial flow, prismatic type graphite moderator, coated particle fuel, passive decay-heat removal, direct cycle electric and/or H₂ production through heat exchanger. This concept is an evolved from the GT-MHR design approach and uses more efficient fuel-to-coolant heat transfer to achieve higher outlet temperatures with the same fuel temperature limits.
- ***Ultra High Temperature Gas Cooled Reactor (UHTGR)*** – Helium cooled, loop type, graphite moderated/reflected, pebble fuel in nominally 1 m columns, coated particle fuel, passive decay-heat removal, direct cycle electric and/or H₂ production through heat exchanger. The concept combines key features of the pebble bed and prismatic approaches to achieve the highest possible outlet temperature and fuel cycle flexibility.

These three classes of reactor systems were analyzed further to determine performance and feasibility, the results of which are presented in this report. These systems all represent high-temperature systems with coolant exit temperatures exceeding 1000°C. High-temperature exit coolant temperatures will be required in the next generation of reactor concepts to maximize electrical generation efficiency and to enable the production of hydrogen by efficient thermochemical cycles. In order to attain thermal efficiencies greater than ~33%, which is the typical thermal efficiency for modern LWR power plants using a Rankine cycle, advanced systems will use a recuperated helium Brayton system. Thermal efficiencies for the recuperated Brayton cycle as high as 60% can be achieved for a gas-turbine inlet temperatures of ~1250°C. Additional reheat and intercooling stages can allow for the Carnot efficiency to be approached.

Thermochemical cycles for hydrogen production also require high temperatures. For the iodine-sulfur process, temperatures greater than 850°C are required (Brown, et al., 2002; Marshall, 2002).

Current high-temperature reactor designs, including the Pebble Bed Modular Reactor (PBMR) (Nicholls, 2001) and the Gas Turbine Modular High Temperature Reactor (GT-MHR) (LaBar, 2002), are proposed to operate with helium exit temperatures in the range of 850°C to 900°C and 40 to 48 % thermal efficiency using the recuperated Brayton cycle. However, experimental reactors have been operated at significantly higher gas exit temperatures. The Ultra High Temperature Reactor Experiment (UHTREX) was operated at LANL in the late 1960s (Simnad, 1971). The UHTREX operated at 3 MW_{th} and maintained helium coolant exit temperatures of 1300°C for a limited operational time.

A significant amount of research work was performed in the 1970's and 1980's on high-temperature nuclear heat for coal gasification (Frohling and Ballensiefen, 1984; IAEA, 1999). The Prototype Plant for Nuclear Process Heat project (PNP project) was based on high-temperature helium-cooled gas-reactor systems similar to the PBMR. Some of the important results of that work were the advancement of high-temperature super alloys and coatings, the development of a He/He heat exchanger design, and the development of the annular/coaxial hot gas duct for helium transfer to and from the reactor. The PNP project design criterion was to utilize helium gas at 950°C to 1000°C.

The most important issue associated with high-temperature reactor development is undoubtedly the most obvious - the effects on material properties at elevated temperatures in both radiation and non-radiation environments. Structural and boundary material properties, including eutectic formation, corrosion, creep, yield strength, and rupture strength, must be considered in the design. Also the cost of using exotic super alloys and refractory metals and coatings must be considered. For moderating materials, the heat conductivity and strength must be addressed at high temperatures in neutron and gamma-ray environments. For fuel materials, fission product retention and fuel failure, in addition to the other described effects, become very important.

Other important issues associated with high-temperature reactors include decay-heat removal, system operation and maintenance, fuel reloading, reactor control, and coolant boundary integrity at elevated temperatures. Decay-heat removal involves maintaining sufficient heat capacity and passive heat removal to maintain the maximum fuel temperatures as low as achievable, even under the most catastrophic failure of the coolant system boundary. System operation and maintenance involves logistical and engineering design parameter studies, many of which cannot be addressed until a working prototype has been operated. For instance, in the current direct helium Brayton cycle reactor concepts, the plate-out of radioactive silver on turbine components may significantly impair turbine maintenance. Fuel reloading requires that acceptable conditions for handling and storing fuel be developed that are reliable and cost effective. Reactor control involves instrumentation operability and the manipulation of control rods via drive systems under high-temperature and high-pressure conditions. Coolant boundary integrity is important since the presence of oxygen at elevated temperatures would prove catastrophic to the fuel barrier integrity for advanced carbon-based fuels.

In proposing and analyzing advanced next-generation reactor concepts in sufficient detail to determine performance, feasibility and cost, it is recognized that there is not sufficient information in all cases to address every issue rigorously. However, many of the important issues can be addressed sufficiently to allow for a determination of the engineering feasibility of the design and a comparison to the current gas-cooled systems, i.e., the PBMR and the GT-MHR, and to current LWR power plants. Some qualitative estimates can be made for cost comparisons to current designs.

2. DESCRIPTON OF SELECTED REACTOR SYSTEMS

The advanced reactor systems chosen for further study all represent high-temperature systems with coolant outlet temperatures exceeding 1000°C. All of the systems proposed are neutronically thermal or near thermal systems in that they maintain a sufficient amount of moderating materials such that the neutrons are slowed down to the ambient temperature (i.e., the thermal temperature) of the reactor. For a moderated reactor at 1200°C, the average neutron energy would be ~5 times that of a neutron at room temperature, 0.025 eV, but at ~0.12 eV, the spectrum is still considered to be in the thermal-energy region. The reactor systems also all use the same basic type of fuel form. Although new and advanced fuel types could be developed in the future, currently the most viable fuel for high-temperature applications is the Triso-coated particle fuel design (Minato, et al., 2000). Advances in the fuel particle design continue to be made, including the use of different coating materials, to allow for operating temperatures greater than 1250°C.

The three reactor systems chosen for further study represent three different levels of advancement in the current high-temperature reactor technology. The AHTR uses a molten-salt coolant with an exit coolant design temperature of 1000°C and requires primarily incremental improvements in high-temperature materials compatibility. The VHTGR uses a helium-gas coolant with an exit coolant design temperature of 1100°C and requires both fuel and materials development. The UHTGR uses a helium-gas coolant with an exit coolant design temperature of 1200°C to 1300°C and requires additional development of the coated fuel particle, innovative piping configurations, and advanced recuperator heat exchanger materials.

The three reactor systems are described in greater detail below, followed by advantages and disadvantages of each system. Each concept is then analyzed in greater detail with respect to the temperature in the fuel, passive safety, heat exchanger issues, criticality, burnup, and reactivity coefficients. Additional issues and conclusions are also discussed. The following descriptions of the reactor systems summarize the overall design concept of each system.

2.1 Advanced High Temperature Reactor – Molten Salt - 1000 °C

Description: Molten-salt cooled (66% LiF - 34% BeF₂ (Flibe, Li enriched to greater than 99.99% in Li-7), prismatic type graphite moderator, coated particle fuel, passive decay-heat removal. Other salt coolant can be considered (Na, Zr) with relatively minor impact on overall performance characteristics.

Application: H₂ production using secondary salt heat exchanger, potential electrical power generation using salt to helium heat exchanger, and helium Brayton cycle.

Configuration: Pool type, graphite moderated and reflected, axial coolant flow.

Fuel Material: Triso-coated particle fuel – UO₂ kernel, SiC coating, ThO₂ can be included in kernel for conversion to U-233.

Enrichment: 8% to 20% U-235.

Fuel Element Configuration: Fuel compacts in rod or annular form, coolant channel around rod or in annular region, hexagonal graphite moderator region in surrounding media. Configurations designed to minimize temperature drop between fuel and coolant.

Maximum Fuel Temperature: 1250°C operational, 1600°C extended transient.

Fuel Coolant ΔT : For 5 W/cc power density, 1 cm radius flow channel, 10% coolant volume fraction, $k = 0.3$ W/cm-K, ΔT max to surface = 60°C, ΔT surface to bulk coolant = 130°C for 800°C inlet, 1000°C outlet.

Coolant Outlet Temperature: 1000°C core exit.

System Pressure: Near ambient (<50 psi), molten salt (Flibe) boiling point at 50 psi ~ 1400°C, at 15 psi ~1300°C.

Power (size): For a 3 m core radius, 6 m core height - 5 W/cc average power density results in 850 MW_{th}, - 10 W/cc, power level ~ 1700 MW_{th}. Passive cooling with molten salt cooling can be effective above 5 and 10 W/cc.

Estimated Efficiency: ~55% at 1000°C for recuperated Brayton cycle, H₂ production efficiency expected to be greater than 50% for S-I cycle.

Refueling: For 5 W/cc average power density, core lifetime is 4.5 to 6.0 years. Partial core replacement and fuel shuffling every 1.5 to 2 years.

Comments: The AHTR requires essentially no fuel development and only incremental improvements in high-temperature materials compatibility. The molten-salt coolant

provides a high-temperature coolant capability at very low pressures. The molten salt adds a significant amount of heat capacity to the system and, with natural convection flow during shutdown, improved passive safety effectiveness. The molten salt has the added benefit of acting as a getter for fission products that could be released from the fuel. The Flibe salt has a melting point of 460°C that presents new design and operations issues for this type of system. This concept also requires high-temperature, low-pressure pumps which may present design and maintenance issues. The AHTR concept is not limited in power by size constraints, since only a low pressure boundary is required that can be made much larger than that of high-pressure helium or water systems.

The AHTR concept is shown in Figure 1. The molten salt is pumped through the core using mechanical pumps. The inlet salt temperature is 800°C to 900°C and the exit temperature is 1000°C. The flow can be baffled to allow greater flow in the radial regions generating greater power, such that the outlet temperature for all of the flow channels is constant. The molten salt is shown to flow into the pool region outside of the core where the primary/secondary counter flow heat exchanger transfers the heat from the primary to the secondary. The secondary system also uses the Flibe molten salt at low pressure. Due to the high heat transfer coefficient of the molten salt, the exit temperature of the secondary can be assumed to be only tens of degrees less than the core exit temperature. Passive heat removal could occur through the vessel wall or by natural convection through the secondary. The reactor would be controlled by control elements inserted into the core and operated via drive mechanisms above the core. The vessel could be built below grade with a small containment building surrounding it. The secondary piping would be required to be insulated. However, since the secondary, like the primary, is at a low pressure, the piping material strength does not need to be great at the elevated temperatures. Both the primary and secondary systems would have to be insulated and heated to maintain the salt in a liquid state during shutdown and maintenance. Auxiliary power would be required to maintain the salt at temperatures greater than the melting point of 460°C, if the decay power from the reactor was not adequate for this purpose during initial operations and refueling conditions.

Advantages of the AHTR Concept

- **Reduced Containment Building Requirements** – Since there is no volumetric expansion of the coolant if the vessel is depressurized, containment-building requirements could be significantly reduced.
- **Low Pressure Vessel** – Compared to LWRs and to helium-cooled reactors, the pressure vessel is not required to function at elevated pressures. An inner liner and insulating material will be required within the vessel to maintain the vessel temperature to within design limits. However, the vessel itself will not experience significant elevated temperatures or stresses.

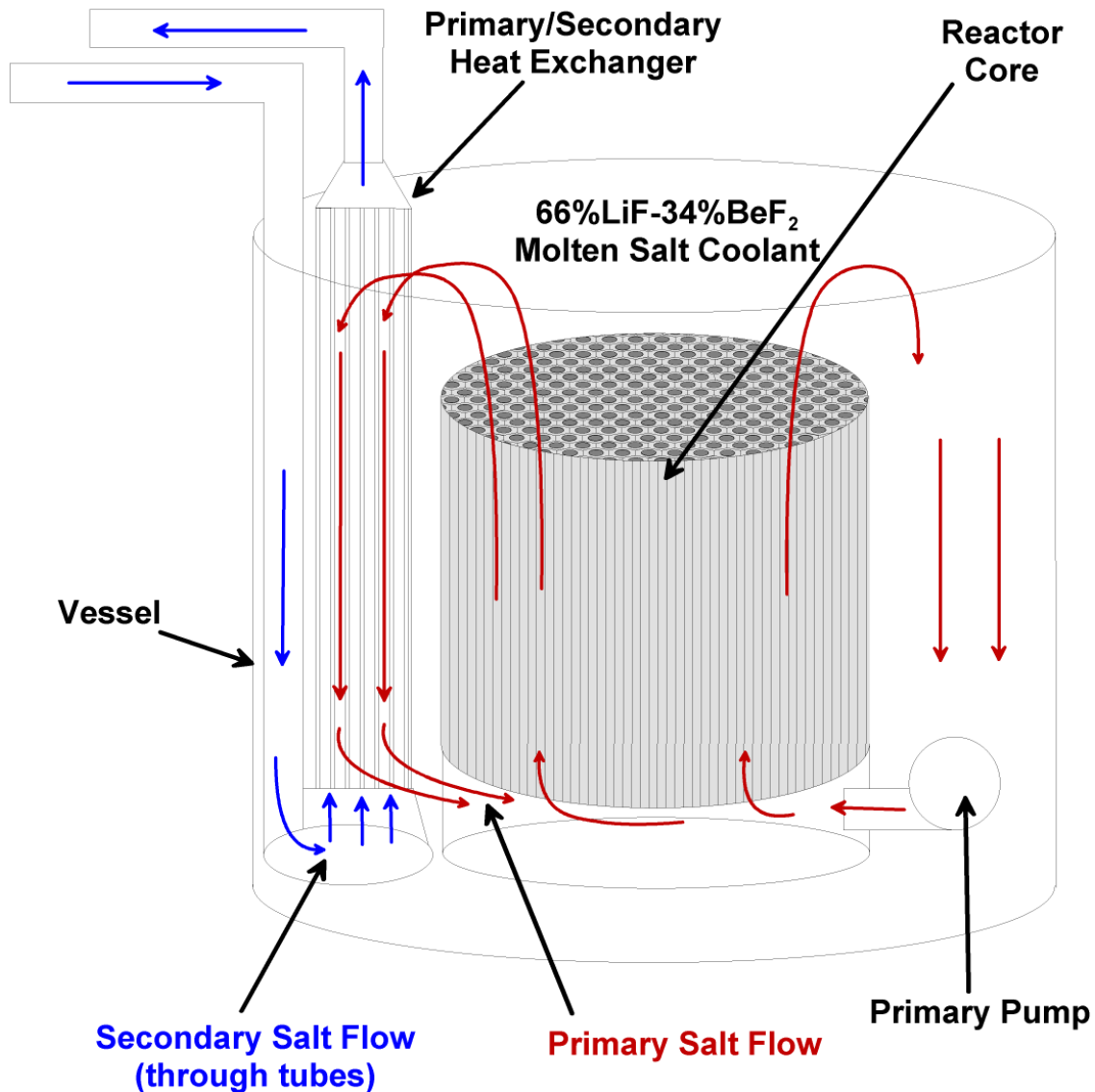


Figure 1. The AHTR – Molten Salt Reactor Concept.

- **Piping** – Compared to helium-cooled reactors, the piping that transfers the coolant outside of the reactor vessel does not operate at high pressures. The piping is required to be insulated internally in order to maintain the boundary at a low temperature. Lined, coated or more exotic alloys could be used for the piping and insulated externally.
- **Primary/Secondary Leakage** – Coolant leakage into the secondary from the primary is not an issue since the secondary can be operated at a slightly higher pressure resulting in flow from the secondary into the primary. Multiple redundant heat exchangers can allow for the shutdown and replacement or repair of a heat exchanger unit.

- **Fission Product Retention and Cleanup** - Fission products that escape from the fuel will be trapped within the salt. The Flibe salt should act efficiently as a getter material chemically trapping all but the noble gaseous fission products. The primary coolant can be processed through an auxiliary system that removes the fission products from the salt.
- **Passive Safety** – The AHTR has more thermal mass and heat transfer capability than helium cooled high-temperature reactor concepts due to the molten-salt coolant. The salt not only adds a significant amount of heat capacity to the system, but natural convective cooling can be used to cool the primary coolant by the secondary system.
- **Instrumentation and Control** – The in-core instrumentation and control rod drive mechanisms pass through a low-pressure boundary that, if breached, does not lead to a catastrophic depressurization of the system.
- **Neutron Generation Time** – The neutron generation time for this concept is on the order of 1 ms, which implies that the response of the reactor to positive reactivity transients is very slow. An addition of \$1 of reactivity at critical would place the reactor on approximately a one second period.

Disadvantages of the AHTR Concept

- **Corrosive Characteristics of the Molten Salt** – Molten salts at elevated temperature can be corrosive. All materials that are in contact or could come in contact with the molten salt must be compatible and corrosion-resistant at highly elevated temperatures. This includes fuel element assemblies, in-vessel structural materials, safety and control rods, pumps and seals. On the positive side, there exists a large amount of information in the area of material compatibility and corrosion rate with molten salts at elevated temperatures. Flibe used in the Molten Salt Reactor Experiment (MSRE) in the 1960s and operated at a temperature of $\sim 700^{\circ}\text{C}$. It has since been rigorously studied in the U.S. and Russia in MSR designs, and in controlled nuclear fusion hybrid concepts as a blanket material.
- **Salt to Helium Heat Exchanger** – Although heat transfer from the molten-salt primary to a molten-salt secondary is straightforward and efficient, heat transfer from the secondary side molten salt to a helium coolant for use in the Brayton cycle will be difficult at these extremely high temperatures. The helium coolant must be pressurized to ~ 1000 psi in order to be useful in the Brayton cycle, and therefore heat exchanger design and fabrication is a significant challenge. Innovative engineering concepts are needed to address the high temperature heat exchange issue.
- **Melt Temperature of Salt** – The melt temperature of Flibe is 460°C . Although not fully explored, it is assumed to be undesirable to allow the salt coolant to freeze within the reactor vessel, the reactor coolant channels, or within the secondary. Hence, the salt coolant must always be maintained above 460°C by using auxiliary heat mechanisms or by reducing the amount of decay-heat removal from the system under shutdown

conditions. This not only will have an effect on the engineering design, but also on the operation and maintenance of systems where the molten salt is present. Refueling of the core will also be an issue, since it will have to be performed remotely due to the extreme environmental conditions. The heat of fusion for Flibe is ~ 440 J/g, which is similar to water.

- **Control Elements in Core** – The AHTR concept will require reactor control elements to be located within the high-temperature region of the reactor core. The design does not lend itself to having cooler regions unless the concept was modularized such that a number of smaller regions were maintained within separate vessels, with the control elements located between the vessels.
- **Compact Fuel Form** – Although not specifically a disadvantage, the AHTR concept does not lend itself to using pebble-bed type fuel as opposed to the compact form, at least not in a pool type configuration. The density of a pebble in the proposed PBMR is ~ 1.9 g/cc. The density of molten Flibe at 700°C is 2.05 g/cc. Hence, the pebbles would tend to have slight buoyancy, especially within an environment where the flow will in the upward direction. For conventional compact rod configurations, more traditional retention mechanisms can be designed into the upper grid plate structure.
- **Fuel Cost** – Although it is difficult to assess the true fuel fabrication cost for the particle fuel/compact form, it is expected to be greater than the fuel costs for LWRs. However, since the fuel costs for LWRs are low compared to the capital cost, a high fuel cost could still allow for the overall plant cost to be significantly lower.

Conclusions

The AHTR concept is a high-temperature reactor system that could be developed in the near term, with no advanced fuel development beyond that which has been tested and used previously. Only incremental improvements in high-temperature materials are required. This concept lends itself most readily to applications that require process heat at $\sim 1000^\circ\text{C}$ or less at relatively low pressures – such as required for large-scale thermochemical hydrogen production. Using the concept for electrical power generation will require additional heat exchanger design.

2.2 Very High Temperature Gas Cooled Reactor - He - 1100°C

Description: Helium-gas cooled, prismatic type graphite moderator, coated particle fuel, passive decay-heat removal.

Application: Direct recuperated Brayton cycle electric, H₂ production using helium-to-helium heat exchanger.

Configuration: Loop type, graphite moderated and reflected, axial coolant flow.

Fuel Material: Triso-coated particle fuel – UO₂ kernel, ZrC coating, ThO₂ can be included in kernel for conversion to U-233.

Enrichment: 8% to 20% U-235.

Fuel Element Configuration: Fuel compacts in rod or annular form, coolant channel around rod or in annular region, hexagonal graphite moderator region in surrounding media.

Maximum Fuel Temperature: 1400°C operational, 1600°C -1800°C extended transient.

Fuel Coolant ΔT : For 5 W/cc power density, 1 cm radius flow channel, 10% coolant volume fraction, $k = 0.3$ W/cm-K, ΔT max to surface = 60°C, ΔT surface to bulk coolant = 100°C for 700°C inlet, 1100°C outlet.

Coolant Outlet Temperature: 1100°C core exit.

System Pressure: 1000 psi

Power (size): 850 MW_{th} at 5 W/cc average power density, 3 m core radius, 6 m core height. Passive cooling limited to ~5 W/cc.

Estimated Efficiency: ~57% at 1100°C for recuperated Brayton cycle, H₂ production efficiency expected to be greater than 50%.

Refueling: For 5 W/cc average power density, core lifetime is 4.5 to 6.0 years. Partial core replacement and fuel shuffling every 1.5 to 2 years.

Comments: The VHTGR concept is very similar to the GT-MHR design concept. The VHTGR includes an advanced fuel design, an advanced fuel element concept, and would operate at a significantly higher exit temperature. The VHTGR requires fuel and materials development, but is limited in power density by the vessel decay-heat removal. This concept represents an advanced, next generation GT-MHR.

The VHTGR concept is shown in Figure 2. The concept shows the He coolant return entering the center region of the core and then flowing upward through the prismatic-type fuel coolant channels. However, the concept could allow for the inlet flow along the outer region of the reactor. Flow through the inner portion allows for additional heat capacity to be utilized during shutdown, no-flow conditions. The inlet coolant temperature is nominally chosen as 800°C. The exit temperature is 1100°C. The flow can be baffled to allow greater flow in the radial regions generating greater power such that the outlet temperature for all of the flow channels is constant. At this temperature and pressure, a coaxial gas transfer duct will be required with the hot gas piping internal to the outer cold gas. The primary gas would be transferred directly to the turbine for power generation. For H₂ production, a He/He heat exchanger would be used to transfer the heat to a secondary system. Passive heat removal would occur through the reactor vessel wall. The reactor would be controlled by control elements inserted into the core and operated via drive mechanisms above the core. Since the primary is at a high pressure, insulating materials are required around the core region and within the pressure vessel to maintain the vessel at a low temperature during operation.

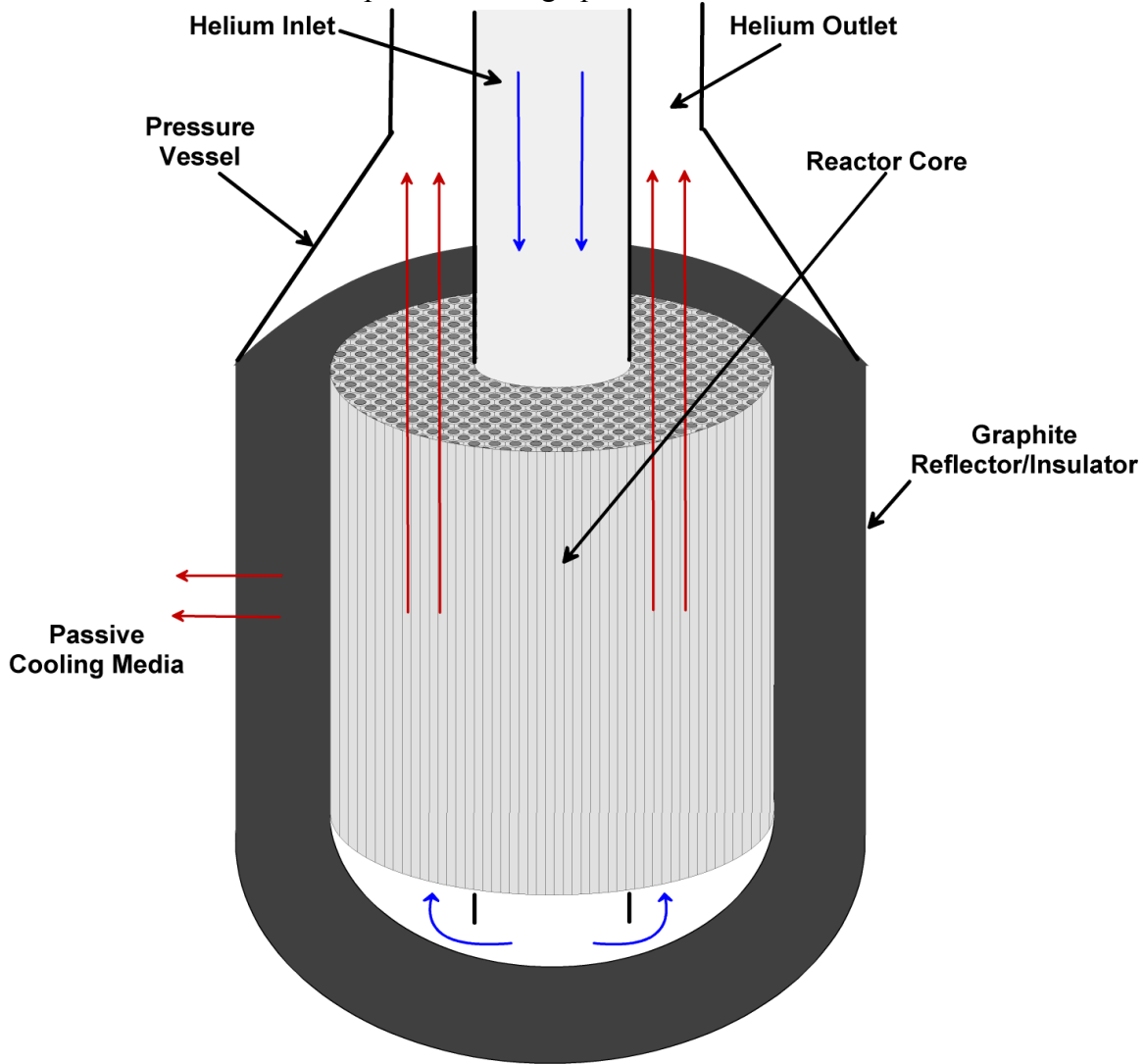


Figure 2. The VHTGR – Helium Gas Cooled Reactor Concept.

Advantages of the VHTGR Concept

- **Minimal Containment Building** – Compared to LWRs, the containment building is not required to be a massive structure since there is only single phase volumetric expansion of the coolant if the vessel is depressurized.
- **Non-Corrosive Coolant** – The helium-gas coolant is inert.
- **Low Temperature Helium During Shutdown** – Compared to the AHTR, most of the reactor systems will be at a low temperature during shutdown and maintenance.
- **Compact Fuel Form** – If the compact fuel form is prismatic with internal cooling channels, the reactor will have better passive cooling capabilities, as compared to a pebble fuel, since the prismatic forms will provide a conductive thermal path to the moderator matrix.
- **Passive Safety** – The VHTGR is designed to be passively safe, with decay-heat removal by conduction through the fuel, moderator, reflector, and pressure vessel to an outside atmosphere. The concept would not be as efficient as the AHTR with the molten-salt nature convection loop. The VHTGR would also be limited in power density and in size due to the heat transfer limitations of the core and the maximum fuel temperature.
- **Direct Brayton Cycle** – The direct recuperated Brayton cycle allows for a direct and highly efficient power conversion to electrical power.
- **Neutron Generation Time** – The neutron generation time for this concept is on the order of 1 ms, which implies that the response of the reactor to positive reactivity transients is very slow.

Disadvantages of the VHTGR Concept

- **Pressure Vessel** – The pressure vessel must operate at a pressure of 1000 psi. An inner liner and insulating material will be required to be within the vessel to maintain the vessel temperature at a low value.
- **Piping** – The piping that transfers the coolant outside of the reactor vessel must be rigorously designed with coaxial tubing since the coolant is at a high pressure and temperature. The piping will be required to have the hot gas transferred using the internal piping and the cold gas transferred within the annular region between the internal and external piping.
- **Fission Products in Primary** – Since a direct Brayton cycle is used for power production, fission products that escape the fuel will be plated on the cold surfaces of the turbine, compressor, and recuperator, and may cause significant maintenance problems.

- **Helium to Helium Heat Exchanger** – For H₂ production, a secondary helium loop will be required to isolate the chemical plant from the primary coolant. A He/He heat exchanger will be required which may be large and will be less efficient as compared to liquid coolants.
- **Compact Fuel Form** – Although the compact fuel form allows for better heat transfer to the vessel wall during shutdown conditions, the compact fuel form is less efficient at transferring heat to the coolant under normal operation, as compared to pebble fuel. The compact fuel also does not lend itself to online refueling, as does the pebble fuel.
- **Instrumentation and Control** – The in-core instrumentation and control rod drive mechanisms pass through a high-pressure boundary.
- **Control Elements in Core** – The VHTGR concept will require reactor control elements to be located within the high-temperature region of the reactor core. The design may allow for the control elements to be placed in the reflector region, which will be cooler. Since the compact fuel form does not allow for online refueling, a fresh core load will be required to be poisoned by control elements.
- **Fuel Cost** – Although it is difficult to assess the true fuel fabrication cost for the particle fuel/compact form, it is expected to be greater than the fuel costs for LWRs. However, since the fuel costs for LWRs are low compared to the capital cost, a high fuel cost could still allow for the overall plant cost to be significantly lower.

Conclusions

The VHTGR concept requires high-temperature fuel and materials development which although will require significant advances, are considered achievable in the timeframe of Gen IV. This concept lends itself most readily to the direct recuperated Brayton cycle for power production. Process heat applications, such as required for large-scale thermochemical hydrogen production, are also viable using a secondary loop and a He/He heat exchanger design.

2.3 Ultra High Temperature Gas Cooled Reactor - He - 1200 °C

Description: Helium-gas cooled, pebble fuel, coated particle fuel, modular design, passive decay-heat removal.

Application: Direct recuperated Brayton cycle electric, H₂ production using helium to helium heat exchanger.

Configuration: Multiple loop type, graphite moderated and reflected, axial coolant flow.

Fuel Material: Triso-coated particle fuel – UO₂ kernel, ZrC or multiple SiC or advanced coatings, ThO₂ can be included in kernel for conversion to U-233.

Enrichment: 8% to 20% U-235.

Fuel Element Configuration: Fuel particles in graphite pebble (spherical) form, graphite moderator regions in surrounding media.

Maximum Fuel Temperature: 1500°C operational, 1800°C extended transient.

Fuel Coolant ΔT : For 5 W/cc power density, 3 cm radius pebble, 40% coolant volume fraction, $k = 0.3$ W/cm-K, ΔT max to surface = 42°C, ΔT surface to bulk coolant 25°C. For 25 W/cc, ΔT max to surface = 208°C, ΔT surface to bulk coolant 36°C

Coolant Outlet Temperature: 1200°C - 1300°C core exit.

System Pressure: 1000 psi

Power (size): 1000 MW_{th} at 25 W/cc average power density, 18 modules in triangular pitch, module size ~0.5 m radius, 4 m core height. Passive cooling limited to ~35 W/cc.

Estimated Efficiency: ~60% at 1200°C for recuperated Brayton cycle, H₂ production efficiency expected to be greater than 50%.

Refueling: For 25 W/cc average power density, core lifetime is 3.0 years. Partial core replacement and fuel shuffling every 1.0 years.

Comments: The UHTGR is an advanced design concept using advanced pebble fuel and a unique modular arrangement of smaller diameter pressure vessels, which allows for greater decay-heat removal. The UHTGR fuel particle requires additional development of multiple coatings (ZrC, SiC, or NbC), innovative fuel and pipe ducting for temperatures greater than 1200°C, and advanced recuperator heat exchanger materials. The pebble fuel form reduces the maximum-to-surface fuel temperature, and the smaller vessels allow for improved decay-heat removal at the vessel boundary.

The UHTGR concept is shown in Figures 3 and 4. The concept is based on higher temperature fuels, pebble fuel, and modular geometry. Figure 3 shows the concept for a single module. The module diameter is ~1 m, and cannot be made critical standalone. The helium coolant return enters the center region of the module and then flows upward through the pebble bed coolant channels. However, the concept could allow for the inlet flow along the outer region of the module. Flow through the inner portion allows for additional heat capacity to be utilized during shutdown, no-flow conditions. The inlet coolant temperature is nominally chosen as 800°C. The exit temperature is 1200°C to 1300°C. At this temperature and pressure, a coaxial gas transfer duct will be required, with the hot gas piping internal to the outer cold gas. The primary gas would be transferred directly to the turbine for power generation. For H₂ production, a He/He heat exchanger would be used to transfer the heat to a secondary system. Passive heat removal would be through the module vessel wall. Since the primary is at a high pressure, insulating materials are required around the fueled region of the module and within the pressure vessel to maintain the pressure vessel wall at relatively low temperatures during operation. The insulating material proposed is 1 mm diameter graphite particles. This region would be separated from the core region with a graphite liner. The insulating particle bed allows some heat loss through the bed and the pressure vessel to the passive coolant media during normal operation. Under shutdown conditions without helium coolant flow through the fuel bed, the heat losses are adequate to allow for the maximum temperatures in the core to be within acceptable limits. The design trade-offs for the modules include the power density, fuel region dimensions, insulating particle size, insulating region dimensions, limitations on the maximum fuel temperature, and the maximum allowable pressure vessel temperature.

Figure 4 shows the module configuration for the complete system. The modules are arranged in an unpressurized vessel that would hold the moderator and the passive coolant media. The passive coolant could be an inert gas, air, or heavy water. The passive coolant would be maintained at a relatively low temperature, and would use natural convection flow under passive cooling conditions. Additional moderating materials would be required within the region between the modules in order to maximize the neutron utilization. The possible configurations include graphite with passive coolant channels next to the modular pressure vessels, or heavy water, which would act as both a moderator and passive coolant. Light water is not acceptable due to the larger neutron cross section for hydrogen versus deuterium. The reactor would be controlled by control elements inserted into the unpressurized region and operated via drive mechanisms above the core. This arrangement allows for much high power densities to be achieved (~25 W/cc), as compared to current GT-MHT and PBMR designs as well as the VHTGR concept.

Advantages of the UHTGR Concept

- **Minimal Containment Building** – Compared to LWRs, the containment building is not required to be a massive structure since there is only single phase volumetric expansion of the coolant if the vessel is depressurized.
- **Non-Corrosive Coolant** – The helium-gas coolant is inert.

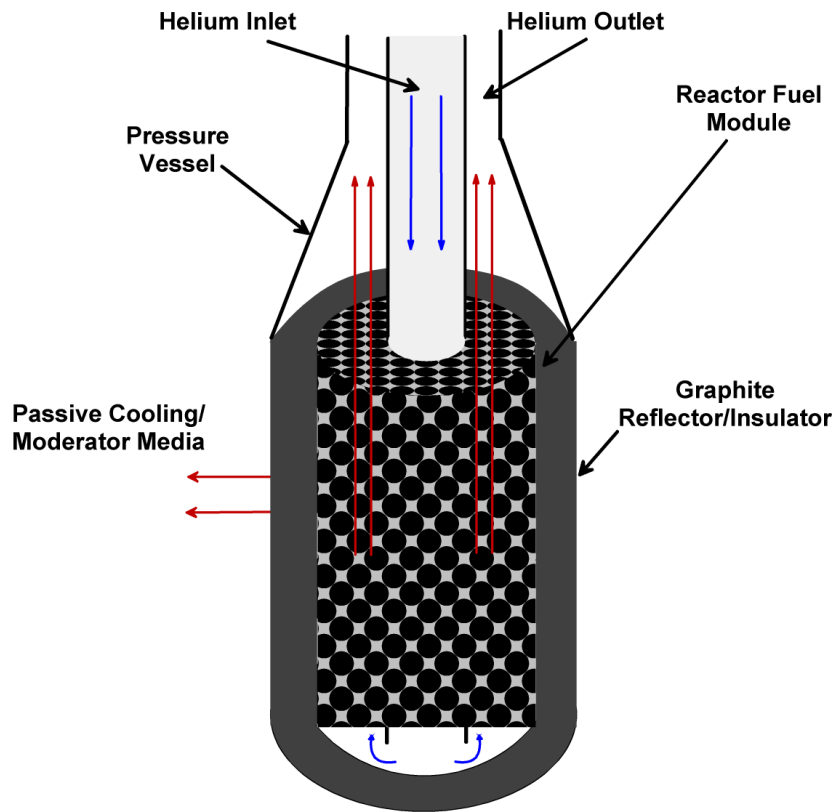


Figure 3. The UHTGR Module Concept – Helium Gas Cooled.

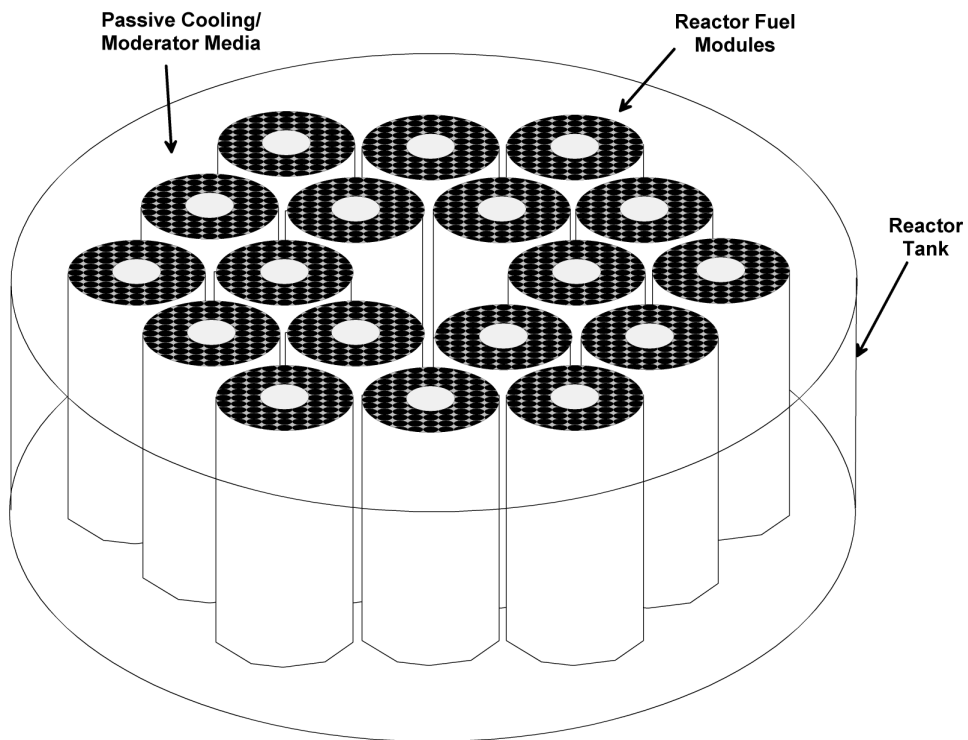


Figure 4. The UHTGR concept – 18 Module Configuration.

- **Low Temperature Helium During Shutdown** – Most of the reactor systems will be at a low temperature during shutdown and maintenance.
- **Pebble Fuel Form** – The pebble fuel form allows for a lower temperature differential between the center of the pebble and the surface, as compared to prismatic forms. The pebble fuel form adds the potential for online refueling.
- **Passive Safety** – The UHTGR is designed to be passively safe, with decay-heat removal by conduction through the fuel, moderator, reflector, and pressure vessel to an outside coolant/moderator. The concept is significantly more efficient at removing decay heat as compared to other pebble bed designs due to the smaller dimension of the module. Hence, the UHTGR can maintain a significantly larger power density under operating conditions and remain passively safe during shutdown.
- **Low Pressure/Low Temperature Moderating Region** – The low pressure and low temperature moderating/passive cooling region surrounding the modules allows for instrumentation and control rods to be easily designed into the system. Since the control rods can easily be moved into and out of this region, the reactor core can maintain a significant reactivity excess for fresh fuel reloading.
- **Direct Brayton Cycle** – The direct recuperated Brayton cycle allows for a direct and highly efficient power conversion to electrical power.
- **Neutron Generation Time** – The neutron generation time for this concept is on the order of 1 ms, which implies that the response of the reactor to positive reactivity transients is very slow.
- **Power Level** – The high power density that can be achieved by the modular design allows the power density to be comparable to a current typical LWR. If an efficiency of 60% could be achieved for a reactor power level of 1000 MW_{th}, the electrical power produced would be 600 MW. Higher power densities to 50 W/cc could be achieved by using radial flow and smaller diameter pebbles. At 50 W/cc, the electrical power generated would be 1200 MW. The rejected power would be 800 MW, which is less than a factor of two than that of a typical LWR (~2000 MW rejected power).

Disadvantages of the UHTGR Concept

- **High Temperature Fuel Coatings** – In order to achieve a coolant exit temperature of 1200°C to 1300°C, a fuel development effort would be required to develop multiple layered fuel particles with ZrC, SiC, and/or NbC.
- **Pressure Vessel** – The pressure vessel surrounding each module operates at a pressure of 1000 psi. An inner liner and insulating material will be required to be within the vessel to maintain the vessel temperature at a low value. The pressure vessel for each module will be required to be fabricated from a metal or alloy with a low thermal neutron

absorption cross section, such as Zircalloy. However, the required thickness of the vessel is less than for the VHTGR since the diameter of a module is only ~1 m.

- **Piping** – The piping that transfers the coolant outside of the reactor vessel must be rigorously designed with coaxial tubing since the coolant is at a high pressure and temperature. The piping will be required to have the hot gas transferred using the internal piping and the cold gas transferred between the internal and external piping.
- **Fission Products in Primary** – Since a direct Brayton cycle is used for power production, fission products that escape the fuel will be plated on the cold surfaces of the turbine, compressor, and recuperator, and may cause significant maintenance problems.
- **Helium to Helium Heat Exchanger** – For H₂ production, a secondary helium loop will be required to isolate the chemical plant from the primary coolant. A He/He heat exchanger will be required, which may be large and will be less efficient as compared to the AHTR.
- **Coolant Leakage** – The primary and secondary systems will be required to operate at 1000 psi - requiring rigorous design, fabrication, and leak testing requirements to be imposed on the system.
- **Fuel Cost** – The fuel particle for UHTGR would be more costly to produce than current Triso-coated particles. The cost /benefit analysis of increased efficiency vs more costly fuel and system components must be addressed. Since the fuel costs for nuclear systems low compared to the capital cost, a high fuel cost could still allow for the overall plant cost to be significantly lower.

Conclusions

The UHTGR seeks to identify an approach for extreme high temperatures, should the benefits of such a system be determined to be necessary. The ultra-high-temperature reactor system would require advances in the coated particle fuel, transfer piping, and high-temperature alloys. Greater efficiencies could be achieved using the recuperated Brayton cycle for power production. The modular design would allow for a larger decay-heat removal capability and hence the potential for a significantly greater power density. Process heat applications, such as required for large-scale thermochemical hydrogen production, are also viable using a secondary loop and a He/He heat exchanger design.

3. FUEL PARTICLE

The very high efficiency concepts examined in this study all depend on coated particle fuel technology to achieve high temperatures with acceptable fission-product retention characteristics. The coated particle fuel approach provides advantages in achieving these goals due to the inherent relative strength of the small container (i.e. the sub-millimeter multicoated particles) in confining fission products resulting from the nuclear reaction. Coated particle fuels have been demonstrated extensively in numerous gas-cooled reactors and test programs. Current particle fuel capabilities are impressive, up to 1250°C for long term operation. The challenge for the VHTGR and UHTGR concepts being considered in this study is to extend this basic proven design to a higher temperature regime by consideration of new materials and configurations.

Coated Particle Fuel Description

Current particle fuel design consists of a fissionable kernel (UC_2 , UCO , UO_2 , other) surrounded by a porous buffer layer of pyrolytic carbon (PyC) to allow for retention of gaseous fission products without excessive pressure build up. This porous PyC layer is surrounded by a non-porous layer of PyC to provide chemical separation of the kernel from the next layer, SiC. The SiC layer provides strength and ultimate fission-fragment retention. A final layer of non-porous PyC is added to keep the SiC in compression and to protect it during handling and fabrication of the final fuel elements. Figure 5 shows the configuration of the Triso-coated particle

High Temperature Options

Current coated particle fuel limitations arise from the temperature limitations of the SiC coating which cannot operate at the temperatures greater than $\sim 1700^\circ C$ for prolonged time periods (Nabielek, et al., 1989; Goodin, 1982; Naoumidis, et al., 1982). Alternative coatings for SiC, such as ZrC, or other carbides such as NbC, need to be developed that extend the temperature range up to $1500^\circ C$. The main barrier for fission product release from fuel particles is the SiC layer. Except for silver, all metallic and gaseous fission products are effectively retained by this barrier. The long term operating temperature for the SiC coating is $1250-1300^\circ C$ with short-term excursions to $1500-1600^\circ C$ having been demonstrated (Ogawa, et al., 1992; IAEA, 1997; Ogawa, et al., 1991)

Zirconium carbide (ZrC) has a melting point of $3540^\circ C$ and melts eutectically with carbon at $2850^\circ C$ (Ogawa, et al., 1985). This temperature is significantly above the acceptable operating point of SiC. Thus ZrC is a prime candidate as a coating material for the higher temperature VHER. ZrC coated particles have shown excellent performance in irradiation tests, even retaining silver and showing higher resistance to chemical attack by palladium (Minato, et al., 2000; Ogawa, et al., 1982). Although higher temperature testing will be required, these test do show the feasibility of ZrC coated fuel.

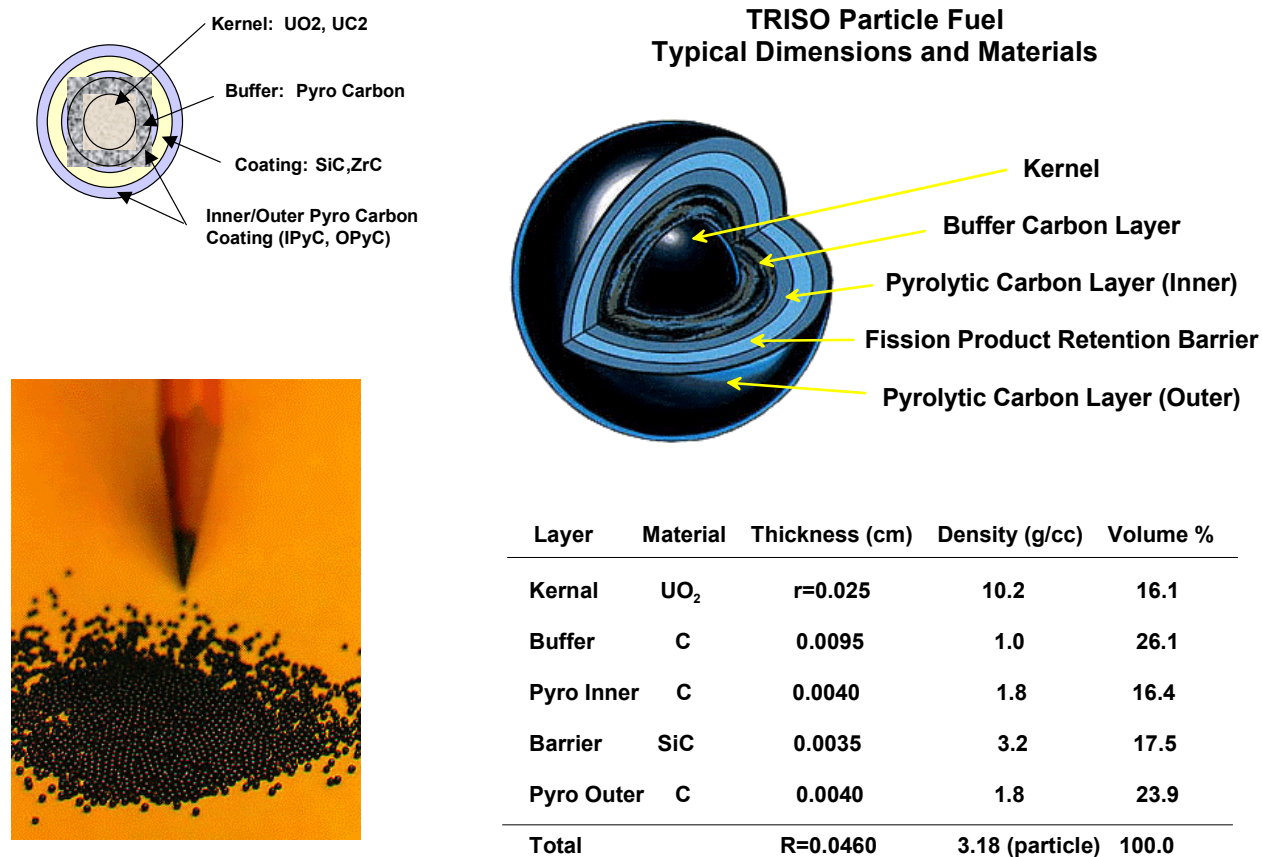


Figure 5. Typical Triso-Coated Particle Fuel Composition, Dimensions, and Density.

Other alternative materials to achieve very high temperatures such as oxide, nitride, or other high temperature coated particle systems have been considered as longer term options. Materials such as BeO, ZrO, or other refractory materials may be considered as a candidate barrier coating. UCZrC or nitrides are other possible options for a kernel suitable for high temperature applications. The traditional buffer is pyrocarbon, but an alternative is BeO. Alternative external coatings might include BeO, ZrO, Nb, ZrBe₁₃, or other refractory materials. These particles could be placed in graphite, oxide or other matrix material. Clearly development times and costs for these fuel types would require significant motivation from a cost / benefit perspective.

Fuel Modeling

In order to assess the potential to extend the operating fuel temperature limits of carbide coated fuel, or to assess the potential for new materials, new fuel modeling capabilities that adequately treat the failure process for high-temperature fuel systems have to be developed, extending models that have been used for present-day gas-reactor fuel systems.

Since the IPyC/SiC/OPyC layer combination acts as the primary structural element in the particle as well as the fission product and pressure barrier, the overall integrity of the fuel system is controlled by the soundness of the IPyC/SiC/OPyC layer, in particular, the SiC layer. Fission products can be released by diffusion through the SiC layer or as a result of the fracture of the SiC layer. While most fission products are retained in the current fuel to temperatures approaching 1600°C, several noble elements, Ag and Pd in particular, are either released (Ag) or chemically react (Pd) with the SiC layer at lower temperatures. As a practical matter, the upper temperature limit for coated particle fuel is dictated by the transport and release of fission products through the SiC layer, assuming that layer fracture does not occur.

During reactor operation, the pyrocarbon layers on either side of the SiC layer undergo swelling (either positive or negative) and creep. As a result, severe internal stresses develop, far exceeding stresses due to internal gas production build-up in the layers. Eventually one or both of the layers will develop cracks. Cracks in the pyrocarbon layers result in failure of the SiC layer with the release of fission products to the primary system. The goal of any fuel design is to prevent or minimize particle failures. However, the problem is very complex, with both mechanical and chemical phenomena playing dominant roles. Moreover, the properties of the individual pyrocarbon layers are anisotropic, and will further change with exposure to the environment. Improved fuel behavior models must be developed to model the mechanical failure of the barrier layers.

4. FUEL ELEMENT

All of the VHER concepts proposed in this report use the carbide fuel particle interspersed within a graphite matrix. The AHTR and VHTGR concepts use a compact fuel form in a prismatic configuration, similar to that proposed for the GT-MHR. The UHTGR concept uses a fuel pebble design similar to the PBMR. Details of the fuel loading, potential fuel element concepts, and maximum fuel temperature are discussed and analyzed for each fuel element design.

4.1 Fuel Loading

The particle fuel form represents the most advanced high-temperature fuel available today, and will most likely continue to lead in technological advances. However, the VHER concepts are not uniquely dependent on the fuel type. As other advanced high-temperature fuels are developed, such as UN fuel developed as part of the SP-100 program, they may also be considered in the proposed VHER concepts. As discussed in the previous section, advances in high-temperature particle fuels will probably be made through advances in particle coating techniques and materials. Use of multiple coatings and coatings of advanced materials may allow for fission product retention at temperatures greater than 1250°C. Advanced fuel concepts are expected to allow for maximum fuel operating temperatures greater than 1500°C.

Particle fuel has been used extensively in thermal gas-cooled reactor designs and proposals. Both pebble bed type reactors and prismatic fueled reactors have been operated using particle fuel embedded within a graphite matrix. The AVR in Germany and Fort St. Vrain reactor in the U.S. demonstrated the effectiveness of particle fuel in pebble and prismatic form, respectively, for power generation (Simnad, 1971). More recently, Japan has begun operation of a 10 MW pebble bed reactor for testing and demonstration purposes (Tang, et al., 2002). Proposed PBMR (Nicholls, 2001), MHTGR (Turner, et al., 1988), and GT-MHR (LaBar, 2002) concepts utilize particle fuel in a pebble and compact graphite matrix forms. The use of thorium has also been proposed in particle fuel to generate U-233, which can be burned in situ or reprocessed.

One problem in using particle fuel in a graphite matrix is maintaining a large enough uranium density within the reactor to allow for high burnup efficiency. A typical LWR (Duderstadt and Hamilton, 1976) operates with a fuel loading of ~ 1.8 g (uranium)/cm³ averaged over the total core volume (fuel + clad + moderator). For a 3% U-235 enriched cycle, the U-235 loading is ~ 0.054 g (U-235)/cm³. The burnup for a typical LWR is $\sim 33,000$ MW-d/metric ton of uranium (MT-U), 1,100,000 MW-d/MT-U-235, or 60,000 MW-d/m³ of total core volume (fuel + clad + moderator). In order to achieve burnup values within this same range, a VHER concept must have a similar fuel density, particularly for the U-235.

Typical particle fuel and pebble fuel composition and elemental densities are shown in Table 1. A typical fuel pebble is illustrated in Figure 6. A typical fuel pebble has a uranium density of ~ 0.08 g/cm³ for a particle-packing fraction of 0.055. This equates to a fuel loading per pebble of ~ 9 g of uranium (Nicholls, 2001). For a pebble bed reactor, the pebbles would be arranged in a close-packed configuration and maintain a loading fraction of ~ 0.6 . At this pebble loading

fraction, the uranium density in the core is $\sim 0.048 \text{ g/cm}^3$. This loading density is ~ 37 times less than that for an LWR. Assuming an 8% U-235 enrichment for the PBMR, the U-235 density is $\sim 0.0038 \text{ g/cm}^3$, which is ~ 14 times less than the U-235 loading density for an LWR.

Table 1. Typical Particle Fuel and Pebble Fuel Elemental Composition.

Element	Particle Fuel (g/cm^3)	Pebble Bed Reactor Fuel (g/cm^3 -pebble) Packing Fraction = 0.055 U loading = 9 g/pebble	Pebble Bed Reactor Fuel (g/cm^3 -pebble) Packing Fraction = 0.22 U loading = 36 g/pebble
U	1.44	0.080	0.320
O	0.20	0.011	0.044
C	1.15	1.76	1.66
Si	0.39	0.022	0.088
U/C	1.25	0.045	0.19

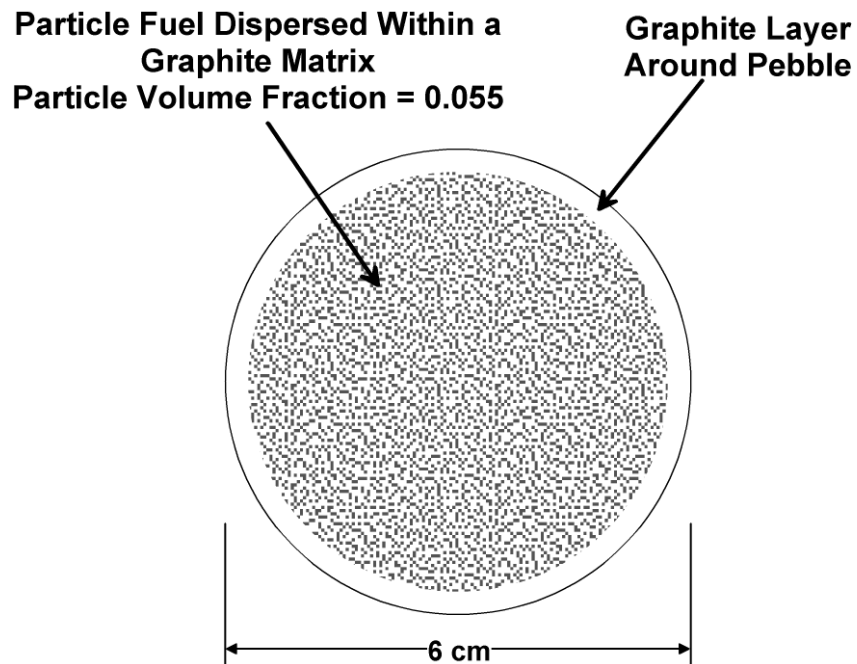


Figure 6. Illustration of a PBMR Fuel Pebble.

Assuming that the particle fuel dimensions are fixed due to the required coating thickness, the only mechanism for substantially increasing the core uranium loading is increasing the packing fraction of the particles within the matrix. Some references (Teuchert, et al., 1978; Teuchert and Maly, 1975) indicate that a packing fraction of ~4 times the loading of the standard pebble, or higher, is achievable, which corresponds to a particle packing fraction of 0.22 or greater. At this packing fraction, the uranium density in the core is ~0.19 g/cm³. This value is approximately a factor of 10 less than that of a typical LWR. For 8% U-235 enrichment, the U-235 density is ~0.015 g/cm³ for the core. This value is 3.6 times lower than that of an LWR. The U-235 loading could be further increased by increasing the enrichment from 8% to 20%, which is a factor of 2.5.

The UHTGR would use a fuel pebble with a fuel loading similar to that described above and shown in Table 2. It will be assumed that, for this concept, the particle packing fraction could be as high as 0.22. The criticality and burnup calculations will use these values with 10% and 20% U-235 enrichment to determine the required core size and burnup history. Silicon (Si) in the form of SiC will be used in the neutronics analysis for the particle coating. It is assumed that other coating materials would have similar neutronic properties as Si.

Table 2. Fuel Loading Density for the UHTGR.

Element	UHTGR Pebble Bed Fuel (g/cm ³ -core) Packing Fraction = 0.055	UHTGR Pebble Bed Fuel (g/cm ³ -core) Packing Fraction = 0.22
U	0.048	0.192
O	0.0066	0.026
C	1.06	0.996
Si	0.013	0.053
U/C	0.045	0.19

The prismatic compact fuel form proposed for the AHTR and VHTGR has the advantage over the pebble bed, in that the coolant volume fraction can be varied depending on the configuration and coolant channel size. For the pebble bed, the coolant volume fraction is fixed at ~40% due to the packing arrangement of the spheres and cannot be changed. For the prismatic form, the loading density for the core is a function of the fuel density, the coolant volume fraction and the volume fraction for other moderating and structural materials. The maximum possible fuel loading density for the prismatic fuel, assuming a 0.055 and 0.22 fuel particle packing fraction, is shown in Table 3. These results assume no cooling channel or other moderating materials. If 10% of the reactor volume was coolant, the fuel loading density would be scaled by 0.9.

Table 3. Maximum Fuel Loading Density for the AHTR and VHTGR.

Element	Prismatic Reactor Fuel (g/cm ³ -max) Packing Fraction = 0.055	Prismatic Reactor Fuel (g/cm ³ -max) Packing Fraction = 0.22
U	0.080	0.320
O	0.011	0.044
C	1.76	1.66
Si	0.022	0.088
U/C	0.045	0.19

4.2 Configuration

The fuel element configuration for the UHTGR concept is a simple pebble bed arranged within the fuel region of each module. The fuel pebble was described in the previous section. The only possible variable for the fuel pebble design, other than the particle loading, is the radius of the pebble. For the PBMR concept, the pebble radius is 3 cm, which is approximately the size of a billiard ball. Changing the size of the pebble, with all of the pebbles identical, does nothing to change the packing fraction of the bed. For a pebble bed core with all of the pebbles the same size, the packing fraction is ~0.6. Changing the size of the pebble will change the thermal and thermal hydraulic parameters. A smaller fuel pebble will allow for a larger surface area per unit volume and a lower centerline fuel temperature for the pebble, for a constant power density. The thermal hydraulic parameters for a pebble are more difficult to assess compared to channel flow, since the coolant flow is not constrained in the radial direction.

For the AHTR and VHTGR concepts utilizing the prismatic fuel form, there exists a significant amount of variability in the design of the fuel elements. The basic representation of the prismatic fuel form is shown in Figure 7. The prismatic fuel is hexagonal-shaped and extends the length of the core. Each fuel element contains a fuel region, moderator region and coolant channel region. Figure 7 depicts an element with an inner cylindrical fuel compact, an annular flow channel and an outer prismatic graphite moderator. For high-temperature reactor concepts, it is important to have the fuel region in close proximity to the coolant in order to maintain the lowest maximum fuel temperature possible. Designs with the coolant channel on the perimeter of the prism, with moderating material between the fuel and coolant channel, are not considered viable for high-temperature concepts.

Maintaining a coolant channel on the outside edge of the fuel compact is a viable configuration for the AHTR molten-salt cooled concept since, during shutdown decay-heat removal, the liquid salt within the channel remains as the main coolant source. This is not true for the He-gas cooled VHTGR concept. In order to maintain a low temperature for the fuel compact and He

coolant, the compact should be in direct contact with the moderator to allow for radial heat conduction to the core boundary. This type of a configuration would also work for molten-salt coolant.

Figure 8 illustrates possible fuel element configurations for a molten-salt cooled system and a He gas-cooled system. The prismatic elements shown have a pitch of 15.24 cm (6 in.) with a cylindrical fuel compact 4.31 cm (1.70 in.) in radius. The coolant volume fraction is 0.025 and the fuel compact volume to the total fuel element volume is ~30%. The dimensions shown are representative values, and are not to be assumed as optimized. Determination of actual design dimensions would include a complex iteration that factors in power density, peaking factors, maximum fuel temperature, coolant temperature, criticality and burnup.

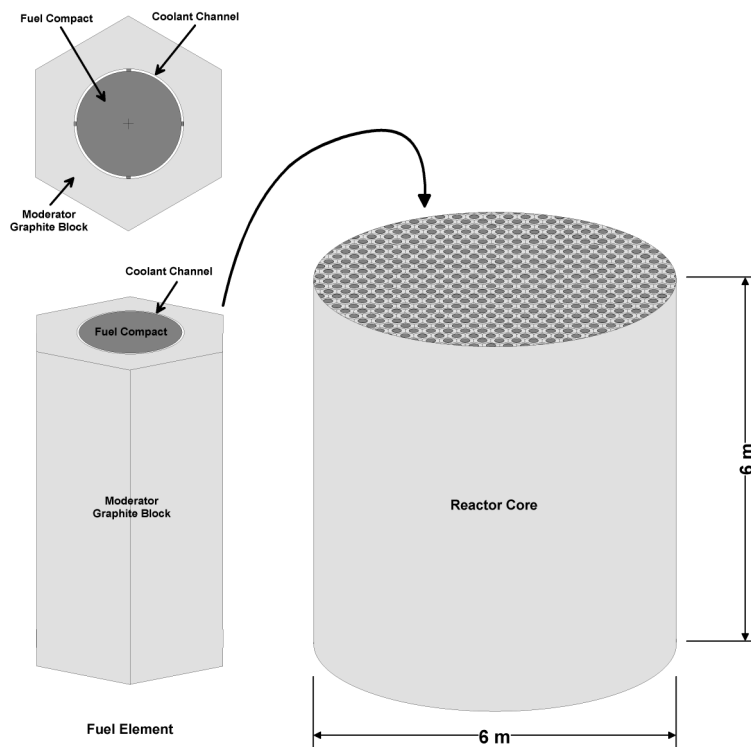


Figure 7. Fuel Element Configuration for the AHTR and VHTGR concepts.

Other possible fuel/coolant/moderator configurations are shown in Figure 9. If a single flow channel is not adequate for maintaining a low temperature differential across the fuel and from the fuel surface to the coolant, the fuel region can be partitioned and cooled by multiple flow paths. Shown in Figure 9 are three variations, which include multiple annular channels and multiple flow holes.

Having additional moderating material is not necessarily required for the prismatic fuel form. It may be desirable to have as high a fuel loading as possible by making the complete prismatic form into fuel. Figure 10 illustrates this concept with multiple flow channels within the prism. Flow channels can be designed to either completely remain within the prism or to also be

maintained along the boundary such that the channels maintain a triangular pitch throughout the core. A prismatic fuel form with multiple flow channels will be necessary if the thermal analysis determines that individual compacts with single flow channels would be too small in size to allow for fabrication and handling.

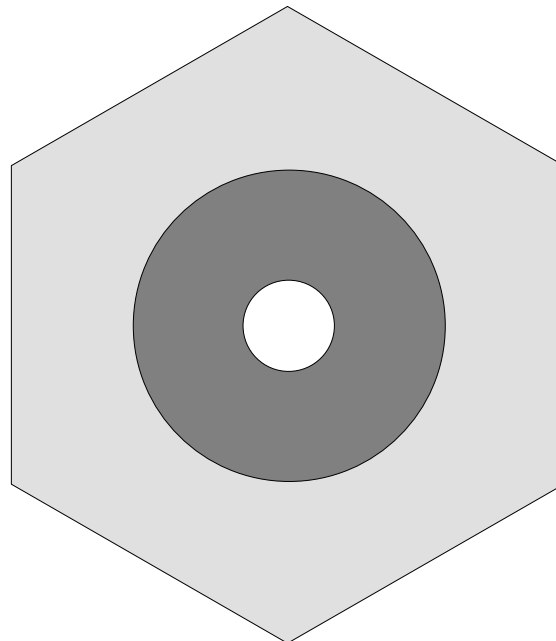
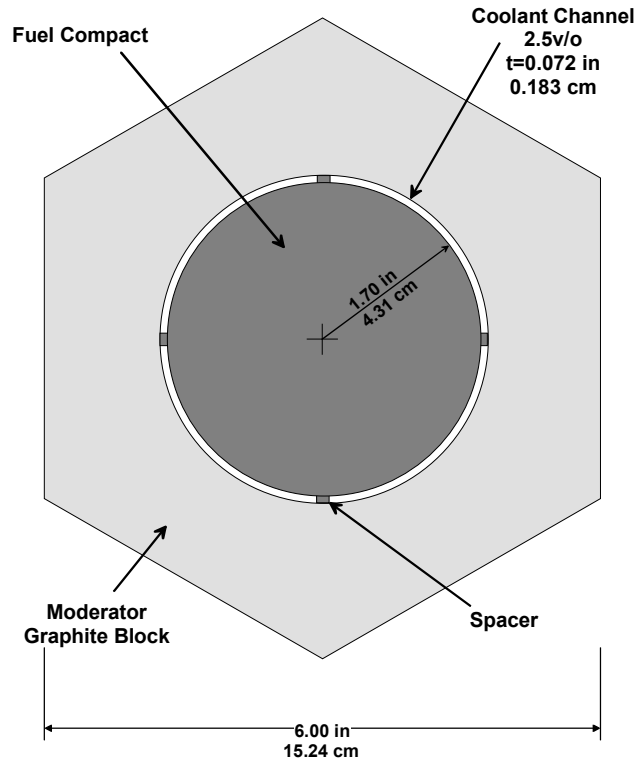


Figure 8. Prismatic Fuel Form With Annular and Inner Cooling Channel.

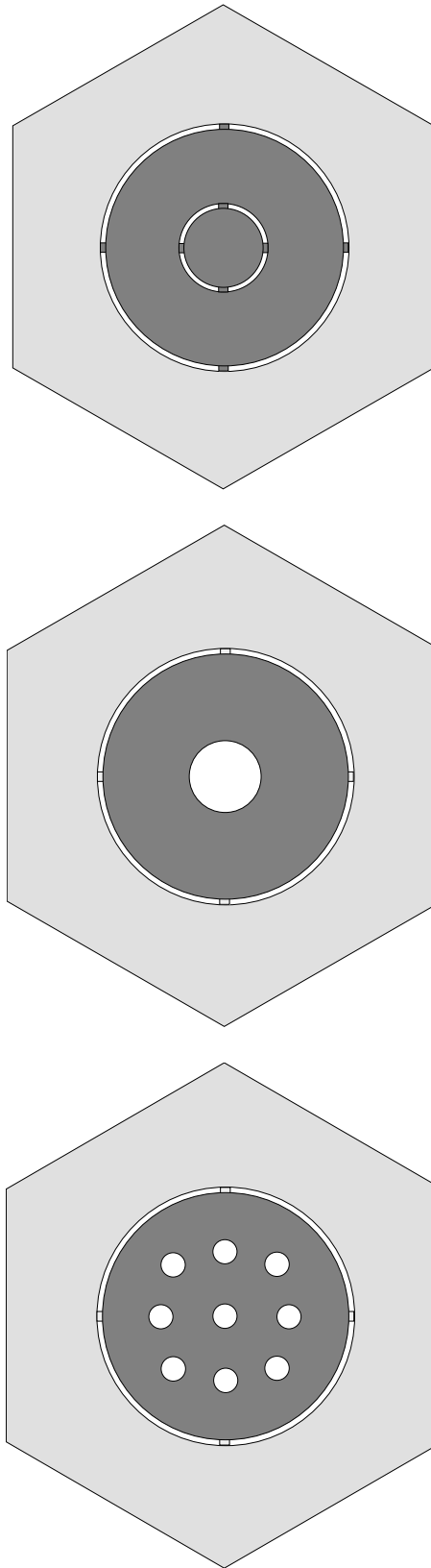


Figure 9. Cooling Channel Options for the Prismatic Fuel Form.

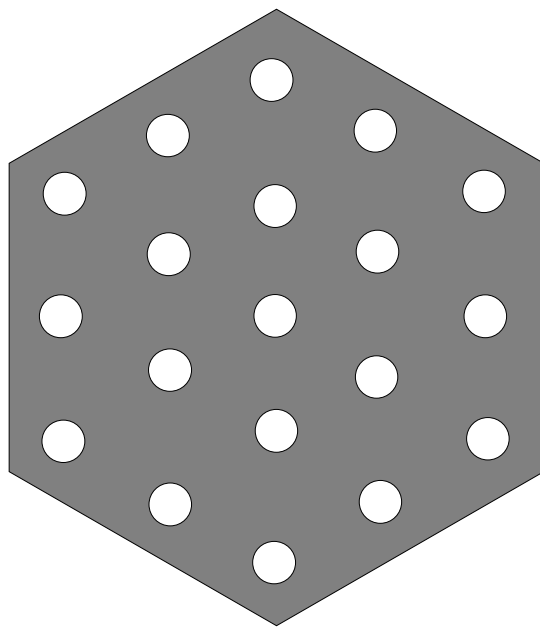
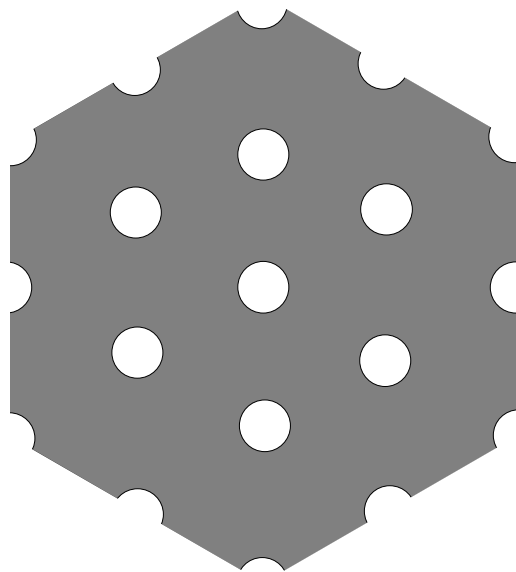


Figure 10. Prismatic Fuel Form Without Additional Moderator.

4.3 Thermal Analysis Modeling

The steady-state thermal analysis for a fuel element with a simple geometry can be performed by finding the analytic solution to the steady-state heat equation. For a fuel region with a constant conductivity (temperature-independent) material and uniform heat source, the radial temperature distribution can be determined for 1) a sphere, 2) a cylindrical fuel compact surrounded by an annular flow channel, and 3) a cylindrical flow channel surrounded by a fuel compact. The steady-state heat equation with a constant conductivity and uniform heat density is as follows:

$$-k \nabla^2 T(r) = q''' \quad (1)$$

where

k = temperature independent conductivity (W/cm-°C),

$T(r)$ = temperature distribution (°C),

q''' = heat density within the fuel (W/cm³),

∇^2 = Laplacian operator – r direction only

$$= \frac{1}{r^2} \frac{d}{dr} r^2 \frac{d}{dr} \quad (\text{for spherical coordinates}),$$

$$= \frac{1}{r} \frac{d}{dr} r \frac{d}{dr} \quad (\text{for a cylindrical coordinates}).$$

Spherical Solution

For a sphere with a radius equal to R , and constant boundary temperature $T(R) = T_w$, the solution to Equation 1 at the center of the sphere is

$$T_{\max} = T(0) = \frac{q'''}{6k} R^2 + T_w \quad (2)$$

The radial heat flux at the surface of the sphere is equal to

$$q''(R) = -k \vec{\nabla} T(r)|_R = -k \frac{dT(r)}{dr}|_R = q''' \frac{V}{A} = q''' \frac{R}{3} \quad (3)$$

where

$q''(R)$ = heat flux at R (W/cm²),

$\vec{\nabla}$ = gradient operator – r direction only = $\frac{d}{dr} \mathbf{r}$ (for spherical and cylindrical coordinates),

$$V = \frac{4}{3} \pi R^3 ,$$

$$A = 4 \pi R^2 .$$

For the heat density given as a core average, q'''_{avg} , packing fraction, pf , radial core peaking factor, F_r , and axial peaking factor, F_z , the heat density for the fuel pebble is

$$q''' = \frac{q'''_{avg}}{pf} F_r \cdot F_z \quad (4)$$

Cylindrical Solution – Cylindrical Fuel/Annular Flow Channel

For a cylindrical fuel compact surrounded by an annular flow channel, the solution for the centerline temperature is

$$T_{\max} = T(0) = \frac{q'''}{4k} R^2 + T_w . \quad (5)$$

where R is the radius of the fuel compact and the other variables are the same as defined for Equation 2.

The radial heat flux at the surface of the cylinder at the coolant interface is equal to

$$q''(R) = q''' \frac{R}{2} . \quad (6)$$

For the heat density given as a core average, q'''_{avg} , the cylindrical fuel and coolant unit within a moderator prismatic fuel element with pitch equal to P , radial core peaking factor, F_r , and axial peaking factor, F_z , the heat density for the fuel region is

$$q''' = q'''_{avg} \frac{\sqrt{3}P^2}{2\pi R^2} F_r \cdot F_z . \quad (7)$$

Cylindrical Solution – Cylindrical Flow Channel/Annular Fuel

For a cylindrical flow channel surrounded by an annular or fuel compact, the solution for the centerline temperature is

$$T_{\max} = T(b) = \frac{q'''}{4k} a^2 \left[\left(1 - \frac{b^2}{a^2} \right) + 2 \frac{b^2}{a^2} \ln \left(\frac{b}{a} \right) \right] + T_w \quad (8)$$

where a is the radius of the flow channel, b is the radius of the fuel compact, and the other variables are the same as defined for Equation 2.

Since $\frac{a^2}{b^2}$ can be defined as the coolant fraction, cf (area of coolant to area of fuel + coolant), Equation 8 can be rewritten as

$$T_{\max} = T(b) = \frac{q'''}{4k} a^2 \left[\left(1 - \frac{1}{cf} \right) + 2 \frac{1}{cf} \ln \left(\frac{1}{\sqrt{cf}} \right) \right] + T_w \quad (9)$$

The radial heat flux at the surface of the cylinder at the coolant interface is equal to

$$q''(a) = q''' \frac{b^2 - a^2}{2a} = q''' \frac{a}{2} \left(\frac{1}{cf} - 1 \right) \quad (10)$$

For the heat density given as a core average, q'''_{avg} , the cylindrical fuel and coolant unit within a moderator prismatic fuel element with pitch equal to P , radial core peaking factor, F_r , and axial peaking factor, F_z , the heat density for the fuel region is

$$q''' = q'''_{avg} \frac{\sqrt{3}P^2}{2\pi(b^2 - a^2)} F_r \cdot F_z \quad (11)$$

If there is no moderator region, and the fuel outer surface is a prism (hexagon) with pitch, P , the hexagon may be approximated as a cylinder with radius b , equal to

$$b = \left(\frac{\sqrt{3}}{2\pi} \right)^{1/2} P = 0.525 P \quad (12)$$

4.4 Thermal Hydraulic Analysis Modeling

The goal of the thermal hydraulic analysis is to determine the temperature difference between the coolant channel wall and the bulk coolant, and to determine the pumping power required to flow the coolant through the reactor. The steady-state thermal hydraulic analysis for flow in a channel with molten-salt or helium coolant is straightforward, since the flow is one-dimensional. For flow in a particle bed, the analysis is more difficult since the flow is not restricted in the radial direction. For a particle bed, empirical relations on a macroscopic level must be used in the analysis.

The temperature difference between the coolant channel wall and bulk coolant is determined from the general equation for convection heat transfer

$$q'' = h (T_w - T_b) \quad (13)$$

where q'' is the heat flux at the surface of the coolant channel wall, h is the local heat transfer coefficient, T_w is the coolant channel wall temperature and T_b is the bulk coolant temperature. The heat transfer coefficient can be found using the Nusselt (Nu) number, defined as

$$Nu = \frac{h L_c}{k_f} \quad (14)$$

where k_f is the conductivity of the fluid and L_c is the characteristic length or equivalent diameter D_e , defined as

$$L_c = D_e = \frac{4 \cdot \text{flow area}}{\text{wetted perimeter}} \quad (15)$$

which is equal to the diameter, D , for a circular flow channel.

The Nusselt number can be determined from correlations developed for the particular flow geometry of interest. For forced-convection fully-developed turbulent flow inside a heated circular tube, the Dittus and Boelter correlation or other appropriate correlation can be used. The Dittus and Boelter correlation (Karlekar and Desmond, 1977) is as follows

$$Nu = 0.023 \text{ Re}^{0.8} \text{ Pr}^{0.4} \quad (16)$$

where Re is the Reynolds number and Pr is the Prandtl number. The Re and Pr numbers are defined as

$$\text{Re} = \frac{\rho v L_c}{\mu} = \frac{v L_c}{\nu} \quad (17)$$

$$\text{Pr} = \frac{\rho C_p \mu}{k_f \rho} = \frac{\rho C_p}{k_f} \nu = \frac{\nu}{\alpha} \quad (18)$$

where ρ is the fluid density, ν is the channel velocity, μ is the viscosity, ν is the kinematic viscosity, C_p is the constant pressure heat capacity, and α is the diffusivity. The flow is considered turbulent if the Re number is greater than 2300. For helium gas, μ , k_f , and C_p are temperature dependent but pressure independent. The velocity can be determined from the mass flow rate in the channel

$$\dot{m} = \rho \nu A_f = G A_f \quad (19)$$

where A_f is the channel flow area. The value $\rho \nu$ is the mass flux, G .

The mass flow rate can be either specified or determined. If the inlet and outlet temperatures for the channel are specified, and the average heat flux in the channel is given, the flow rate can be determined by

$$Q = q''_{avg} A_s = \dot{m} C_p (T_{out} - T_{in}) \quad (20)$$

where Q is the total channel heating, q''_{avg} is the average channel heat flux, A_s is the channel surface area, T_{out} is the channel outlet temperature, and T_{in} is the channel inlet temperature.

The pressure drop and pumping power through the flow channel and reactor core can be determined by calculating the friction losses through the channel. The friction losses for turbulent flow can be calculated using the formulation

$$\Delta P_{friction} = f \frac{L}{D_e} \frac{\rho \nu^2}{2} \quad (21)$$

where f is the Darcy-Weisbach friction factor, and L is the channel length. For turbulent flow in a smooth surface circular channel, the friction factor can be approximated (Incropera and DeWitt, 1985) as

$$f = \frac{0.184}{\text{Re}^{0.2}} \quad (22)$$

The pumping power for a single flow channel (to overcome the friction losses in the channel) is

$$W_{ch} = \Delta P_{friction} A_f \nu \quad (23)$$

where W is the pumping power for a single channel. The total pumping power is found by summing over the total number of channels in the core.

For a pebble bed core, the localized Nusselt number, and hence the heat transfer coefficient, can be derived from empirical correlations using the average velocity of the coolant in the core (Stroh, 1979).

4.5 Thermal and Thermal Hydraulic Analysis for the VHER Concepts

The thermal and thermal hydraulic analysis for the AHTR and VHTGR were performed for a circular flow channel using the Mathcad engineering analysis software and the equations developed in the previous section. The Mathcad analysis allows for parametric comparisons to be made on different variables, including the channel diameter, coolant fraction, power density, conductivity, and inlet and outlet temperatures, to determine the temperature difference from the peak to the coolant channel wall, ΔT_{fw} , from the wall to the bulk coolant, ΔT_{wc} , and the pumping power. From this analysis the conceptual design and feasibility of the concept can be further deduced.

AHTR Prismatic Fuel Element – Molten Salt (Flibe) Coolant

The Mathcad-developed thermal and thermal hydraulic analysis code was run for the AHTR concept using molten-salt (Flibe) coolant. The fuel element analyzed is shown in Figure 11. The fuel element is a prismatic fuel compact with a circular flow channel and no additional solid moderator. The fuel elements are stacked in a core similar to that shown in Figure 7. In order to solve for the temperature distribution within the element, the boundary of the prism (hexagon) is replaced with a circular boundary with an equivalent radius. The boundary is assumed to be insulated such that no heat transfer occurs between fuel elements. Equations 8 to 12 were used to solve for the conduction in the fuel compact.

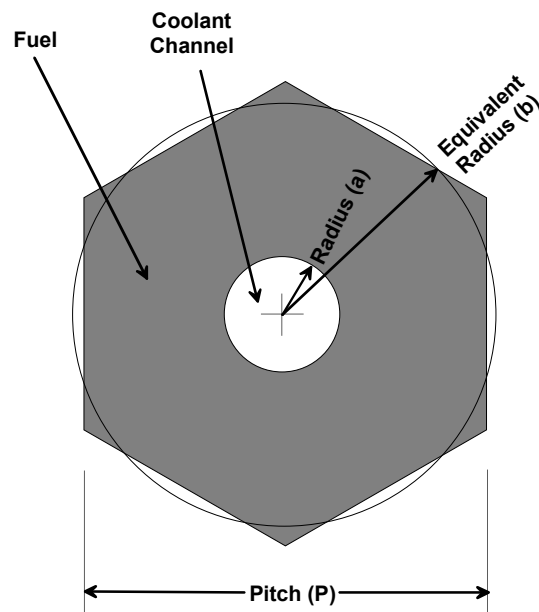


Figure 11. Prismatic Fuel Element Used for Thermal Hydraulic Analysis.

To solve for the temperature difference between the peak at the boundary edge and the coolant channel wall, ΔT_{fw} , the channel radius, coolant fraction, average power density, and thermal conductivity in the fuel compact region are required. The fuel compact is made up of a pressed and sintered mixture of fuel particles and graphite. Determining the thermal conductivity for the compact is difficult, especially under irradiated conditions. For irradiated and annealed graphite, the thermal conductivity is found to range between 0.15 and 0.6 W/cm-°C (Touloukian, 1967). The Peach Bottom HTGR fuel compact is referenced as having a thermal conductivity of 0.3 W/cm-°C (Simnad, 1971).

Figures 12 and 13 show the results of the analysis for a 5 and 10 W/cc power density assuming a constant thermal conductivity of 0.3 W/cm-°C. The results are for coolant fractions of 0.025, 0.05, 0.1, 0.2, 0.3, 0.4, and 0.5, and coolant radii from 0 cm to 3 cm. For a constant coolant fraction, ΔT_{fw} is proportional to the average power density, the square of the coolant channel radius, and inversely proportional to the conductivity.

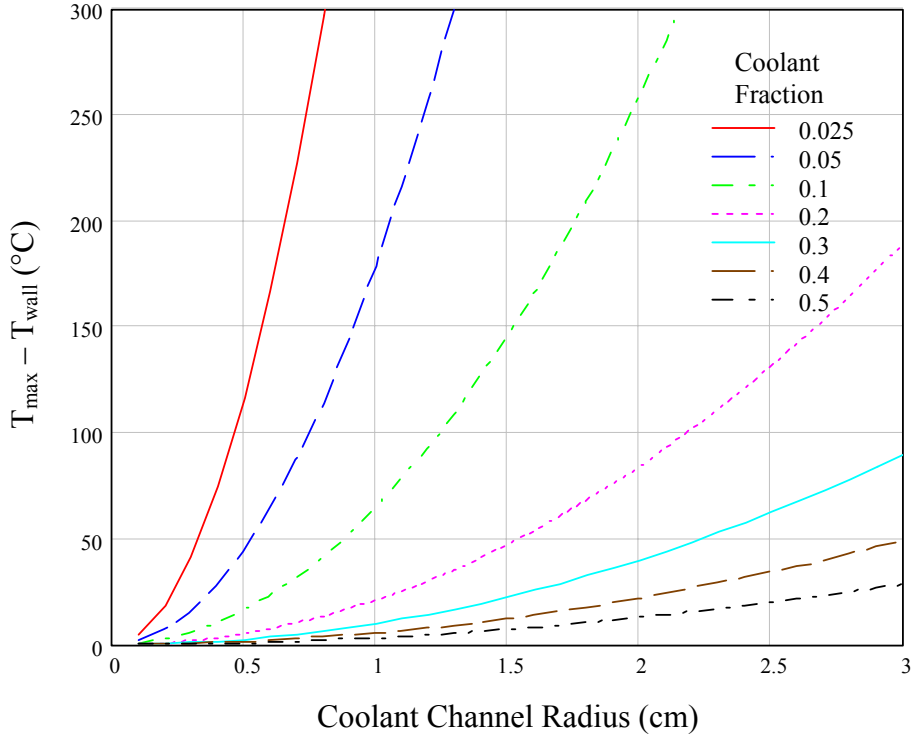


Figure 12. Fuel Compact Peak to Wall Temperature Difference – 5 W/cc, 0.3 W/cm- $^{\circ}\text{C}$.

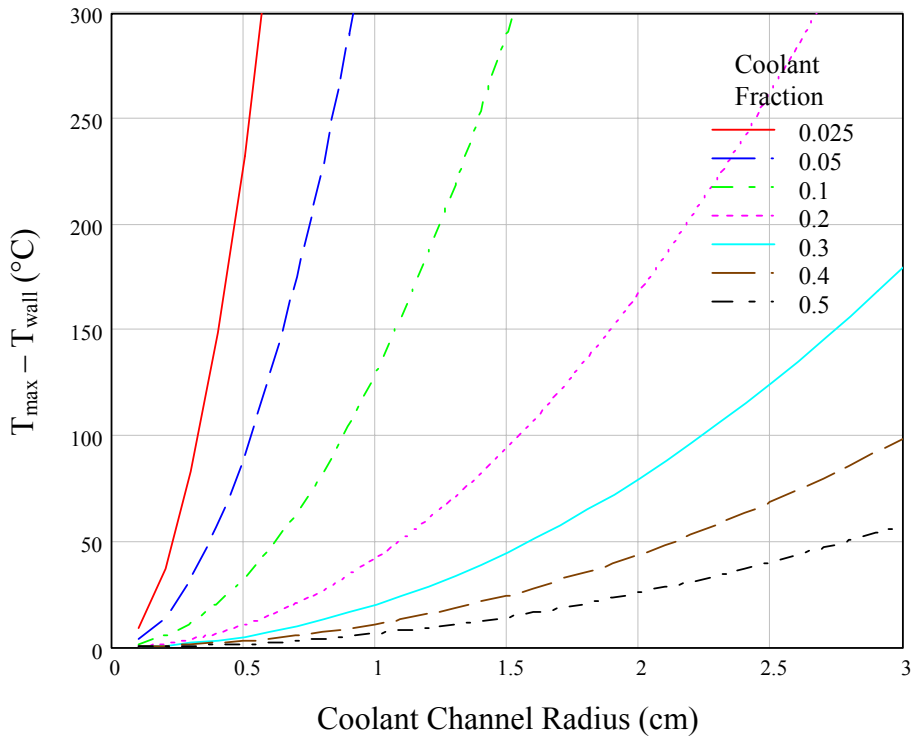


Figure 13. Fuel Compact Peak to Wall Temperature Difference – 10 W/cc, 0.3 W/cm- $^{\circ}\text{C}$.

To solve for the temperature difference between the coolant channel wall and the bulk coolant channel wall, ΔT_{wc} , the channel radius, coolant fraction, average power density, core height, inlet and outlet temperatures, molten-salt density, heat capacity of the molten salt, and thermal conductivity of the molten salt are required. The molten-salt density, heat capacity, and thermal conductivity are relatively constant with temperature. The molten-salt properties used in the analysis are shown in Table 4.

Table 4. Flibe Molten Salt Thermo-Physical Properties.

Material Property	Value
density	2.05 g/cm ³
kinematic viscosity	0.028 cm ² /s
heat capacity	2.34 J/g-°C
thermal conductivity	0.0109 W/cm-°C

Figures 14 and 15 show the results of the analysis for a 5 and 10 W/cc average power density, assuming a reactor core height of 7 m, an inlet temperature of 800°C, and an outlet temperature of 1000°C. The results are for coolant fractions of 0.025, 0.05, 0.1, 0.2, 0.3, 0.4, and 0.5, and coolant radii from 0 to 3 cm. Note that the temperature differences compared to Figures 12 and 13 are in the same range, that is, for the AHTR the ΔT is not dominated by conduction or convection.

For a reactor power of 1000 MW_{th}, and an average power density in the core of 5 W/cc, the total reactor volume would be 2×10^8 cm³. Assuming a core height of 7 m, the radius of the core would be 3 m. Depending on the fuel loading, control element location, and burnup, the radial and axial peaking factors may be significantly greater than one. For an actual reactor design, the fuel loading, burnable poison loading, and burnup would be optimized to maintain the peaking factors as close to unity as possible. For the AHTR thermal hydraulic analysis, it will be assumed that the maximum value for the axial and radial peaking factors multiplied together is no greater than two. Assuming the axial peaking occurs at the core center, and the fission density is symmetric about the centerline, the peak fuel temperature for the AHTR can be determined. At the axial core center, the bulk Flibe coolant temperature is 900°C, assuming an inlet temperature of 800°C and an outlet temperature of 1000°C. Assuming the peak fuel operating temperature cannot exceed 1250°C, the peak fuel-to-bulk coolant temperature difference is 350°C.

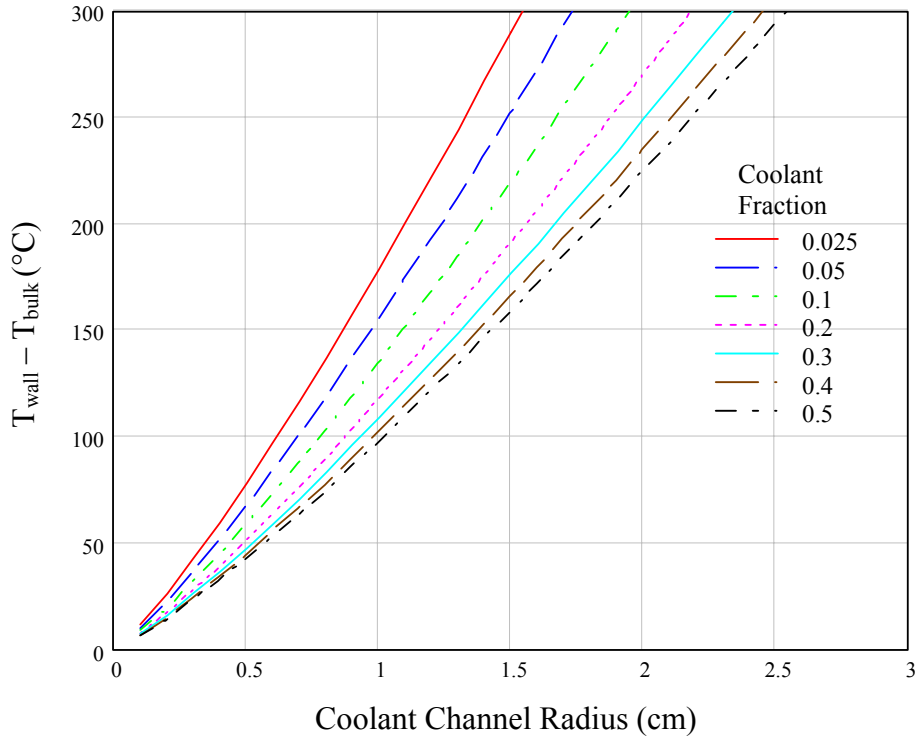


Figure 14. AHTR Wall to Bulk Coolant Temperature Difference – 5 W/cc.

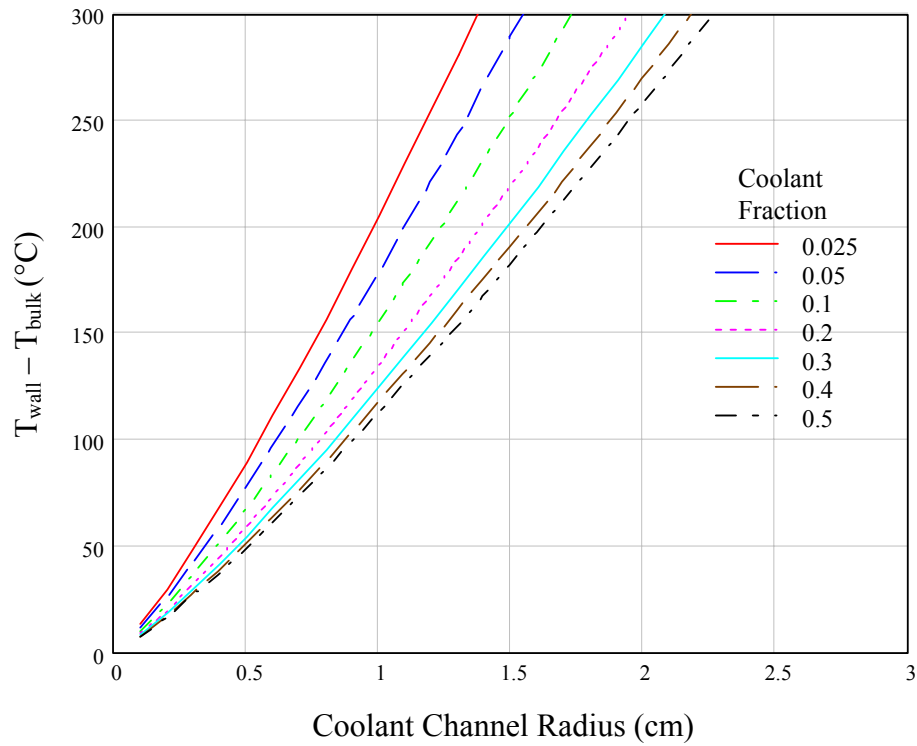


Figure 15. AHTR Wall to Bulk Coolant Temperature Difference – 10 W/cc.

Table 5 shows the results for the channel radius, fuel element radius, and pitch at a given coolant fraction such that the peak fuel-to-bulk coolant temperature difference of 350°C is not exceeded. Smaller coolant channels would allow for a smaller temperature difference. Figures 13 and 15 were used in the Mathcad analysis for a peak power density in the AHTR of 10 W/cc. The results are given to the nearest 0.05 cm. The results show that under these conditions, the fuel element radius remains relatively constant. For a coolant volume fraction of 0.1, the peak temperature will not be exceeded for a coolant radius of 1.15 cm and a pitch of 6.85 cm.

Table 5. AHTR Maximum Coolant Channel and Fuel Radius (Tmax = 1250°C).

Coolant Volume Fraction	Coolant Channel Radius – a (cm)	Fuel Radius – b (cm)	Pitch – P (cm)
0.025	0.50	3.30	6.25
0.05	0.80	3.50	6.65
0.10	1.15	3.60	6.85
0.20	1.60	3.60	6.90
0.30	1.95	3.50	6.70
0.40	2.15	3.40	6.55
0.50	2.35	3.30	6.35

The pumping power required to overcome the friction losses through the core is calculated using Equations 21 to 23. The results are shown in Figure 16 for a 1000 MW_{th} power level AHTR, an average core power density of 5 W/cc, and a 7 m core height. The results show that the pumping power is trivial, especially for coolant volume fractions greater than 0.1 and coolant channel radii greater than 0.5 cm. For a coolant volume fraction of 0.1, and a coolant channel radius of 1.15 cm, the pumping power required for the reactor is ~2 kW, which is a trivial 0.0002% of the total core power.

The thermal and thermal hydraulic analysis results for the AHTR fuel element show that this concept is feasible, from a maximum operating fuel temperature perspective, if size constraints are maintained on the pitch and coolant channel in relation to the power density. A typical configuration would be one with a coolant volume fraction of 0.1, coolant channel radius of 1.15 cm, and a fuel radius of 3.6 cm or a pitch of 6.85 cm. Additional moderating material can be placed around the fuel, if required from a neutronic perspective. Multiple prisms could be joined to form a larger prism with multiple flow channels, similar to that shown in Figure 10, if fabrication and/or handling required larger dimensions of the fuel element.

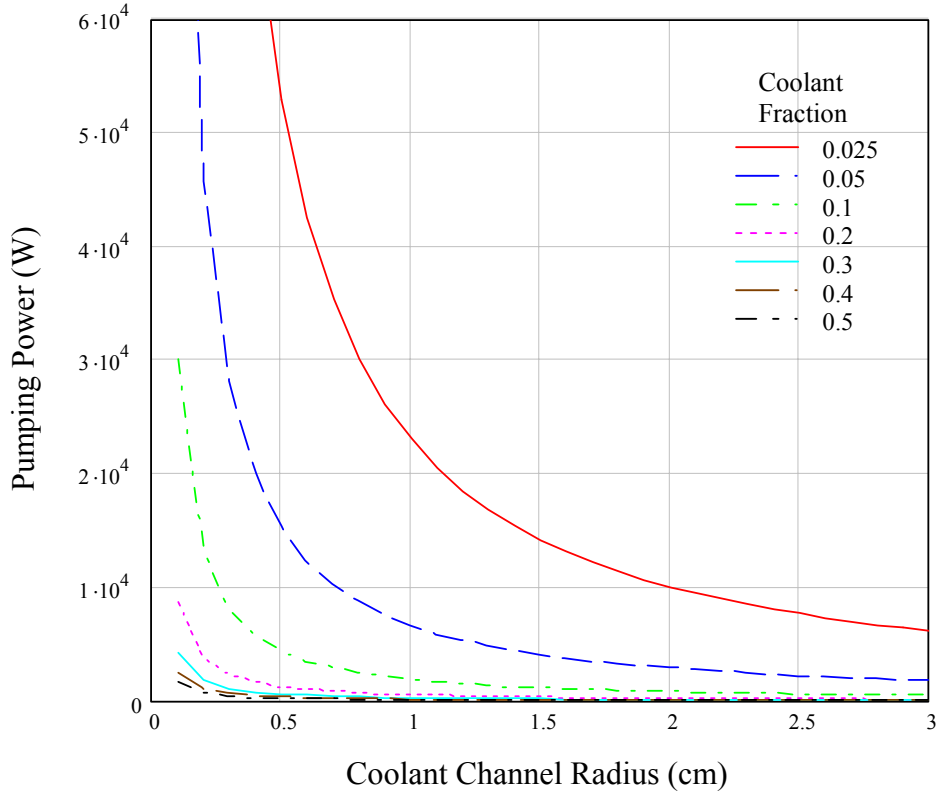


Figure 16. Pumping Power Required for the AHTR.

VHTGR Prismatic Fuel Element – Helium Coolant

The same Mathcad analysis was performed for the VHTGR concept, except that helium was used as the coolant. Since the fuel form is the same for the VHTGR as for the AHTR, the results for the conduction within the fuel element are the same. The results are shown in Figures 12 and 13. To solve for the temperature difference between the coolant channel wall and the bulk coolant channel wall, ΔT_{wc} , the channel radius, coolant fraction, average power density, core height, inlet and outlet temperatures, He gas density, viscosity of the He, heat capacity of the He, and thermal conductivity of the He are required. For He, the viscosity, heat capacity and thermal conductivity are temperature- but not pressure-dependent. The He properties used in the analysis are shown in Table 6.

Figures 17 and 18 show the results of the analysis for a 5 and 10 W/cc average power density assuming a reactor core height of 7 m, an inlet temperature of 700°C, and an outlet temperature of 1100°C. The results are for coolant fractions of 0.025, 0.05, 0.1, 0.2, 0.3, 0.4, and 0.5, and coolant radii from 0 to 3 cm. Note that the temperature differences compared to Figures 12 and 13 are in the same range.

Table 6. He Thermo-Physical Properties at 1000 psi and 900°C.

Material Property	Value
density	0.0031 g/cm ³
viscosity	0.00041 g/cm-s
heat capacity	5.20 J/g-°C
thermal conductivity	0.0030 W/cm-°C

For a reactor power of 1000 MW_{th}, and an average power density in the core of 5 W/cc, the total reactor volume would be 2×10^8 cm³. Assuming a core height of 7 m, the radius of the core would be 3 m. Depending on the fuel loading, control element location, and burnup, the radial and axial peaking factors may be significantly greater than one. For an actual reactor design, the fuel loading, burnable poison loading, and burnup would be optimized to maintain the peaking factors as close to unity as possible. For the VHTGR thermal hydraulic analysis, it will be assumed that the maximum value for the axial and radial peaking factors multiplied together is no greater than two. Assuming the axial peaking occurs at the core center, and the fission density is symmetric about the centerline, the peak fuel temperature for the VHTGR can be determined. At the axial core center, the bulk He coolant temperature is 900°C, assuming an inlet temperature of 700°C and an outlet temperature of 1100°C. Assuming the peak fuel operating temperature cannot exceed 1400°C, the peak fuel-to-bulk coolant temperature difference is 500°C.

Table 7 shows the results for the channel radius, fuel element radius, and pitch at a given coolant fraction such that the peak fuel-to-bulk coolant temperature difference of 500°C is not exceeded. Smaller coolant channels would allow for a smaller temperature difference. Figures 13 and 18 were used in the Mathcad analysis for a peak power density in the VHTGR of 10 W/cc. The results are given to the nearest 0.05 cm. The results show that under these conditions, the fuel element radius remains relatively constant. For a coolant volume fraction of 0.1, the peak temperature will not be exceeded for a coolant radius of 1.55 cm and a pitch of 9.30 cm.

The pumping power required to overcome the friction losses through the core is calculated using Equations 21 to 23. The results are shown in Figure 19 for a 1000 MW_{th} power level VHTGR, an average core power density of 5 W/cc, and a 7 m core height. The results show that the pumping power is significant as compared to the AHTR, especially for coolant volume fractions less than 0.2 and coolant channel radii less than 0.5 cm. For a coolant volume fraction of 0.1, and a coolant channel radius of 1.55 cm, the pumping power required for the reactor is ~ 2.5 MW, which is 0.25% of the total core power.

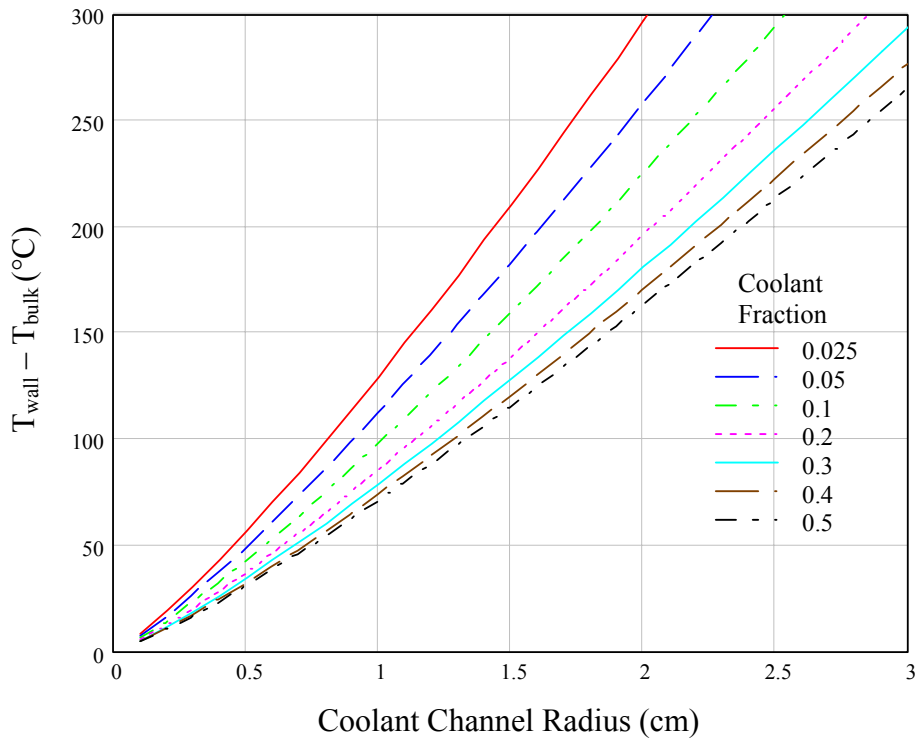


Figure 17. VHTGR Wall to Bulk Coolant Temperature Difference – 5 W/cc.

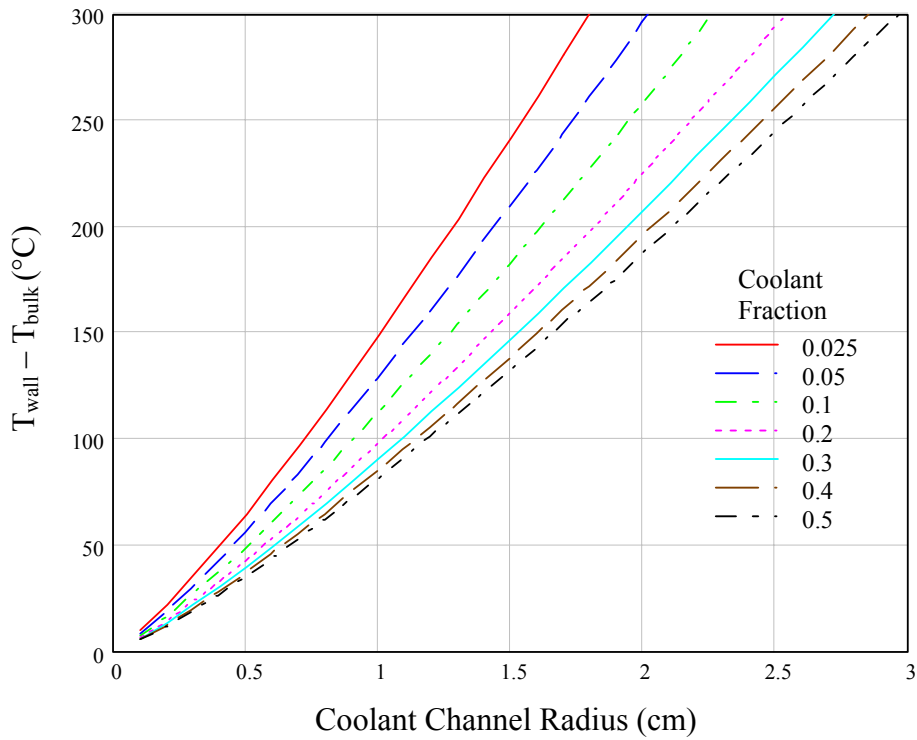


Figure 18. VHTGR Wall to Bulk Coolant Temperature Difference – 10 W/cc.

Table 7. VHTGR Maximum Coolant Channel and Fuel Radius (Tmax = 1400°C).

Coolant Volume Fraction	Coolant Channel Radius – a (cm)	Fuel Radius – b (cm)	Pitch – P (cm)
0.025	0.65	4.15	7.95
0.05	1.00	4.50	8.60
0.10	1.55	4.85	9.30
0.20	2.35	5.20	9.90
0.30	2.95	5.35	10.20
0.40	3.40	5.40	10.25
0.50	3.80	5.40	10.25

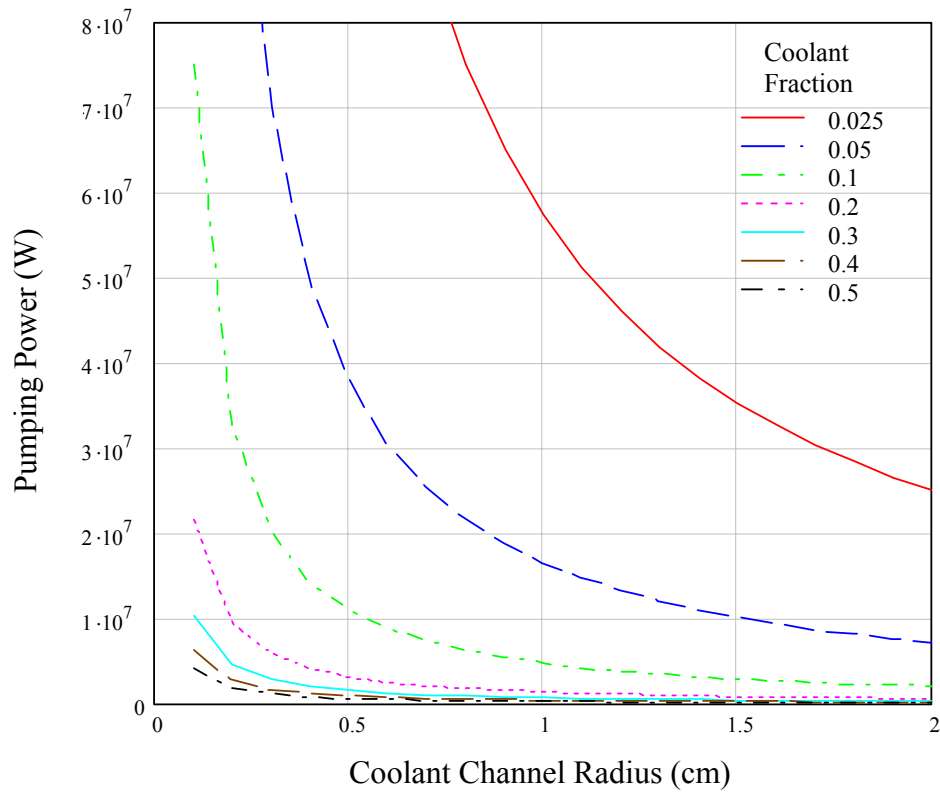


Figure 19. Pumping Power Required for the VHTGR.

In conclusion, the thermal and thermal hydraulic analysis results for the VHTGR fuel element show that this concept is feasible, from a maximum operating fuel temperature perspective, if size constraints are maintained on the pitch and coolant channel, and the power density is maintained in the 5 W/cc range. A typical configuration would be one with a coolant volume fraction of 0.1, a coolant channel radius of 1.55 cm and a fuel radius of 4.85 cm or a pitch of 9.30 cm. Additional moderating material can be placed around the fuel, if required from a neutronic perspective. Multiple prisms could be joined to form a larger prism with multiple flow channels, similar to that shown in Figure 10, if fabrication and/or handling required larger dimensions of the fuel element.

UHTGR Fuel Pebble Element – Helium Coolant

Empirical correlations for the Nusselt number (Stroh, 1979) and pressure drop for a packed bed (Bird, Stewart, and Lightfoot, 1960) or column can be used to find the heat transfer coefficient and pumping power for the UHTGR concept. Equations 2 to 4 can be used to determine the temperature difference across the fuel pebble. The UHTGR concept is assumed to have 18 identical modules with He coolant at 1000 psi and a packed bed using the standard size pebble of 6 cm diameter. Each module has an annular fuel region, as shown in Figure 3, with an inner radius of 20 cm, an outer radius 47 cm, and height of 400 cm. The pebble bed is assumed to have a packing fraction of 0.6, operates at a constant power density, and is cooled by axial flow through the bed. The inlet temperature is 850°C and the outlet temperature is 1250°C. Assuming the maximum operating temperature of the fuel is 1500°C, the maximum temperature difference at the axial core centerline is 450°C.

The results for the analysis are shown in Table 8 for 5, 25, and 50 W/cc core average power densities. The conductivity of the pebble is assumed to be 0.3 W/cm-°C. The temperature difference in the pebble and the pumping power are the limiting conditions for operating at high power densities. A power density of 50 W/cc would only be acceptable if smaller pebbles were used. A pebble $1/\sqrt{2}$ (0.707) the size of a standard pebble radius (2.12 cm) would result in a factor of 2 decrease in the temperature difference. To achieve 50 W/cc, the pumping power would be reduced by changing the design to radial flow through the bed instead of axial flow. For a 25 W/cc power density, the design is feasible using the standard 3-cm radius pebble. The constraints on the maximum operating temperature of 1500°C can be met while having an outlet temperature of 1250°C. A single module would operate at a power level of ~57 MW_{th} with the total 18 module core operating at ~1000 MW_{th}. The pumping power is 6% of the total power. A lower pumping power could be achieved by designing radial flow into the concept.

Table 8. UHTGR Thermal Hydraulic Results.

Power Density (core average) W/cc	ΔT pebble center to surface ($^{\circ}\text{C}$)	ΔT pebble surface to coolant ($^{\circ}\text{C}$)	Pumping Power Through Core (MW)
5	42	25	0.03
25	208	36	3.5
50	417	41	28.0

In conclusion, the UHTGR concept is feasible, from a thermal and thermal hydraulic view, in achieving extremely high core outlet temperatures and achieving higher power densities as compared to the AHTR and VHTGR designs. This design concept – modular pebble bed design with higher power densities – would also work for lower core exit temperatures using the current 1250°C limitation on the maximum fuel temperature for the standard fuel pebble.

5. PASSIVE DECAY HEAT REMOVAL

The pressure vessel, internal thermal barriers, and reactor core must be integrally designed to ensure that the safety and performance goals will be met for both normal operating conditions and off normal conditions. In order to maintain inherent safety in the design, decay-heat removal under passive conditions without forced flow, must be included in the design.

The design of the pressure vessel and passive decay-heat removal for the VHER concepts differ significantly. For the AHTR concept, the pressure within the vessel is very low (<50 psi). The coolant is a corrosive liquid (Flibe molten salt) at a high temperature. Passive decay-heat removal can be through convection through the core and conduction through the pressure vessel wall, or, more robustly, through natural-circulation salt flow within the primary heat exchanger. For the VHTGR and UHTGR concepts, the pressure within the vessel is high (1000 psi). The coolant is an inert gas (helium) at a high temperature that may contain impurities, such as oxygen. Passive decay-heat removal can only be achieved by conduction through the core, thermal barrier, and pressure vessel wall.

Important design considerations for the VHER concepts are the pressure vessel and internal insulating materials. Since the coolant temperatures are very high under normal operating conditions, a thermal barrier must exist between the coolant and pressure vessel. The barrier allows the vessel to be operated at a lower temperature, thus ensuring the vessel's mechanical integrity. Conventional materials used for pressure vessels, including mild steels and stainless steel, do not have sufficient mechanical strength at elevated temperatures above ~600°C. Super alloys of nickel and refractory alloys can be used at higher temperatures but also have temperature limitations. The thermal barrier can be graphite brick with a relatively low thermal conductivity, or other materials that are compatible with the coolant. The thermal barrier must be designed to maintain the pressure vessel at a low temperature during normal operation and, for the VHTGR and UHTGR concepts, allow enough heat flow (~1% of the total power) so that the maximum allowable fuel temperature is not exceeded under passive cooling conditions. The pressure vessel radius and thickness, operating pressure, power density, thermal barrier thickness, heat capacity, and conductivity, fuel region radius, heat capacity, and conductivity, and ultimate heat sink characteristics all play important roles in optimizing the passive safety and operational performance of the system. For the AHTR with natural convection passive safety, the thermal barrier is only required to maintain the vessel wall at a low temperature, during both operational and passive cooling conditions.

The results presented in this section are representative in nature, and should be considered as illustrative. The results are largely dependent on the variables discussed above. More in-depth analyses would be required to ensure that a system would perform as an intended.

The decay or shutdown power and energy fraction is shown in Figure 20 for a 10-year continuous operating history at a constant power level. The curves were generated using the Wigner-Way formula (Lewis, 1977)

$$P_d(t) = 0.0622 P_0 [t^{-0.2} - (t_0 + t)^{-0.2}] \quad (24)$$

where $P_d(t)$ is the decay power level, P_0 is the reactor power prior to shutdown, t_0 is the time, in seconds, of power operation before shutdown, and t is the time, in seconds, elapsed since shutdown. The energy deposited over time can be found by integrating Equation 24. At 50 hours the energy fraction is ~ 1000 s. Dividing by 50 hours give an average decay power fraction of 0.0056 or 0.56% of the operating power level prior to shutdown.

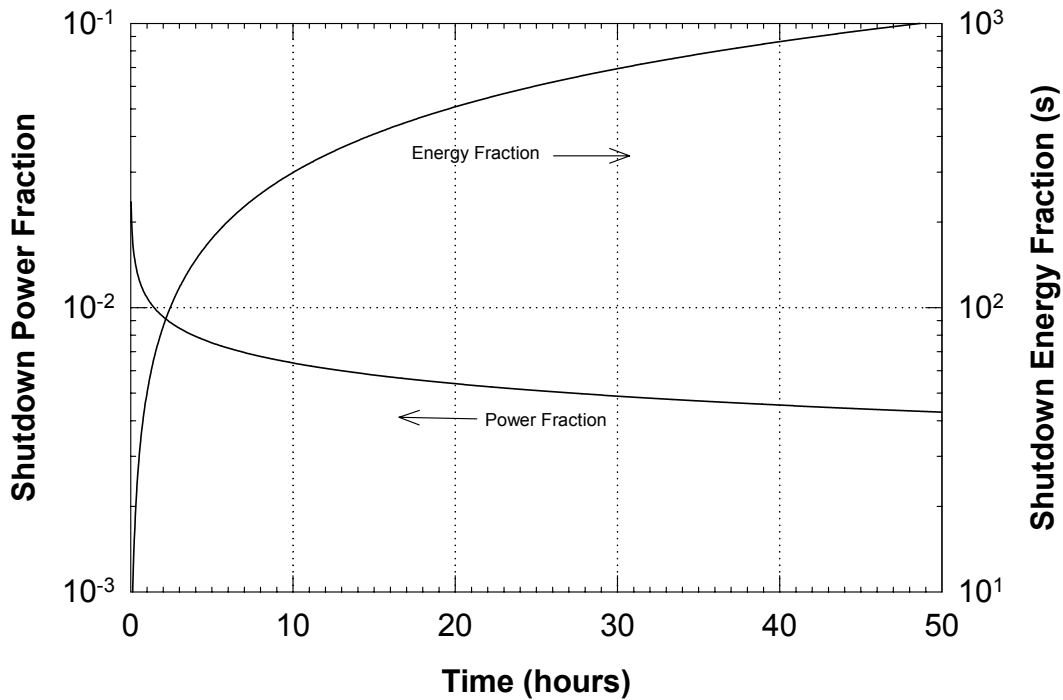


Figure 20. Decay Power and Energy Fraction Following a 10-Year Operating History.

5.1 AHTR – Passive Heat Removal Analysis

Two passive decay-heat removal case studies were performed for the AHTR concept: 1) conduction or natural convection through the core, with conduction through a thermal barrier and pressure vessel to an air heat sink; and 2) natural convection through the core to a heat exchanger with natural convection to a heat sink.

A plan view (not to scale) is shown in Figure 21 for the AHTR concept with natural-convection passive cooling through the heat exchanger (see Figure 1). For passive cooling by conduction through the vessel wall, the configuration would be similar, but with a thicker insulating thermal barrier. Under normal operating and shutdown conditions, pumps located at the bottom of the pool would pump the Flibe molten salt through the core and primary/secondary heat exchanger. The secondary side of the heat exchanger would also use molten-salt coolant. A schematic diagram of the primary and secondary systems is shown in Figure 22. The schematic shows the secondary system with three coolant paths. One path would be through an auxiliary heat exchanger that would be used for both passive cooling and maintaining the molten salt above the

melting point of 460°C under shutdown conditions. The other two heat exchangers would be used for process heat applications and for heat transfer to helium for Brayton cycle power generation. The design details of the heat exchangers and secondary system were not considered for this study. If passive cooling were through the vessel wall as opposed to natural convection through a heat exchanger, an air region outside of the pressure vessel would be cooled by an additional air heat exchanger within the containment building.

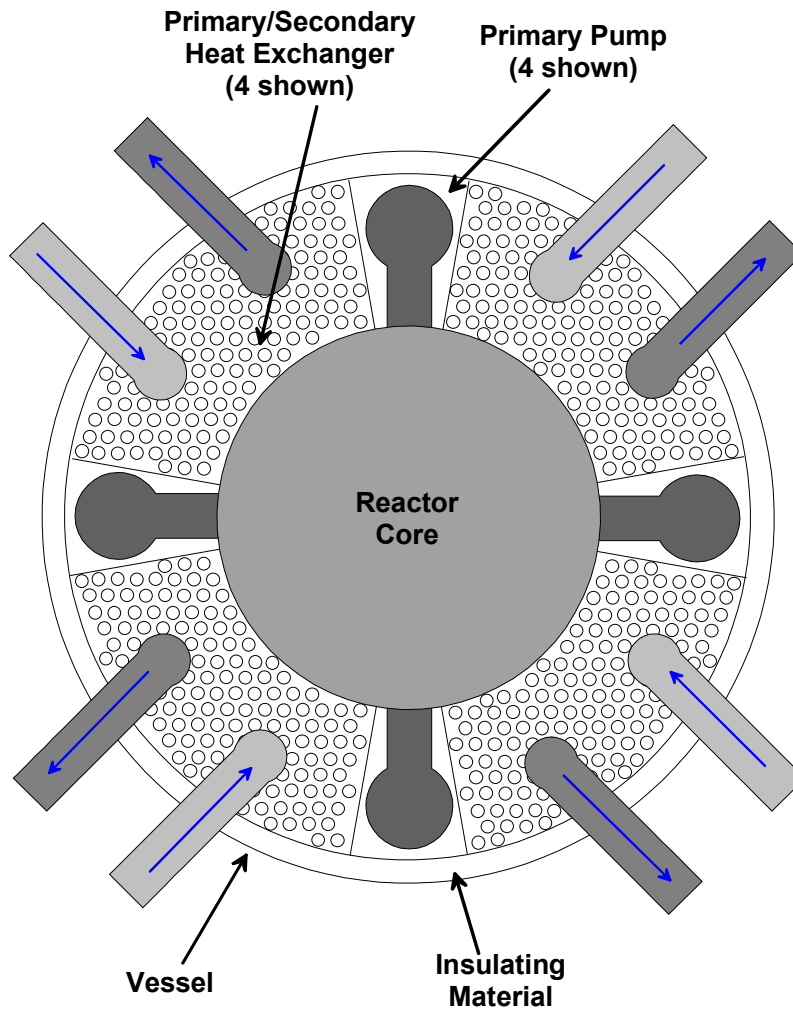


Figure 21. Plan View of the AHTR Concept.

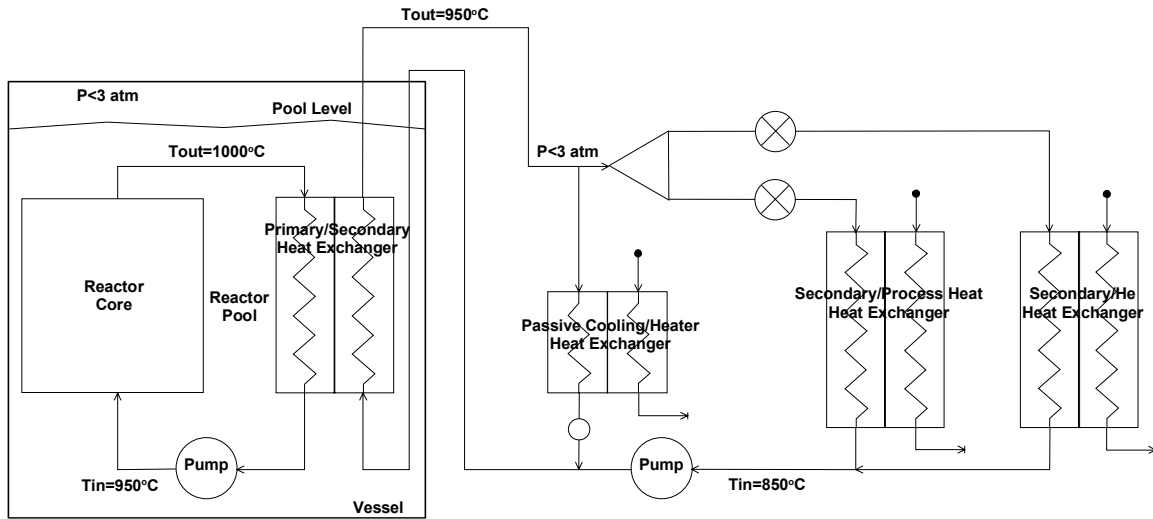


Figure 22. Schematic Diagram of the AHTR Cooling System.

For the first case study, a one-dimensional (radial) transient conduction calculation was performed to determine the maximum core temperature and vessel temperature as a function of time, allowing for passive cooling through the vessel wall to air. The dimensions, materials, and thermal properties for this study are shown in Table 9. The conductivity and heat capacity of the materials were assumed to be constant with temperature. The boundaries at the Flibe interface were assumed to be natural convective. An appropriate Nusselt number and heat transfer coefficient were derived for these boundaries. The boundary from the vessel to the air heat sink was also assumed to be convective (Hosegood, 1988). The natural convection heat transfer coefficient for air was increased an order of magnitude since the air would be flowing by the vessel under natural circulation flow.

Table 9. Dimensions and Properties for the AHTR Passive Heat Removal Analysis.

Region	Radius or Thickness (cm)	Conductivity (W/cm-K)	Density x Heat Capacity (J/cm ³ -K)
Core - Graphite	300	0.63	3.235
Reflector - Flibe Molten Salt	100	0.0109	4.797
Thermal Barrier - Graphite	100	0.63	3.235
Vessel - Hastelloy-N	5	0.214	5.047

The results are shown in Figures 23 and 24 for the core operating at 5W/cc for 10 years prior to shutdown. No radial or axial peaking factors were assumed in the analysis. Figure 23 shows the results assuming radial heat conduction through the core, which would be representative of a no-flow condition. Figure 24 shows the results assuming flow through the core, either by the pumps

or by natural circulation. For both cases, the initial temperature of the core and Flibe reflector is assumed to be a constant 900°C, an arbitrary value chosen as representative. At time equal to zero, the vessel maximum temperature is calculated to be ~350°C.

For Figure 23, a maximum core temperature of 1650°C is reached at ~35 hours after shutdown. The reflector salt temperature and maximum vessel temperature, however, begin decreasing after time equal to zero. Other calculative results show that a thinner thermal barrier, or one with a higher conductivity, would allow for a low maximum core temperature, but a higher vessel temperature. A calculation using the same input, but with a 5-cm graphite thermal barrier, resulted in a maximum core temperature of 1520°C at ~25 hours after shutdown. However, the initial vessel temperature, prior to shutdown, is calculated to be 740°C, which would be unacceptable as a design point. Lowering the power density, decreasing the radius of the core, increasing the heat capacity of the core, or increasing the conductivity of the core would decrease the maximum core temperature.

For Figure 24, a core temperature and salt temperature of 1325°C is reached at 70 hours after shutdown, but is still increasing. The vessel temperature increases after time equal to zero and is at a temperature of ~450°C at 70 hours after shutdown. The effect of allowing the coolant to circulate through the core results in a lower core temperature and extends the peak of the transient. Like the previous case, other calculative results show that a thinner thermal barrier, or one with a higher conductivity, would allow for a low maximum core temperature, but a higher vessel temperature. A calculation using the same input, but with a 5-cm graphite thermal barrier, resulted in a maximum core temperature of 980°C at ~20 hours after shutdown. Again, the initial vessel temperature, prior to shutdown, is calculated to be 740°C, which would be unacceptable as a design point. Lowering the power density, decreasing the radius of the core, or increasing the heat capacity of the core, would decrease the maximum core temperature.

The results for the flow condition would most likely represent the state of the system if passive cooling through the vessel wall were to be used in the design approach. The vessel could be maintained at lower temperatures if a highly convective coolant, such as water, was used as the outer coolant media. Since the molten salt would not be in direct contact with the vessel, and the vessel is at a low pressure, using water as the ultimate heat sink is not an unreasonable design concept. Also, an inner liner, fabricated from a high-temperature refractory metal, could be used to further isolate the molten salt from the vessel.

In conclusion, this case study shows that passive decay-heat cooling of the AHTR concept through the vessel is feasible and could be optimized to work for a power density of ~5 W/cc and radial core size of 300 cm. Alternative cooling media at the vessel boundary, such as water, should be investigated further.

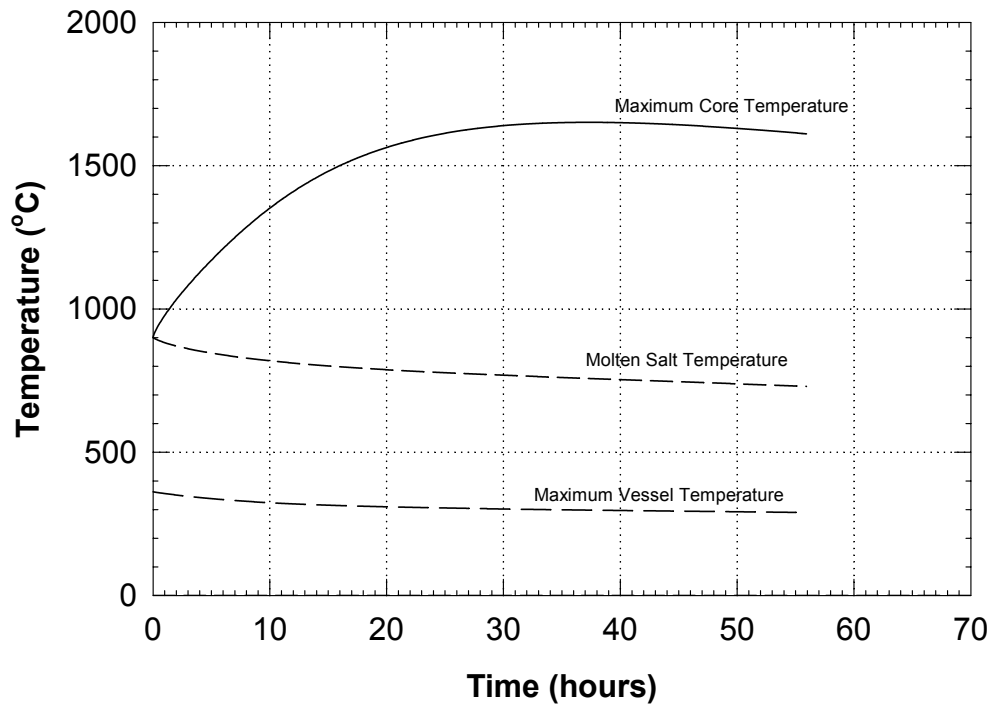


Figure 23. Passive Cooling Results for the AHTR With Conduction Through the Core.

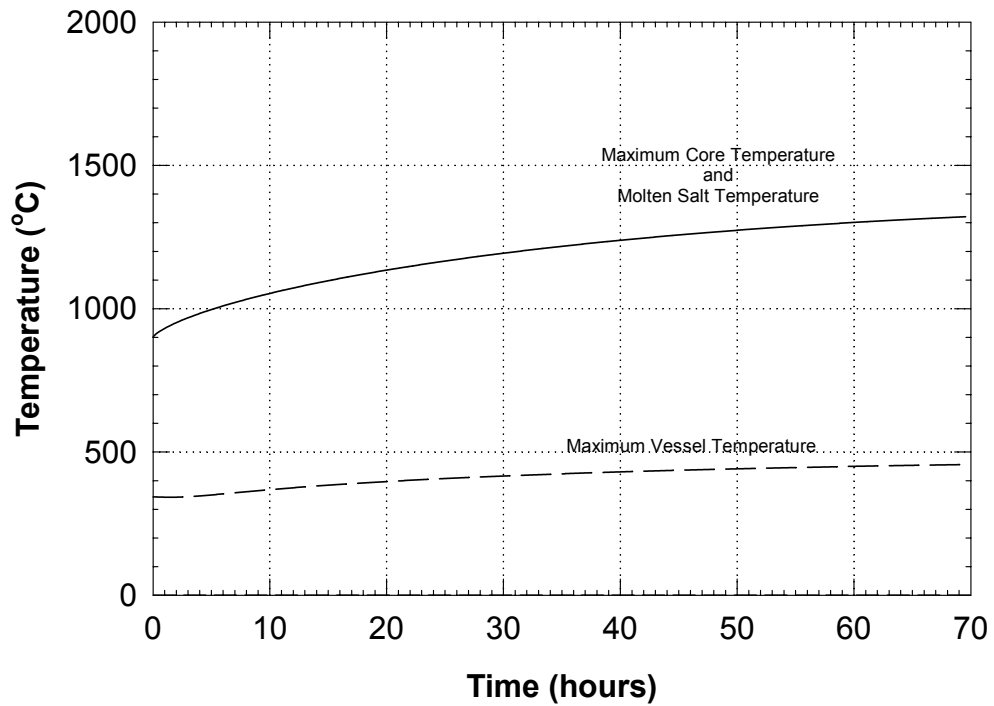


Figure 24. Passive Cooling Results for the AHTR With Flow Through the Core.

For the second case study, a one-dimensional (axial) steady-state calculation was performed to determine if natural circulation could be established under shutdown conditions, while maintaining the maximum core temperature at an acceptable value. The reactor core was assumed to be 300 cm in radius and 600 cm in height, with 10% coolant volume. The initial reactor power was 1,000 MW, equivalent to 5.9 W/cc. No axial or radial peaking was assumed. The coolant channels in the reactor were 1.5 cm in radius. For this analysis, the shutdown power level was assumed to be a constant 1%, or 10 MW. The vessel was 500 cm in radius, with heat exchanger tubes 1.5 cm in radius filling ~50% of the free volume. The ultimate heat sink was assumed to be a radiator at a constant temperature of 942°C (1215 K). The radiator, or redundant combination of radiators, could be located outside of the containment building and would be cooled primarily by thermal radiation. The radiator could be fed at all times and covered, or otherwise insulated, under normal operating conditions. In order to dissipate 10 MW of heat at 1215 K, the surface area required would be 80 m².

The results of the analysis are shown in Figure 25. For the Flibe molten salt, the volumetric coefficient of expansion is 0.0003 /K. The secondary flow is established with the higher density molten salt in the radiator and downcomer section of the heat exchanger. The temperature at the inlet to the heat exchanger is 942°C, the same temperature as the radiator. The outlet temperature of the heat exchanger is calculated to be 1119°C. The total flow rate in the secondary is 25 kg/s. The cooling of the salt in the pool by the heat exchanger allows for a higher density salt within the pool as compared to the core, which enables the natural circulation flow. The inlet temperature to the core is calculated to be 942°C and the outlet 1123°C. The total mass flow rate through the core is 23 kg/s. The maximum coolant wall temperature is calculated to be 1154°C. The maximum fuel temperature would only be a few degrees higher than this value. This temperature is significantly below the 1600°C maximum allowable transient temperature for SiC particle fuel.

In conclusion, using natural circulation flow as the passive cooling design feature for a molten-salt cooled system is an acceptable alternative to passive cooling through the pressure vessel. Although more design analysis would be required, this methodology could allow for significantly lower temperatures in the core under passive cooling conditions.

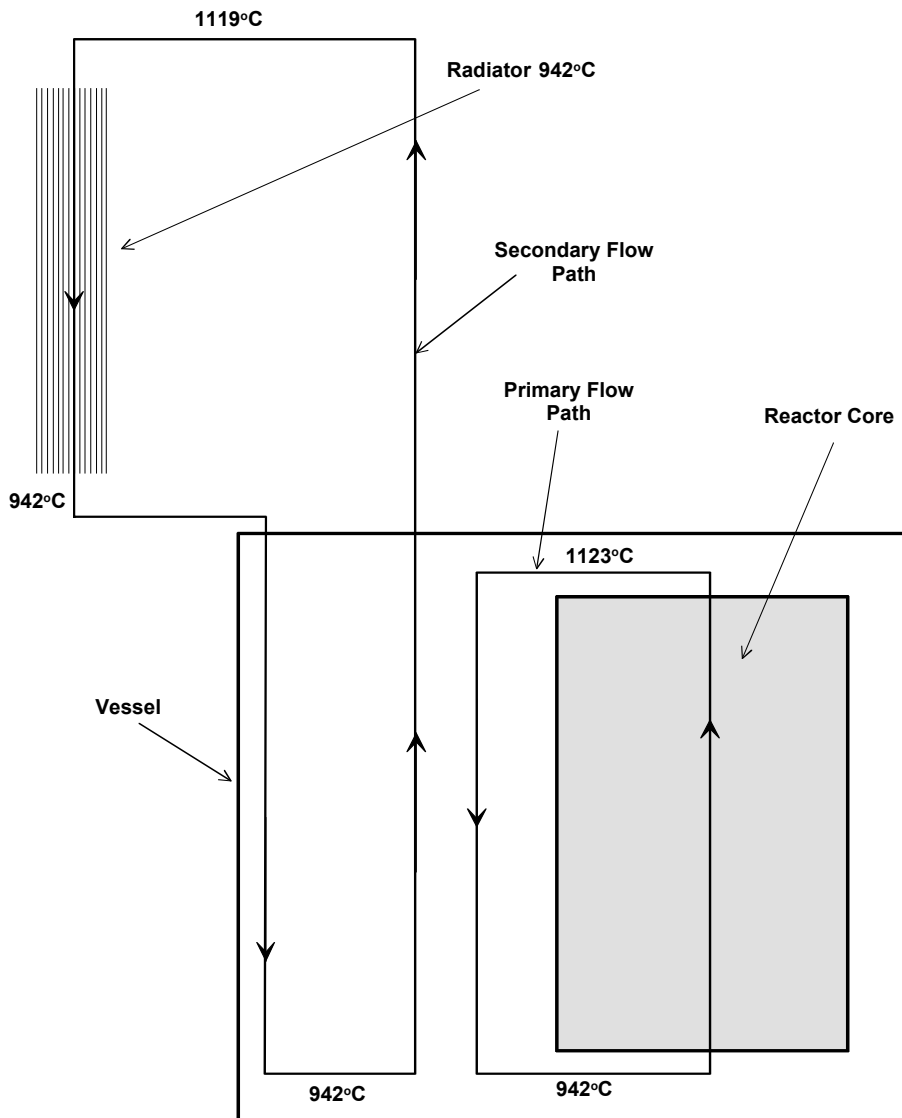


Figure 25. Natural Circulation Passive Cooling Results for the AHTR.

5.2 VHTGR – Passive Heat Removal Analysis

A one-dimensional (radial) transient conduction calculation, similar to the AHTR analysis, was performed for the VHTGR concept to determine the maximum core temperature and pressure vessel temperature as a function of time, allowing for passive cooling through the vessel wall to air. The dimensions, materials, and thermal properties for this study are shown in Table 10. See Figure 2 for a representative illustration of the VHTGR. The boundary from the pressure vessel to the air heat sink was assumed to be convective. The natural convection heat transfer coefficient was increased an order of magnitude since the air would be flowing by the vessel under natural circulation flow.

Table 10. Dimensions and Properties for the VHTGR Passive Heat Removal Analysis.

Region	Radius or Thickness (cm)	Conductivity (W/cm-K)	Density x Heat Capacity (J/cm ³ -K)
Core - Graphite or Graphite Pebble	200	0.63 or PB Correlation	3.235 or 1.941 for PB
Reflector/Thermal Barrier - Graphite	100	0.0109	4.797
Pressure Vessel – Stainless Steel	5	0.190	4.360

The results are shown in Figures 26 for the core operating at 5W/cc for 10 years prior to shutdown. No radial or axial peaking factors were assumed in the analysis. Figure 26 shows the results assuming radial heat conduction through the core, reflector and pressure vessel. The initial temperature of the core is assumed to be a constant 800°C, an arbitrary value chosen as representative. At time equal to zero, the vessel maximum temperature is calculated to be ~320°C.

For the solid graphite core calculation, a maximum core temperature of 1275°C is reached at ~15 hours after shutdown. The maximum vessel temperature, however, begins decreasing after time equal to zero. Other calculative results show that a thinner thermal barrier, or one with a higher conductivity, would allow for a low maximum core temperature, but a higher vessel temperature. Lowering the power density, decreasing the radius of the core, increasing the heat capacity of the core, or increasing the conductivity of the core would decrease the maximum core temperature.

The same calculation was performed except that the thermal conductivity for a pebble-bed core (Stroh, 1979) with 6-cm diameter pebbles was used. A maximum core temperature of 1580°C is reached at ~21 hours after shutdown. This illustrates why the pebble-bed reactor concepts have small diameters and have greater length than would be designed from a neutronics perspective.

In conclusion, this analysis shows that passive decay-heat cooling of the VHTGR concept through the vessel is feasible and could be optimized to work for a power density of ~5 W/cc and radial core size of greater than 200 cm. Alternative cooling media at the vessel boundary, such as water, should also be investigated.

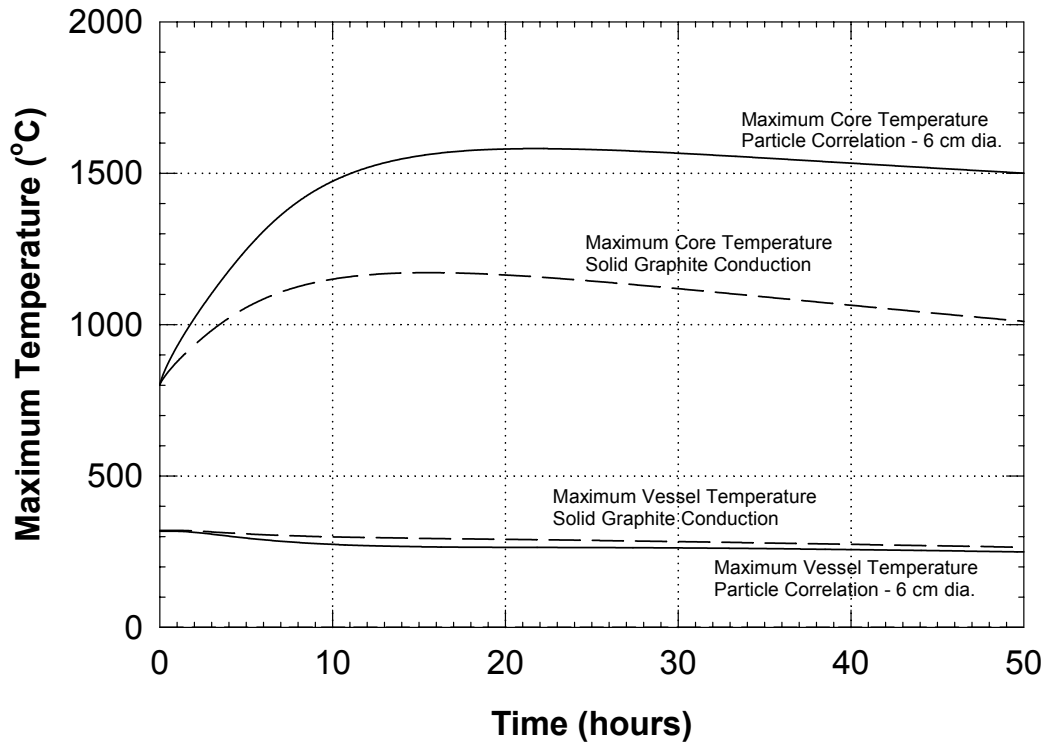


Figure 26. Passive Cooling Results for the VHTGR.

5.3 UHTGR – Passive Heat Removal Analysis

A one-dimensional (radial) transient conduction calculation, similar to the VHTGR analysis, was performed for a UHTGR module to determine the maximum core temperature and pressure vessel temperature as a function of time. Both air and water cooling of the pressure vessel wall were analyzed. The dimensions, materials, and thermal properties for this study are shown in Table 11. Representative illustrations of the UHTGR module and configuration are shown in Figures 3 and 4. The boundary from the pressure vessel to the air or water heat sink was assumed to be convective. The natural convection heat transfer coefficient was increased an order of magnitude for air cooling, since the air would be flowing by the vessel under natural circulation flow. For this analysis, the helium return is through the center of the module through a graphite pebble bed with pebbles 6 cm in diameter. The coolant reaches the bottom of the module and flows axially through the fuel bed to the outlet. The fuel bed is 6-cm diameter pebbles. A graphite thermal barrier is outside of the fuel bed and is composed of 1-mm diameter graphite spheres. The smaller spheres allow for a lower conductivity in the barrier. Outside of the graphite barrier is the pressure vessel. A graphite liner would be used to separate the inner region from the fuel bed, and the fuel bed from the graphite thermal barrier. The inner graphite bed allows for additional heat capacity during shutdown cooling.

Table 11. Dimensions and Properties for the UHTGR Passive Heat Removal Analysis.

Region	Radius or Thickness (cm)	Conductivity (W/cm-K)	Density x Heat Capacity (J/cm ³ -K)
Inner Core - Graphite Pebble	20	PB Correlation 6 cm dia.	1.941
Core – Graphite Pebble	27	PB Correlation 6 cm dia	1.941
Reflector/Thermal Barrier - Graphite Particle	10	PB Correlation 0.1 cm dia	1.941
Pressure Vessel – Zirconium Alloy	3	0.126	2.128

The results are shown in Figure 27 for the core operating at 35 W/cc for 10 years prior to shutdown. No radial or axial peaking factors were assumed in the analysis. The initial temperature of the core is assumed to be a constant 1200°C, an arbitrary value chosen as representative. At time equal to zero, the vessel maximum temperature is calculated to be ~400°C for air cooling and 175°C for water cooling.

For the air cooling calculation, a maximum core temperature of 1790°C is reached at ~4 hours after shutdown. The maximum vessel temperature increases to 575°C and then begins to decrease. For the water cooling calculation, a maximum core temperature of 1690°C is reached at ~3 hours after shutdown. The maximum vessel temperature increases slightly to 200°C and then begins to decrease. Other calculative results show that a thinner thermal barrier, or one with a higher conductivity, would allow for a low maximum core temperature, but a higher vessel temperature. Lowering the power density, decreasing the radius of the core, increasing the heat capacity of the core, or increasing the conductivity of the core would decrease the maximum core temperature.

In conclusion, this analysis shows that passive decay-heat cooling of the UHTGR module through the vessel is feasible and could be optimized to work for a power density of ~35 W/cc. Alternative cooling media at the vessel boundary, such as water, should also be further investigated. Other configurations for the module are also possible, such as return coolant flow outside of the fuel bed, flow within a two-region fuel bed, or radial coolant flow through the bed.

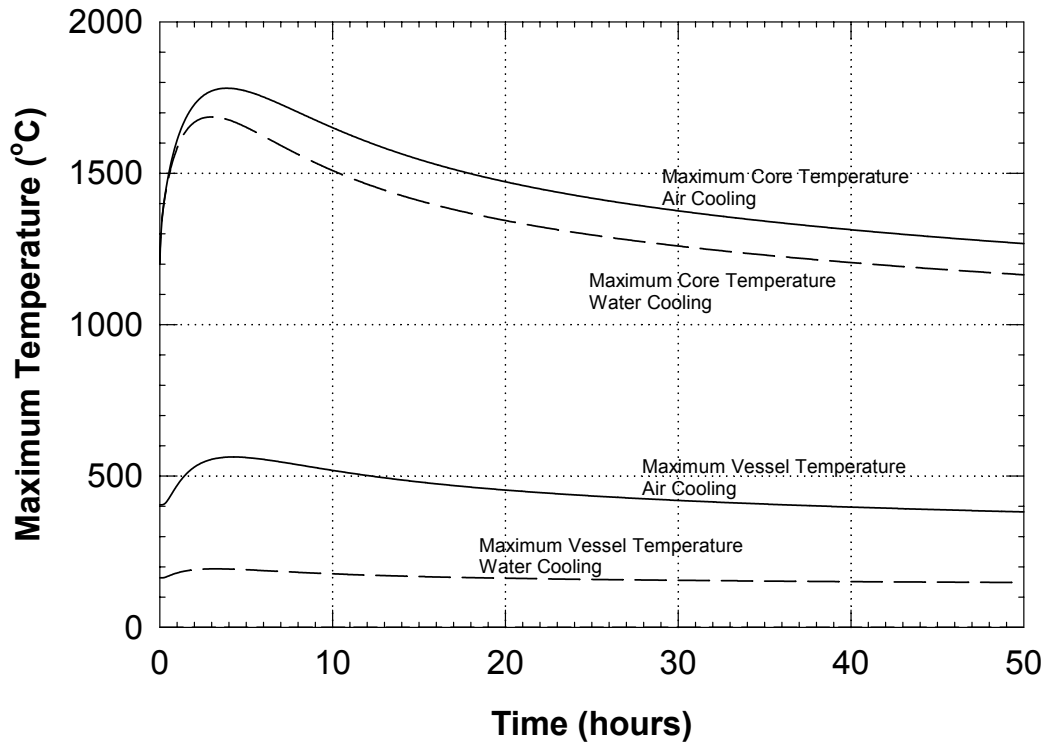


Figure 27. Passive Cooling Results for the UHTGR Module.

6. MATERIAL ISSUES

Material issues associated with nuclear reactors and coolants operating at temperatures greater than 1000°C dominate the challenges facing the VHER concepts. Most common metallic materials become very soft at temperatures approaching 1000°C. The rupture strength (rupture at 10⁵ hours) for 304 and 316 stainless steels is ~10 ksi at 600°C, and 2 ksi at 800°C (Lyman, 1961). Advanced high-temperature alloys such as INCOLOY-800H (Fe-Ni-Cr), HASTELLOY-X (Ni-Cr-Mo), and INCONEL-617 (Ni-Cr-Co-Mo) have rupture strengths ranging from 3 ksi to 9 ksi at 800°C, but drop to less than 1 ksi at 1000°C (Nickel, et al, 1984). Refractory metals and alloys such as Nb (Nb-1Zr), Ta (Ta-8W-2Hf), Mo (TZM), and W can have rupture stresses greater than 40 ksi, but are also typically very brittle and susceptible to oxidation at high temperatures. Corrosion and material compatibility at temperatures approaching 1000°C are also important. Flibe molten salt is corrosive. Helium with trace quantities of oxygen, H₂O, CO, or CO₂ can also be corrosive.

6.1 Coolant

For the VHTGR and UHTGR concepts, helium would be used as the coolant. Helium is an inert monotonic ideal gas with a high thermal conductivity relative to other gasses. He-4 is the dominant isotope of natural helium (~100%) and maintains virtually no neutron absorption cross section. Hence, helium will not become activated. The difficulty in using helium is in maintaining it at a high-purity level, oxygen-free. At high temperatures, oxygen as an impurity can readily attack metals.

For the AHTR concept, Flibe molten salt has been selected as the leading candidate for both the primary and secondary coolant. However, there exist a vast number of mixtures of different types of molten salts, some of which may have greater application to the AHTR concept. For this study, only Flibe was considered since it was used in the MSRE, has been proposed for use in other molten-salt reactor concepts, and has been extensively reviewed, studied, and considered in fusion applications (MacPherson, 1985; Bettis and Robertson, 1970; McCoy, et al., 1970; Grimes, 1970; Ignatiev, et al., 1999; Moriyama, et al., 1988; Zinkle, 1998). Flibe is a mixture of 66% LiF and 34% BeF₂. Its melting temperature is 458°C and heat of fusion is ~440 J/g. Flibe maintains superficial properties similar to water but has a density twice that of water. It has a high heat capacity and relatively high thermal conductivity. Flibe is ideal for high-temperature applications in that it maintains a low vapor pressure. At 1400°C the vapor pressure is 50 psi; at 1300°C the vapor pressure is 15 psi. In order to maintain a low neutron absorption cross section for the Flibe, the Li must be enriched in Li-7, to remove as much of the high absorption cross section Li-6 as possible. The other constituents of the Flibe maintain a low neutron absorption cross section. Flibe is also stable at high temperatures and under high-radiation environments. It is postulated that Flibe would also act as a getter for tramp fission products that might diffuse through the fuel and fuel element to the coolant. Like all molten salts, Flibe is very corrosive, and must be matched with compatible materials such as graphite, nickel alloys, and refractory metals.

6.2 Core Materials

Core materials include the fuel elements, structural materials, control rods, liners, reflectors, and thermal barriers. For the helium cooled systems, the main issues include high-temperature effects, radiation damage, thermal expansion, and to a lesser extent, corrosion due to impurities in the helium. For the Flibe coolant, the above issues are important, but the corrosion effect due to the molten salt is the dominant effect.

The material that is most dominant in the VHER concepts is graphite. Graphite is carbon that has been formed into an allotropic crystalline structure under heat and pressure. There are numerous types of graphite. Nuclear grade graphite has very small quantities of impurities. Graphite has been used extensively in the past as a thermal reactor material, since carbon has a very small neutron absorption cross section, is a low- Z element, and is easily manufactured and machined. Graphite also allows for high-temperature applications in inert environments due to its stability and high sublimation point ($>3000^{\circ}\text{C}$). Graphite can be used as an effective solid moderator or reflector. Graphite has little tensile strength and can only be used in blocks, particles, or as liners. Graphite can be made with very low thermal conductivity in a porous or pressed powder form, or with a reasonable thermal conductivity in a solid form. Radiation damage of graphite at low temperatures ($<300^{\circ}\text{C}$) can allow for the accumulation of stored energy, sometimes referred to as the Wigner energy. At higher temperatures the damage is readily annealed out of the material. The major drawback to using graphite is that it readily oxidizes in air at temperatures greater than $\sim 400^{\circ}\text{C}$ (Glasstone and Sesonske, 1967). This was a major contributor to the damage at one of the British plutonium production reactors at Windscale, and at Chernobyl.

For the AHTR concept, graphite would be used for the fuel elements and internal structures. It could also be used for the thermal barrier, or as a liner maintaining a boundary between the salt and the thermal barrier. Graphite has been used and proposed as the moderator and reflector material in molten-salt reactor concepts, where the fuel is an integral component of the salt (McCoy, et al., 1970; Ignatiev, et al., 1999). For temperatures at least as high as 700°C , graphite has been shown to perform well in Flibe molten salt, with minimal corrosion. Graphite forms carbides with virtually all metals above $\sim 600^{\circ}\text{C}$. Some exceptions include Rhenium and Copper. Hence structural materials, core materials, and control rods that contact graphite must be designed to be compatible with the graphite at high temperatures.

Refractory alloys or other high-temperature alloys could be used in the VHER concepts as liners. Some refractory elements, like W and Ta, have high neutron absorption cross sections and may not be suitable for liners in which neutrons must pass. W and Ta alloys may be used as control rods or as cladding materials for poisons, such as B_4C .

Thermal barriers for the VHER concepts can be low thermal-conductivity graphite or ceramics, if a liner is used to maintain a boundary from the coolant to the barrier. Graphite has already been discussed, and can be made to have a low thermal conductivity. Alumina/Silica and Calcia/Silica ceramics have thermal conductivities in the range of 0.001 W/cm-K and relatively good compressive strength. Low density carbides could also be used as thermal barriers.

6.3 Pressure Vessel, Piping, Heat Exchangers, Pumps

Pressure Vessel

The pressure vessel is one of the most important structural components for the VHER concepts. For the VHTGR and UHTGR, the pressure vessel must maintain an operating pressure of 1000 psi, operate at modest temperatures (300°C to 500°C), endure a high-radiation environment, and allow for heat to transfer through it for passive decay-heat cooling. For the AHTR concept, the vessel will operate at a low pressure. If natural circulation cooling through a heat exchanger is used for passive decay-heat cooling, the vessel could operate at a temperature less than 300°C.

For the AHTR concept, the vessel can be a mild steel or stainless steel, if it can be shown that no molten salt would ever come in contact with the vessel. If the molten salt could come in contact with the vessel, then Hastelloy-N or a refractory metal would be required. The vessel for the AHTR would not be required to be very thick. Since the vapor pressure of the coolant is very low at 1000°C, the thickness of the vessel will be governed by the molten-salt weight and the system over-pressure. This pressure will not be greater than about 10 psi. If natural circulation cooling is used, the vessel could be located below grade with no required cooling passages.

For the VHTGR concept, the pressure vessel can also be made from a mild steel or stainless steel. However, since the vessel must maintain a pressure of 1000 psi, it will be required to have a much greater thickness than for the AHTR. Assuming a core radius of 300 cm, an inner reflector/thermal barrier thickness of 100 cm (total radius equal to 400 cm), a pressure of 1000 psi, and a design stress of 20 ksi, the thickness of the vessel would be 20 cm (~8 in.). For a core radius of 200 cm, and an inner reflector/thermal barrier thickness of 100 cm (total radius equal to 300 cm), the thickness of the vessel would be 15 cm (~6 in.). These results are based on the hoop stress for a thin-walled pressure vessel, which is valid when the vessel wall thickness is less than 10% of the vessel radius. The size and thickness of the VHTGR pressure vessel would be the same or larger than that of a typical LWR.

For the UHTGR concept, the pressure vessel would be required to be fabricated from a low neutron absorption alloy such as Zircaloy, since the modules that make up the design concept together form a critical configuration that is very neutron-efficient. Assuming a 20 ksi design stress, a vessel radius of 50 cm, and a pressure of 1000 psi, the thickness of the vessel would be 2.5 cm (~1 in.). Although this vessel would be smaller than for the VHTGR, it would be required from a more expensive material. The pressure vessels for the UHTGR would also be exposed to a much larger fast neutron flux that could lead to greater radiation induced embrittlement.

AHTR – Piping, Heat Exchangers, Pumps

The piping, heat exchangers, and pumps that are located with the AHTR vessel operate in a low-pressure environment. However, as discussed previously, the Flibe molten salt is corrosive and must be used with compatible material.

A significant amount of research has been performed in the area of material compatibility of Flibe and metals in both the advanced molten-salt reactor concepts and in the fusion blanket concepts. Work performed on the MSRE, dating back to the 1960's, showed that Ni-based Hastelloy-N, modified with small quantities (~1%) of Ti or Hf (1%) resulted in excellent resistance to corrosion, good high-temperature strength, and improved resistance to radiation embrittlement (McCoy, et al., 1970). Other work performed recently in the U.S., Japan, and Russia has confirmed that Ni-based alloys and modified versions of Hastelloy-N have excellent corrosion resistance up to 700°C (Ignatiev, et al., 1999; Moriyama, et al., 1988; Zinkle, 1998). It is not clear what the corrosion effects would be at 1000°C.

Although refractory metals and refractory metal alloys are usually brittle, they have very high melting points and have been shown to have excellent corrosion resistance to Flibe. Table 12 shows the results from Ghoniem (1998) and Zinkle (1998) for the estimated operating range for refractory alloys in Flibe. Ghoniem based the maximum temperature limit on the corrosion rate due to dissolved impurities in Flibe salts in a fusion reactor blanket. Zinkle based the operating range on radiation effects and corrosion in fusion blankets. With the exception of Vanadium, these refractory metals are candidates for use in the AHTR concept.

Table 12. Operating Temperatures for Refractory Metal Alloys in Flibe.

Material	Melt Temperature (°C)	Ghoniem Results - Maximum Temperature (°C)	Zinkle Results – Temperature Range (°C)
Vanadium (V) V-4C-4Ti	1900	600	400-700
Niobium (Nb) Nb-1Zr	2470	1000	550-1000
Tantalum (Ta) Ta-8W-2Hf	3020	1000	700-1200
Molybdenum (Mo) TZM	2620	1000	750-1200
Tungsten (W)	3410	1400	800-1400

The piping transferring the molten-salt coolant from the heat exchanger to the process heat facility, or to another heat exchanger for electric power production, will be required to be insulated and/or within an inert media. Thermal insulation could be used with the transfer piping that would maintain the outer boundary at low temperature. If the outer boundary were at a relatively low temperature (~300°C), it could be exposed to air without oxidation concerns. If not internally insulated, the piping could be jacketed and maintained within an inert environment such as nitrogen or helium. Exposing high-temperature (1000°C) Ni-based alloys or refractory metal to an air environment would result in rapid oxidation reaction and failure of the piping.

Table 13 shows the results from work by Ghoniem for refractory metal alloys in helium with 100-ppm oxygen contamination. The results show estimated upper temperature limits. 100 ppm is equivalent to 0.01% oxygen contamination. These temperatures are on the order of 200°C lower than the estimates for Flibe. Piping at 1000°C in an inert media would have to maintain oxygen getters to ensure minimal oxygen contamination. The piping could also be coated with a high-temperature material that would act as a barrier to oxidation.

Table 13. Operating Temperatures for Refractory Metal Alloys in He With 100 appm O.

Material	Melt Temperature (°C)	Ghoniem Results - Maximum Temperature (°C)
Vanadium (V) V-4C-4Ti	1900	550
Niobium (Nb) Nb-1Zr	2470	800
Tantalum (Ta) Ta-8W-2Hf	3020	800
Molybdenum (Mo) TZM	2620	900
Tungsten (W)	3410	1200

VHTGR and UHTGR – Piping, Heat Exchangers

A significant amount of research work was performed in the 1970's and 1980's on helium-cooled high-temperature reactors and systems (Frohling and Ballensiefen, 1984; Demel, 1981; Proceedings, 1984; Proceedings, 1988; IAEA, 1999). The PNP project concentrated on high-temperature helium-cooled gas reactor systems for coal gasification. The goal was to use helium gas at 950°C to 1000°C. Some of the important results of the work were the advancement of high-temperature super alloys and coatings, the development of a He/He heat exchanger design, and the development of the annular/coaxial hot gas duct for high-temperature helium transfer to and from the reactor.

The VHTGR and UHTGR concepts would take advantage of this work and use similar design approaches for the transfer piping and heat exchangers. However, the goal of the VHTGR and UHTGR concepts would be to attain reactor exit temperatures of 1100°C and 1250°C, respectively.

A number of new alloys and coatings were developed and tested as part of the PNP project. Some of these alloys include INCOLOY-800H, an austenitic steel (Fe-32Ni-20Cr-Ti-Al) for service up to 850°C; HASTELLOX (Ni-22Cr-18Fe-9Mo-W), INCONEL-617 (Ni-22Cr-9Mo-12Co), and THERMON 4972 (Ni-22Cr-28Fe-12W-1Nb), all Ni-based alloys for service up to 950°C. All of these alloys were found to have good corrosion and oxidation characteristics in air. These alloys were also found to have some rupture strength remaining at 950°C - 1000°C, about 1.5 ksi (Nickel, et al, 1984). Coated layers of ZrO₂ and Y₃O₂ with a Ni-Cr-Al-Y sub-layer were studied to allow for service temperatures up to 1000°C.

These super alloys can be used in the piping ducts and heat exchangers for the VHTGR and UHTGR concepts by including the annular/coaxial ducting methodology in the design. The key to allowing for high-pressure and high-temperature gas transfer is by requiring that the cold return gas circulate on the outer portion of the transfer duct or heat exchanger. If the gas return is at 600°C, the rupture strength for INCONEL-617 is ~30 ksi, which is within an acceptable range for maintaining a reasonable wall thickness. Assuming the acceptable design stress is 15 ksi at 600°C and 1000 psi, with a 3-in. radius outer pipe, the wall thickness required is ~0.2 in. Since the He gas pressures within the inner and outer ducts are approximately the same, the inner wall of the coaxial duct can maintain much less strength at the elevated temperature. The outer wall would maintain foil radiative barriers, or other insulating material, to minimize the heat losses from the piping or heat exchanger. The only drawback to this approach would be in the event of a pressure loss within the outer boundary, allowing the inner piping to rupture.

For the VHTGR concept, it is unclear if the technology currently exists such that temperatures of 1100°C could be reached for transferring He gas. Certainly for the UHTGR concept at 1250°C, new advances in materials and coating would be required, along with a significant research and development program.

7. CRITICALITY AND BURNUP

Criticality, reactivity, and burnup calculations were performed for the VHER concepts in order to determine reactor size requirements, refueling time, and temperature coefficients for low density highly carbon moderated systems. In addition, the void coefficient of reactivity was analyzed for the AHTR Flibe cooled concept. The Monte Carlo neutronics code MCNP, version 4B (Briesmeister, 1997), was used extensively to perform the calculations. The burnup analysis was performed using the burnup code BURNCAL (Parma, 2002), which uses MCNP-4B to perform the neutronics portion of the analysis.

Many preliminary scoping calculations were performed to better understand the neutron physics, neutron efficiency, and other variables associated with a carbon dominated reactor system. Additional calculations using Th-232 in different configurations were performed to determine conversion and breeding potential for the VHER concept using a carbon moderator. From these results, more detailed analyses were performed for specific systems. The goal of the burnup analysis was to determine, for specific reactor systems, the core lifetime, fuel utilization, and waste volume as compared to current LWR technology. The analyses presented in this report will focus on this aspect of the work. In addition, the results presented use the fuel element information presented in Chapter 4, with particular emphasis on maintaining the fuel loading within the bounds previously established for particle fuel interspersed within a graphite matrix. Advanced fuel forms could allow for higher uranium loadings to be achieved, which would be beneficial in extending the core lifetime and allowing for the addition of Th-232 in the fuel. However, since this would be highly speculative and possibly unachievable, given the particle nature of the current advanced fuel form, the analyses presented here only considers current uranium loading densities.

The standard measure for burnup is in watt-days (WD) or Megawatt-days (MWD), where the power value is total thermal power generated. The mass of heavy metal or uranium in the initial inventory of fuel is usually designated in metric tons (MT) equal to 1000 kg.

Three metrics will be used in this report to measure burnup performance:

1. Power x Time / Core Volume (WD/cc);
2. Power x Time / Heavy Metal (U) Loading (MWD/MTU);
3. Power x Time / Fissile (U-235) Loading (MWD/MTU-235).

The value for WD/cc can be found by multiplying the power density by the number of days with the effective multiplication (k_{eff}) greater than 1.0. The value for MWD/MTU is found by dividing WD/cc by the initial loading density of the uranium in g/cm^3 . The value for MWD/MTU-235 is found by dividing MWD/MTU by the initial fuel enrichment.

For this report it is also useful to determine the burnup performance in terms of electrical power generated. For a typical LWR, the values for these metrics are as follows:

1. 60,500 WD/cc (thermal) \Rightarrow 20,000 WD/cc (electrical);
2. 33,000 MWD/MTU (thermal) \Rightarrow 11,000 MWD/MTU (electrical);
3. 1,100,000 MWD/MTU-235 (thermal) \Rightarrow 350,000 MWD/MTU-235 (electrical).

The first metric, WD/cc, allows for a burnup comparison on the total volume of waste generated, including void space within the fuel assemblies. The second metric, MWD/MTU, is the standard comparison used for LWRs, based on heavy metal loading. The third metric, MWD/MTU-235, allows for a comparison based on the effective utilization of the U-235.

7.1 Infinite Reactor Calculations

Infinite reactor burnup calculations were performed for 20% and 10% enriched U-235 fuel, with varying uranium to carbon weight ratios (U/C), in order to determine the moderation characteristics and burnup performance for infinite systems. Figures 20 and 21 present the results for the 20% and 10% enrichments, respectively. The calculations were performed for a power density of 5 W/cc and with the moderator temperature at 900°C. Since carbon has a very small capture cross section, reducing the U/C ratio results in a higher value of k_{∞} . Hence, the system cannot become over-moderated with carbon. For the 20% enriched analysis, U/C ratios from 0.01 to 0.6 are viable from a burnup perspective. Note, however, that using the current fuel loading capability (see Tables 2 and 3), the maximum U/C loading currently achievable is ~ 0.2 , assuming no void space. For the 10% enriched analysis, U/C ratios from 0.01 to 0.10 are viable, since k_{∞} is below 1.0 at time equal to zero for U/C ratios greater than 0.15.

Burnup performance based on the U-235 utilization and thermal power generated is shown in Figures 28 and 29 for each U/C value. Using this metric and the overall core lifetime, U/C ratios from 0.02 to 0.05 are found to be acceptable fuel loadings for homogeneous systems. This range of values was studied in more detail for finite VHER reactor systems.

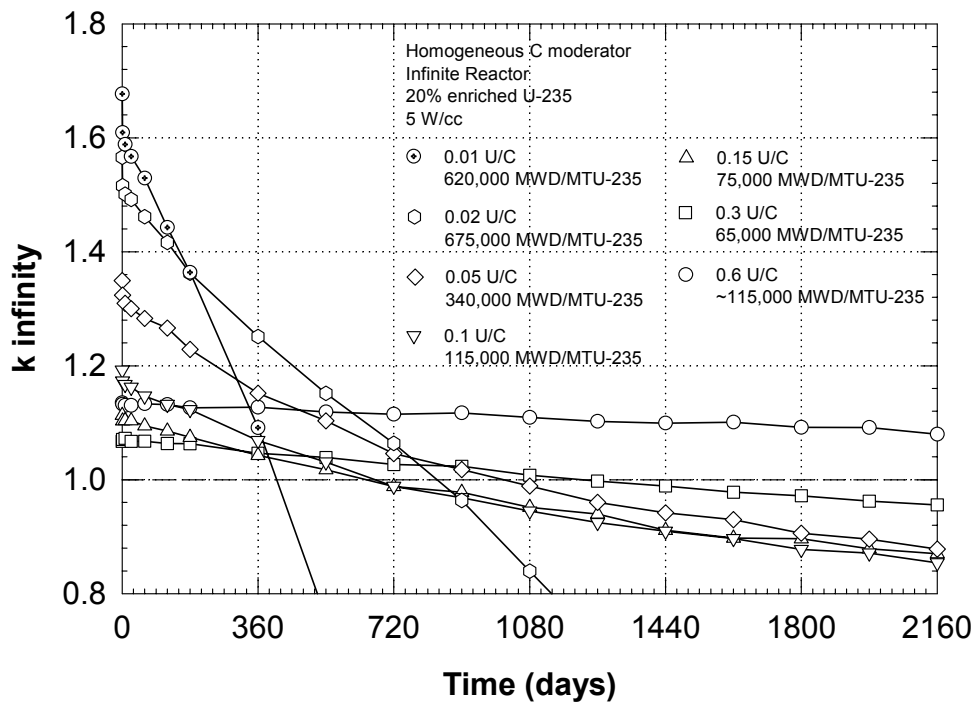


Figure 28. Burnup Results for 20% Enriched U-235 Infinite Reactor.

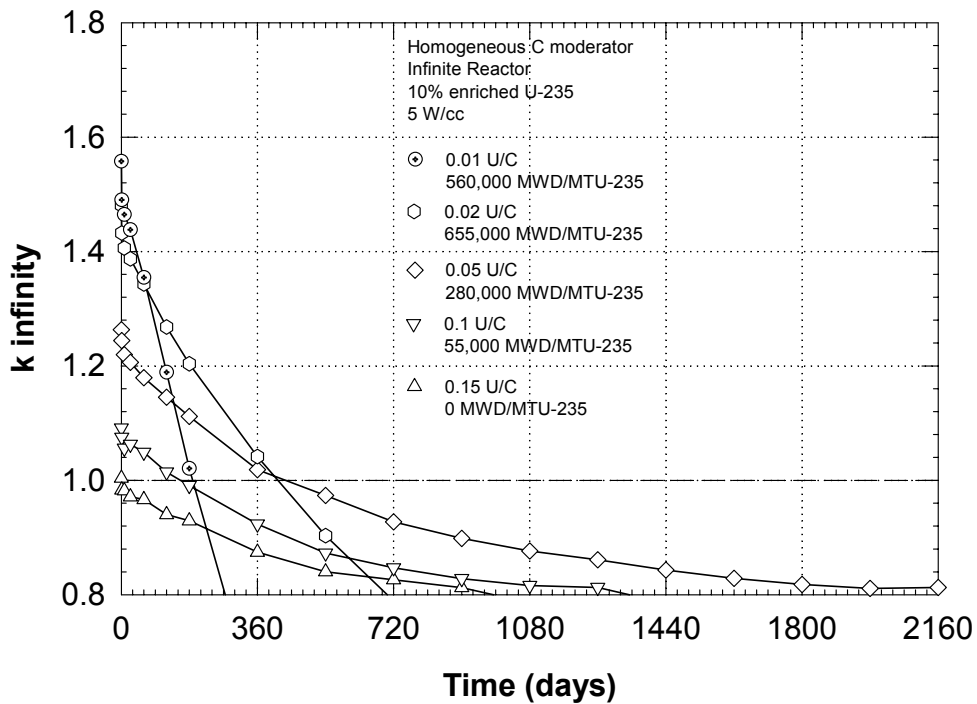


Figure 29. Burnup Results for 10% Enriched U-235 Infinite Reactor.

7.2 AHTR Neutronics Analysis

For the AHTR concept, two fuel element configurations were analyzed in a finite reactor geometry: 1) homogeneous - a cylindrical homogeneous fuel element with a 10% volume fraction coolant channel with Flibe coolant; and 2) heterogeneous - a cylindrical homogeneous fuel element within a prismatic graphite moderator and a coolant channel around the fuel, as shown in Figure 8a. The reactor size was 300 cm in radius and 600 cm in height. At 5 W/cc average power density, the reactor would generate ~850 MW of thermal power. A 100 cm Flibe reflector completely surrounded the core and a 100 cm carbon reflector surrounded the Flibe in the radial direction. The moderator and reflector was set to 900°C.

The Flibe coolant void reactivity coefficient was analyzed for the homogeneous element configuration with 10% coolant fraction, a fuel element radius of 3 cm and a U-235 enrichment of 10%. The results are shown in Figure 30 for U/C weight ratios ranging from 0.02 to 0.1. The results show that for U/C ratios less than ~0.05, complete voiding of the coolant from the core could result in a significant positive reactivity addition. Results for the inner and outer quarters of the core voided were within two standard deviations from the result with the complete core voided. For a U/C equal to 0.02, voiding the complete core resulted in a reactivity addition of ~\$1.00. Other calculations, with poison added (B-10 or Th-232) to reduce k_{eff} to 1.0 for the normal condition, resulted in a negative reactivity effect. Hence, for a “real” reactor system that would include poison control, it is unclear if a positive reactivity condition could exist.

Figure 31 shows the fission generation time for the cases used to generate Figure 30. The results for the un-voided nominal condition are shown. The results for the voided cases are not significantly different. The results show that the fission lifetime increases with decreasing U/C ratio. Values vary between ~1.3 ms for 0.02 U/C to 0.3 ms for 0.1 U/C. These values are significantly greater than that of an LWR, which ranges from 0.01 to 0.1 ms. For a 1 ms generation time and a positive reactivity insertion of \$1.0, the reactor period would be ~0.8 s, which is a very slow transient response.

Although having a U/C ratio of less than 0.05 could be an acceptable configuration for an AHTR reactor concept, the analysis presented hereafter will concentrate on a U/C of 0.05.

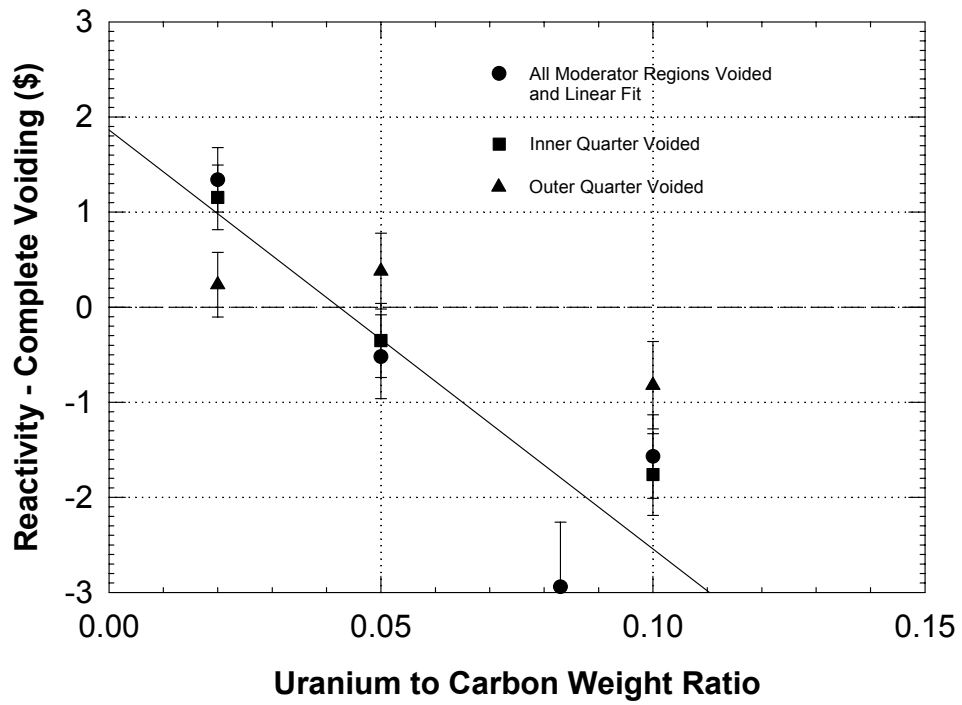


Figure 30. Void Reactivity for the 10% Coolant Fraction AHTR.

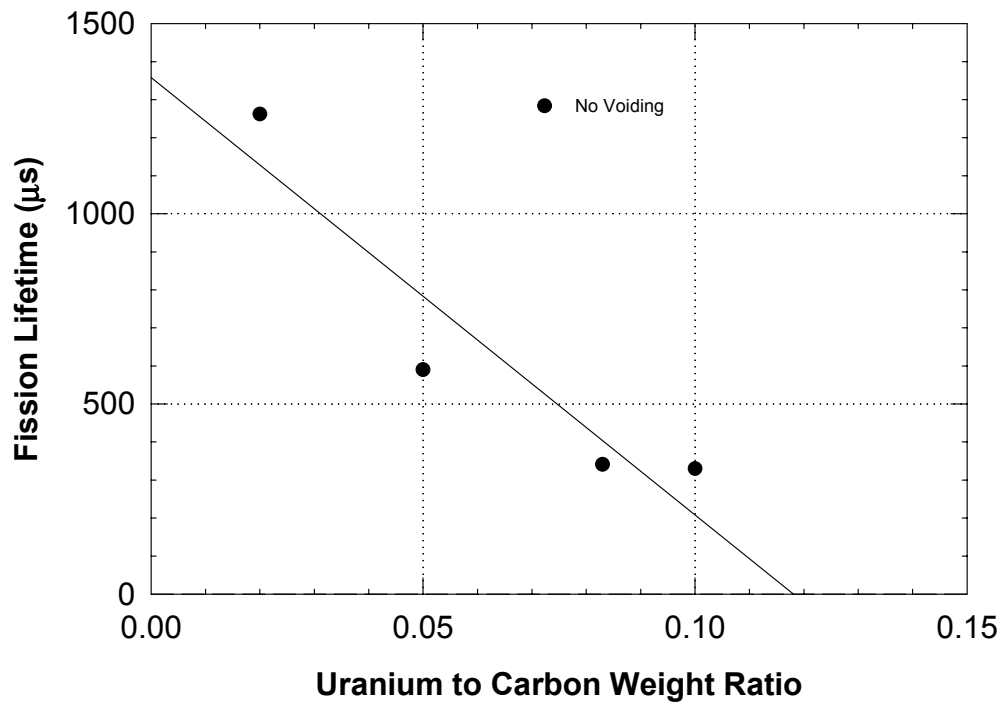


Figure 31. Fission Lifetime for the 10% Coolant Fraction AHTR.

Burnup calculations were performed for the homogeneous fuel element AHTR reactor system with 0.05 U/C, 10% coolant fraction, and 10% U-235 enriched fuel. The results are shown in Figure 32 for an average reactor power density of 5 W/cc. The core was divided into three equal area radial regions to allow for the fuel to be shuffled from the outer region to the inner region at specified reload intervals. At each shuffling, new fuel was placed in the outer third region of the core. Shuffling allows for the fuel to be burned for a significantly longer duration, as compared to a single burn and complete reload with fresh fuel. For the initial loading, the core lifetime was ~540 days. After several partial reloads, the reactor has reached an equilibrium condition in fission product and actinide inventory. The last partial reload shows the burnup duration to be ~280 days. Multiplying this value by three gives the core lifetime of ~840 days.

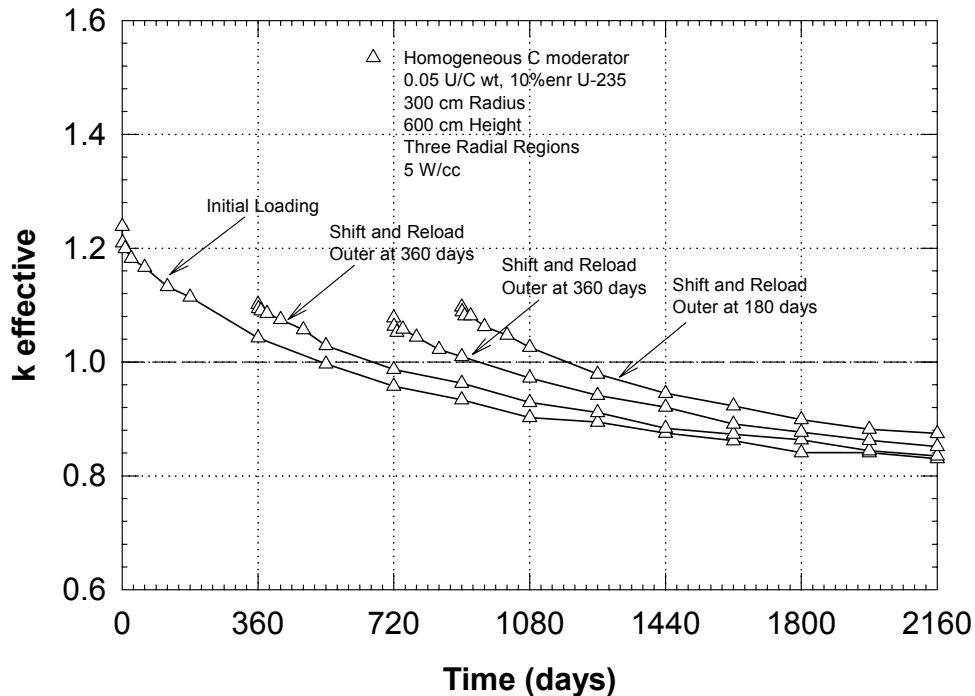


Figure 32. Burnup Results for the AHTR With 0.05 U/C Homogeneous Fuel Element.

The burnup performance metrics are calculated as follows, assuming thermal power and a 55% electrical power generation efficiency:

1. 4,200 WD/cc (thermal) \Rightarrow 2,300 WD/cc (electrical);
2. 55,400 MWD/MTU (thermal) \Rightarrow 30,500 MWD/MTU (electrical);
3. 554,000 MWD/MTU-235 (thermal) \Rightarrow 305,000 MWD/MTU-235 (electrical).

Comparing the electrical power generation results to that of an LWR, the 1st metric (WD/cc) is almost an order of magnitude lower than that of an LWR. If the fuel was disposed of without reprocessing or waste reduction, the volume of waste would be ~9 times that of an LWR,

assuming the fuel rods of the LWR are also not reprocessed or allowed for waste reduction. The other two metrics are close to that of an LWR.

In order to potentially achieve longer burnup durations, analyses were performed where the fuel region was separated from the moderator region, allowing for more neutron thermalization to occur outside of the fuel region. Using a heterogeneous fuel element, described earlier and shown in Figure 8a, the potential exists for significantly increasing the resonance escape probability of the neutrons. For this case, the fuel region was loaded with the maximum uranium loading of 0.32 g/cm^3 , shown in Table 3. The overall U/C weight ratio of 0.05 was maintained for the fuel element by adjusting the size of the moderating region. The results for this case are shown in Figure 33 and 34. The same fuel-shuffling scheme was used as for the homogeneous fuel element. The last shuffle and reload shown in Figure 34 allows for a burnup duration of ~ 650 days or a core lifetime of ~ 1950 days (~ 5.5 years).

The burnup performance metrics are calculated as follows, assuming thermal power and a 55% electrical power generation efficiency:

1. 33,700 WD/cc (thermal) \Rightarrow 18,500 WD/cc (electrical);
2. 112,500 MWD/MTU (thermal) \Rightarrow 61,900 MWD/MTU (electrical);
3. 1,125,000 MWD/MTU-235 (thermal) \Rightarrow 618,800 MWD/MTU-235 (electrical).

Comparing the electrical power generation results to that of an LWR, the 1st metric (WD/cc) is now almost the same value as that of an LWR. This condition assumes that the fuel region can be separated from the moderator region for disposal. If the fuel cannot be separated from the moderating graphite, the 1st metric will be ~ 3.5 times less than the value shown. The other two metrics exceed that of an LWR, the U-235 utilization by almost a factor of two.

Other cases were analyzed to determine if the initial k_{eff} and radial peaking factor could be lowered to values close to 1.0 for the duration of the burnup. The results indicate that adding boron poison that depletes over the core lifetime and allowing for a center radial region of graphite within the core allows for adequate control of k_{eff} and radial peaking factors.

The problem using the heterogeneous type element is that the power density in the fuel region is higher than for the homogeneous element. For the case presented, the power density in the fuel region is $\sim 15 \text{ W/cc}$. In order to maintain low temperatures within the fuel, and still maintain core exit temperatures of 1000°C , the coolant channel must be of adequate size, or a number of cooling channels must be incorporated into the fuel region as shown in Figure 9.

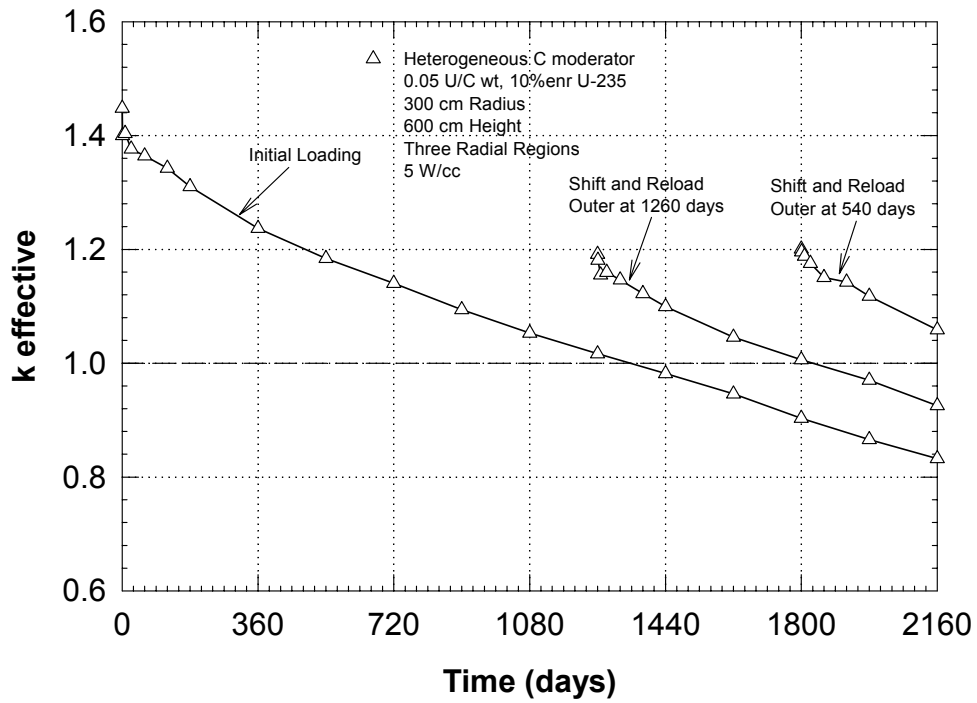


Figure 33. Burnup Results for the AHTR With 0.05 U/C Heterogeneous Fuel Element.

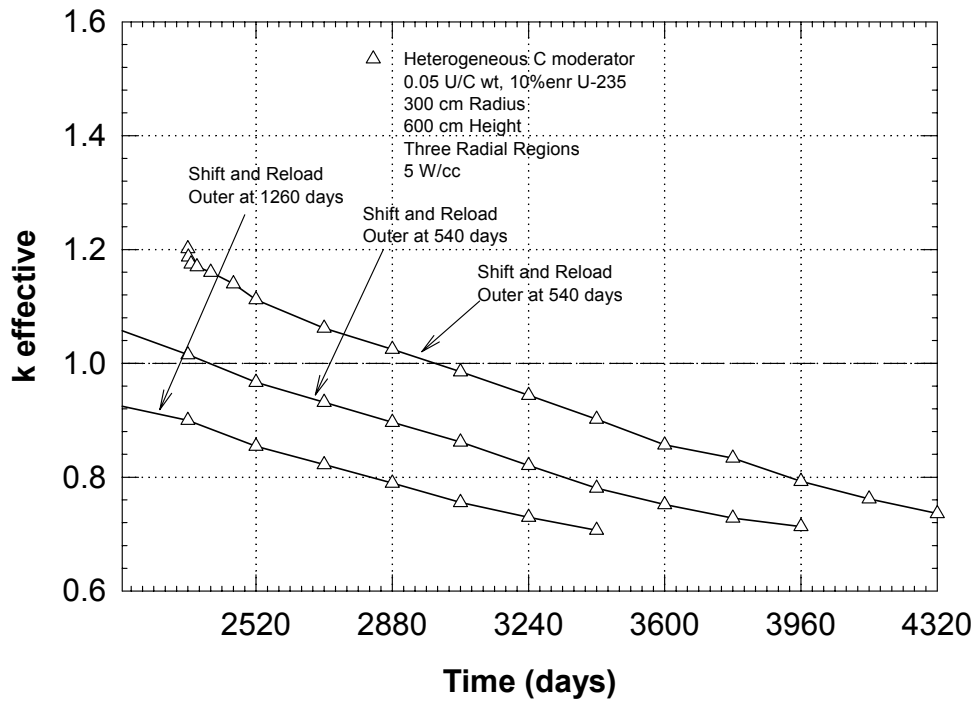


Figure 34. Burnup Results for 0.05 U/C Heterogeneous Fuel Element (Continued).

7.3 VHTGR Neutronics Analysis

No specific criticality or burnup calculations were performed for the VHTGR concept. The VHTGR concept is very similar neutronically to the AHTR, except that the coolant is helium instead of Flibe molten salt. Both concepts use the same type of prismatic fuel element design. For the VHTGR, the helium does not play a role in the neutronics analysis since it has a very small capture cross section and is at a relatively low atomic density. The Flibe coolant acts as a moderator and is similar to carbon in its scattering properties. Hence, all of the analysis performed for the AHTR is applicable to the VHTGR, with the exception of the void reactivity coefficient. The VHTGR will not have a void coefficient of reactivity. Therefore for the VHTGR, the U/C weight ratio can be less than 0.05 if required.

In order to passively cool the VHTGR, the fuel elements will be required to be cooled by channel holes versus annular channels, such that the prismatic elements and the fuel can remain in direct contact and allow for thermal conduction across the core. For the heterogeneous prismatic fuel element, the fuel cylinder would be in direct and intimate contact with the moderator graphite. This may not allow for the fuel to be separated from moderating material, requiring a larger waste volume unless the fuel is reprocessed.

7.4 UHTGR Neutronics Analysis

Criticality and burnup calculations were performed for the UHTGR concept using 18 modules as shown in Figures 3 and 4. The module dimensions and regions are shown in Figure 35. A module consists of an inner graphite region, an annular fuel region, an insulating region, and the pressure vessel. Not included in the neutronic analysis are the liners separating the different regions. The module shown in Figure 3 depicts the helium coolant entering the central graphite region and flowing downward to the bottom of the module, then axially upward through the fuel bed. The flow configuration does not change the neutronic characteristics of the core. For this analysis, the inner moderator region is graphite pebbles loaded in a cylinder with a radius of 20 cm. The fuel bed, 27 cm in thickness, is made up of fuel pebbles with material densities shown in Table 2. The particle coating was assumed to be SiC. Although Si in the form of SiC may or may not be the actual material used in the fuel, it is expected that other coating materials will have similar neutronic characteristics. Surrounding the fuel bed is an insulating graphite particle bed, 5 cm in thickness, and a Zircalloy pressure vessel, 3 cm in thickness. The module fuel region is 400 cm in height. The total fuel volume for a single module is $2.27 \times 10^6 \text{ cm}^3$.

Calculations were performed for an 18-module configuration on a triangular pitch of 120 cm, with graphite (C) or heavy water (D₂O) at 20°C in the region between the modules. Both packing fractions in Table 2 (0.055 and 0.22) were analyzed with 8% and 20% U-235 enriched fuel. Power densities of 5 and 50 W/cc in the fuel bed were investigated. Burn time results for a complete core reload (i.e., with no shuffling) are shown in Tables 14 and 15 for carbon and D₂O within the regions between the modules with a 0.22 particle packing fraction in the fuel pebbles. The results show that using higher enriched fuel and heavy water allows for longer burn times. The burn times are also not found to scale linearly with power density, due to the effect of fission product poisoning.

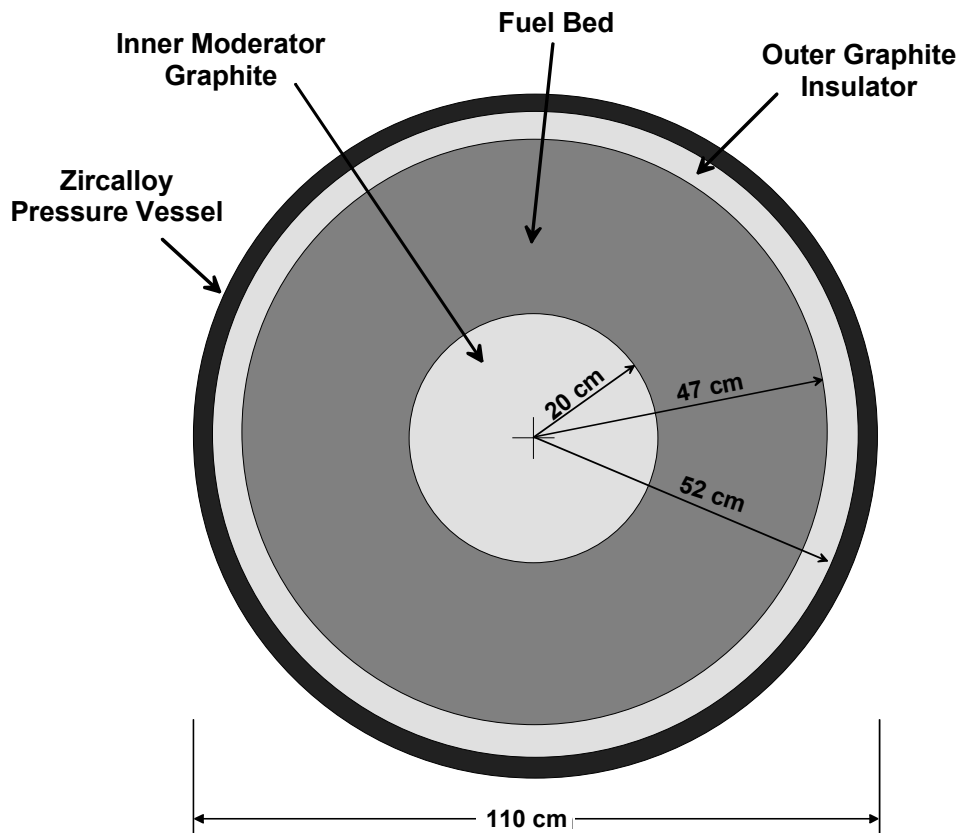


Figure 35. Dimensions for the UHTGR Module.

Table 14. Burnup Results for the UHTGR Using Graphite Moderator.

Power Density (W/cc Fuel Bed)	Burn Time for 8% Enrichment (days)	Burn Time For 20% Enrichment (days)
5	360	2700
50	24	180

Table 15. Burnup Results for the UHTGR Using Heavy Water Moderator.

Power Density (W/cc Fuel Bed)	Burn Time for 8% Enrichment (days)	Burn Time For 20% Enrichment (days)
5	1080	>2880
50	60	360

The result for the graphite moderated system at 5 W/cc and 8% enrichment is similar to the result obtained for the AHTR homogeneous fuel element. Allowing for fuel shuffling and reloading, as was performed for the AHTR, would allow for a significant increase in the burn time duration.

A shuffle and reload analysis was performed for a heavy water moderated condition with 0.22 particle packing and 20% U-235 enriched fuel. The complete reload case is shown in Table 15 with a resulting burn time of 360 days. The reactor was divided into three regions: the inner six modules; the middle six modules; and the outer six modules. Similar to the AHTR analysis, the modules were shuffled outside-to-in with fresh fuel reloaded into the outer modules. For a power density of 50 W/cc, a burn time of 180 days was calculated for a partial reload, equal to a core lifetime of 540 days.

For the last result, 50 W/cc and a core lifetime of 540 days, the burnup performance metrics are calculated as follows, assuming thermal power and a 60% electrical power generation efficiency:

1. 27,000 WD/cc (thermal) \Rightarrow 16,200 WD/cc (electrical);
2. 140,600 MWD/MTU (thermal) \Rightarrow 84,400 MWD/MTU (electrical);
3. 703,100 MWD/MTU-235 (thermal) \Rightarrow 421,900 MWD/MTU-235 (electrical).

Comparing the electrical power generation results to that of the AHTR with the heterogeneous fuel element, the results were found to be ~30% less for the UHTGR. The AHTR result was obtained using 5 W/cc. For a lower power density condition in the UHTGR, the results would be expected to equal or exceed those of the AHTR.

8. CONCLUSIONS

A technical and feasibility analysis of the VHER concepts has been presented in detail in this report. The information is shown in a summary type fashion in Table 16 which associates a semi-quantitative figure of merit for each concept for a given category or subject area. Although rating the concepts in each area is somewhat subjective, the positive and negative aspects of each design are apparent.

Table 16. Figure of Merit for the VHER Concepts

Parameter	AHTR	VHTGR	UHTGR
Fuel Design	●	⊙	⊙
Coolant Characteristics	○ ⁻	●	●
System Pressure/ Pressure Vessel	● ⁺	○	○
Passive Safety	● ⁺	●	●
Thermal Efficiency	●	●	●
Containment Building	●	●	●
Process Heat Applicability	● ⁺	●	●
Proliferation Resistance	●	●	●
Burnup Efficiency	●	●	●
Fuel Cost	○?	○?	○?
Overall Technical Feasibility	⊙	⊙	○
Unique Aspects Should be Investigated Further	●	●	●

- ⁺ Highly Positive
- Positive
- ⊙ Neutral (Neither Positive or Negative)
- Negative
- ⁻ Highly Negative

The AHTR concept has some unique features that set it apart from the other concepts. Using a molten salt coolant allows this design to have highly positive advantages in the areas of system pressure, passive safety, and process heat applicability. Other positive aspects are in the areas of the fuel design and potential thermal efficiency. Since this concept would use existing particle fuel technology, no research oriented fuel development effort would be required. A highly negative aspect of the design is that the molten salt has corrosion and freeze/thaw issues. An uncertainty for all of the VHER concepts is in the area of fuel cost. It is assumed that the

fuel costs could be made competitive with LWR fuels. However, this assumption would need to be investigated further. Also fuel enrichments of 10% or 20% are required for these systems in order to maintain a respectable U-235 loading in the dilute carbide fuel particle and element. There are no unique technical issues that would hinder development of the AHTR concept. The Flibe molten salt has been studied in depth for molten salt type reactors and for fusion blanket coolants. This concept should proceed as the next logical power reactor, especially for process heat applications.

The VHTGR concept is similar to current designs for prismatic gas cooled reactors such as the GT-MHR. The VHTGR concept exit temperature is proposed to be 1100°C. The positive aspects of this concept over the AHTR are the characteristics of the helium coolant and the potential to use a direct Brayton cycle. Some evolutionary advances in the fuel design would be required. Passive decay cooling and process heat applicability are less positive compared to the AHTR design. A negative aspect of the design is the pressure vessel and piping. Transfer of high-temperature and high-pressure gas presents unique engineering challenges. This concept should continue to be studied, especially for high efficiency Brayton cycle electric power production.

The UHTGR concept represents a more revolutionary design allowing for exit temperatures of up to 1200°C. This concept is similar to the current PBMR design, but uses smaller modular pressure vessels. The positive and negative aspects of this concept are the similar as for the VHTGR, with the potential for even higher exit temperatures. The negative aspects of the concept center on material issues and overall technical feasibility. It is not evident that a 1200°C exit temperature has any cost benefit or unique application compared to the other designs. The unique feature of the UHTGR – the modular design feature – should be investigated further even if 1200°C exit temperatures are not achievable or required. The modular design with pebble fuel would allow for higher power densities, more effective passive cooling, potential for online refueling, smaller pressure vessels, and potentially higher plant generating capacity.

The role of high-temperature reactor systems is essential if the role of nuclear energy is to expand. The near term approach of the U.S. should be to take advantage of existing technology, material performance, and fuel designs using high heat capacity and low pressure. Designs that mitigate high-temperature material performance may be more important than improved material properties. The benefits of extremely high exit temperatures must be weighed against the cost and technological risk associated with the design. The designs presented in this report must be further studied and pursued with regard to cost and feasibility estimates in order to better understand their potential impact on the next generation power reactor.

9. REFERENCES

Bettis, E. S.; Robertson, R. C. (1970) "The Design and Performance Features of a Single-Fluid Molten-Salt Breeder Reactor," *Nucl. Appl. Tech.*, **8**, 190, 1970.

Bird, R. B.; Stewart, W. E.; Lightfoot, E. N. (1960) *Transport Phenomena*, John Wiley and Sons, New York, NY, 1960.

Brown, L. C.; Eesenbruch, G. E.; Schulz, K. R.; Marshall, A. C.; Showalter, S. K.; Pickard, P. S.; Funk, J. F. (2002) "Nuclear Production of Hydrogen Using Thermochemical Water-Splitting Cycles," Proceeding of the International Congress on Advanced Nuclear Power Plants (ICAPP), Hollywood, FL, June 9-13, 2002.

Briesmeister, J. F. editor (1997) "MCNP - A General Monte Carlo N-Particle Transport Code, Version 4B," LA-12625-M, Los Alamos National Laboratory, Los Alamos, NM, March 1997.

Demel, O.; editor (1981) "High Temperature Metallic Materials for Application in Gas-Cooled Reactors," Proceedings of a Specialists' Meeting Organized by the International Atomic Energy Agency, Vienna, Austria, May 4-6, 1981.

Duderstadt, J. J.; Hamilton, L. J. (1976) *Nuclear Reactor Analysis*, John Wiley and Sons, New York, NY, 1976.

Frohling, W.; Ballensiefen, G. (1984) "Special Issue on the High-Temperature Reactor and Nuclear Process Heat Applications," *Nuclear Engineering and Design*, Vol. 78, No. 2, April 1984.

Ghoniem, N. M. (1998) "Chemical Compatibility and High-Temperature Limits for Structural Materials," APEX Study Meeting, Sandia National Laboratories, Albuquerque, NM, July 1998.

Glasstone, S.; Sesonske, A. (1967) *Nuclear Reactor Engineering*, Van Nostrand Reinhold Company, New York, NY, 1967.

Goodin, D. T. (1982) "Accident Condition Performance of Fuels for High-Temperature Gas-Cooled Reactors," *J. Am. Ceram. Soc.*, **65**, 238, 1982.

Grimes, W. R. (1970) "Molten-Salt Reactor Chemistry," *Nucl. Appl. Tech.*, **8**, 137, 1970.

Hosegood, S. B. (1988) "An Independent Engineer's View of the Modular HTGR," *Nucl. Eng. Des.*, **109**, 221, 1988.

IAEA (1997) "Fuel Performance and Fission Product Behaviour in Gas Cooled Reactors," IAEA-TECDOC-978, November, 1997.

IAEA (1999) "Hydrogen as an Energy Carrier and its Production by Nuclear Power," IAEA-TECDOC-1085, May 1999.

Ignatiev, V. V.; Grebenkine, K. F.; Zakirov, R. Y. (1999) "Experimental Study of Molten Salt Reactor Technology for Safe, Low-Waste and Proliferation Resistant Treatment of Radioactive Waste and Plutonium in Accelerator-Driven and Critical Systems," in *Proc. of the Global '99 International Conference*, 1999.

Incropera, F. P.; DeWitt, D. P. (1985) *Fundamentals of Heat and Mass Transfer*, John Wiley and Sons, New York, NY, 1985.

Karlekar, B. V.; Desmond, R. M. (1977) *Engineering Heat Transfer*, West Publishing Company, New York, NY, 1977.

LaBar, M. P. (2002) "The Gas Turbine - Modular Helium Reactor: A Promising Option for Near Term Deployment," Proceeding of the International Congress on Advanced Nuclear Power Plants (ICAPP), Hollywood, FL, June 9-13, 2002.

Lewis, E. E. (1977) *Nuclear Power Reactor Safety*, John Wiley and Sons, New York, NY, 1977.

Lyman, T., editor (1961) *Metals Handbook, 8th Edition*, American Society for Metals, Metals Park, OH, 1961.

MacPherson, H. G. (1985) "The Molten Salt Reactor Adventure," *Nucl. Sci. Eng.*, **90**, 374, 1985.

Marshall, A. C. (2002) "An Assessment of Reactor Types for Thermochemical Hydrogen Production," SAND2002-0513, Sandia National Laboratories, Albuquerque, NM, February 2002.

McCoy, H. E.; Beatty, R. L.; Cook, W. H.; Gehlbach, R. E.; Kennedy, C. R.; Koger, J. W.; Litman, A. P.; Sessions, C. E.; Weir, J. R. (1970) "New Developments in Materials for Molten-Salt Reactors," *Nucl. Appl. Tech.*, **8**, 156, 1970.

Minato, K.; Ogawa, T.; Koya, T.; Sekino, H.; Tomita, T. (2000) "Retention of Fission Product Caesium in ZrC-Coated Fuel Particles for High-Temperature Gas-Cooled Reactors," *J. Nucl. Mater.*, **279**, 181, 2000.

Moriyama, H.; Sagara, A.; Tanaka, S.; Moir, R. W.; Sze, D. K. (1998) "Molten Salts in Fusion Nuclear Technology," *Fusion Eng. Des.*, **39**, 627, 1988.

Nabielek, H.; Schenk, W.; Heit, W.; Mehner, A. W.; Goodin, D. T. (1989) "The Performance of High Temperature Reactor Fuel Particles at Extreme Temperatures," *Nucl. Technol.*, **84**, 62, 1989.

Naoumidis, A.; Benz, R.; Rottmann, J. (1982) "Identification of Silicon in Small Quantities of SiC-Coated and SiC(TRISO)-Coated Nuclear Fuel Particles," *High Temp. High Press.*, **14**, 53, 1982.

- Nicholls, D. (2001) "The Pebble Bed Modular Reactor," *Nuclear News*, **44**, 35, 2001.
- Nickel, H.; Schubert, F.; Schuster, H. (1984) "Evaluation of Alloys for Advanced High-Temperature Reactor Systems," *Nucl. Eng. Des.*, **78**, 251, 1984.
- Ogawa, T.; Ikawa, K.; Fukada, K.; Kashimura, S.; Iwamoto, K. (1985) "Research and Development of ZrC-Coated UO₂ Particle Fuel at the Japan Atomic Energy Research Institute," Proceedings of Nuclear Fuels Performance Conference, London, March 25-25, 1985.
- Ogawa, T.; Ikawa, K. (1986) "Reactions of Pd With SiC and ZrC," *High Temp. Sci.*, **222**, 179, 1986.
- Ogawa, T.; Minato, K.; Fukuda, K.; Numata, M.; Miyanishi, H.; Sekino, H.; Matsushima, H.; Itoh, T.; Kado, S.; Takahashi, I. (1991) "A Model to Predict the Ultimate Failure of Coated Fuel Particles During Core Heatup Events," *Nucl. Technol.*, **96**, 314, 1991.
- Ogawa, T.; Fukuda, K.; Kashimura, S.; Tobita, T.; Kobayashi, F.; Kado, S.; Miyanishi, H.; Takahashi, I.; Kikuchi, T. (1992) "Performance of ZrC-Coated Particle Fuel in Irradiation and Postirradiation Heating Tests," *J. Am. Ceram. Soc.*, **75**, 2985, 1992.
- Parma, E. J. (2002) "BURNAL: A Nuclear Reactor Burnup Code Using MCNP Tallies," SAND2002-3868, Sandia National Laboratories, Albuquerque, NM, November 2002.
- Proceedings (1984) "Heat Exchanging Components of Gas-Cooled Reactors," Proceedings of a Specialists Meeting Organized by the International Atomic Energy Agency, Dusseldorf, Germany, April 16-19, 1984.
- Proceedings (1988) "High Temperature Metallic Materials for Gas-Cooled Reactors," Proceedings of a Specialists Meeting Organized by the International Atomic Energy Agency, Cracow, Poland, June 20-23, 1988.
- Simnad, M. T. (1971) *Fuel Element Experience in Nuclear Power Reactors*, Gordon and Breach Science Publishers, New York, NY, 1971.
- Stroh, K. R. (1979) "Thermal-Hydraulic Analysis Techniques for Axisymmetric Pebble Bed Nuclear Reactor Cores," LA-7709-T, Los Alamos National Laboratories, Los Alamos, NM, March 1979.
- Tang, C.; Tang, Y.; Zhu, J.; Qiu, X.; Li, J.; Xu, S. (2000) *J. Nucl. Sci. Tech.*, **37**, No. 9, 802, 2000.
- Teuchert, E.; Maly, V. (1975) "Numerical Research on the Pebble Bed Reactor," in *Advanced Reactors: Physics, Design and Economics*, J. M. Kallfelz and R. A. Karam, editors, Pergamon Press, New York, NY, 1975.
- Teuchert, E.; Rutten, H. J.; Werner, H. (1978) "Performance of Thorium Fuel Cycles in the Pebble-Bed Reactor," *Nucl. Tech.*, **38**, 374, 1978.

Touloukian, Y. S., editor (1967) *Thermophysical Properties of High Temperature Solid Materials*, The MacMillan Company, New York, NY, 1967.

Turner, R. F.; Baxter, A. M.; Stansfield, O. M.; Vollman, R. E. (1988) "Annular Core for the Modular High-Temperature Gas-Cooled Reactor (MHTGR)," *Nucl. Eng. Des.*, **109**, 227,1988.

Zinkle, S. J. (1998) "Summary of Physical Properties for Lithium, Pb-17Li, and $(\text{LiF})_n\text{BeF}_2$ Coolants," APEX Study Meeting, Sandia National Laboratories, Albuquerque, NM, July 1998.

DISTRIBUTION:

1	MS 0727	T. L. Sanders, 6406
1	MS 0736	T. E. Blejwas, 6400
1	MS 0736	J. R. Guth, 6420
5	MS 1136	P. S. Pickard, 6424
10	MS 1141	E. J. Parma, 6424
2	MS 1146	A. J. Suo-Anttila, 6423
1	MS 1146	M. E. Vernon, 6424
1	MS 1146	S. A. Wright, 6424
1	MS 0188	H.R. Westrich, 01011
1	MS 9018	Central Technical Files, 8945-1
1	MS 0899	Technical Library, 9616
1	MS 0612	Review & Approval Desk, 9612 For DOE/OST